

**FLOOD MODELING & RISK FORECASTING FOR AL-BATIN
WATERSHED, SAUDI ARABIA**

Ahmed Mohammed Al-Areeq

CIVIL ENGINEERING

April, 2016

**FLOOD MODELING & RISK FORECASTING FOR AL-BATIN
WATERSHED, SAUDI ARABIA**

BY

Ahmed Mohammed Al-Areeq

A Thesis Presented to the
DEANSHIP OF GRADUATE STUDIES

KING FAHD UNIVERSITY OF PETROLEUM & MINERALS

DHAHRAN, SAUDI ARABIA

In Partial Fulfillment of the
Requirements for the Degree of

MASTER OF SCIENCE

In

CIVIL ENGINEERING

April, 2016

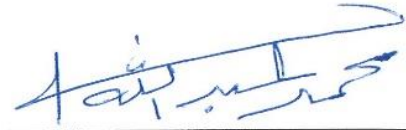
KING FAHD UNIVERSITY OF PETROLEUM & MINERALS
DHAHRAN-31261, SAUDI ARABIA

DEANSHIP OF GRADUATE STUDIES

This thesis, written by **Ahmed Mohammed Al-Areeq** under the direction of his thesis advisor and approved by his thesis committee, has been presented and accepted by the Dean of Graduate Studies, in partial fulfillment of the requirements for the degree of **MASTER OF SCIENCE IN CIVIL ENGINEERING**.



Dr. Salah U. Al-Dulaijan
Department Chairman



Dr. Muhammad A. Al-Zahrani
(Advisor)



Dr. Salam A. Zummo
Dean of Graduate Studies



Dr. Mohammed S. Al-Suwaiyan
(Member)

26/4/16

Date

13 / April / 2016



Dr. Shakhawat Chowdhury
(Member)

©Ahmed Mohammed Al-Areeq

2016

Dedicated

To

My mother

My wife, my children, and to the soul of my father

ACKNOWLEDGMENTS

First and foremost, all praise and thanks to Allah Subhanahu wa Ta'ala for making this thesis possible. My deep thanks and sincere gratitude to my thesis advisor, Dr. Muhammad A. Al-Zahrani, for his efficient, enthusiastic, constructive advice, motivation, immense knowledge and guidance towards the successful completion of this research, which was funded by the Deanship of Scientific Research (DSR) at King Fahd University of Petroleum & Minerals (KFUPM) through project number RC1305-1&2. Thanks are also extended to Prof. Hatim Sharif, consultant of the funded research project, for his support, suggestions, notations and comments which cannot be quantified. Special thanks go also to my committee members, Prof. Mohammed S. Al-Suwaiyan and Dr. Shakhawat Chowdhury, for their support. Thanks also go to the Dammam and Hafar Al-Batin Municipalities for providing the required data that were used in this study.

I wish to express my sincerest appreciation to my mother and brothers for their support, encouragements, and prayers. Deep thanks to my brother, Dr. Nabil, for his moral support at all times. To all my friends both at home and abroad, most especially Ahmed, thank you. Special gratitude to the entire Yemeni community at KFUPM.

I gratefully acknowledge King Fahd University of Petroleum & Minerals for supporting my M.S. studies. On the other side, I would like to convey my sincere thanks and appreciation to my home institution, Thamar University – Yemen, for granting me a scholarship to continue my graduate studies abroad.

Finally, thanks to my dear wife for her patience and moral support. She always stood by me through the good and bad times.

TABLE OF CONTENTS

ACKNOWLEDGMENTS	V
TABLE OF CONTENTS	VI
LIST OF TABLES	IX
LIST OF FIGURES	X
LIST OF ABBREVIATIONS	XIII
ABSTRACT	XVI
ARABIC ABSTRACT	XVIII
CHAPTER 1 INTRODUCTION	1
1.1 Problem Definition	3
1.2 Objectives of the Study	4
CHAPTER 2 LITERATURE REVIEW	7
2.1 Rainfall-Runoff Processes	8
2.2 Hydrologic Models	9
2.3 Hydraulic Models	13
2.4 Modeling Flash Floods in Arid Zones	22
2.5 Floods in Saudi Arabia	24
CHAPTER 3 STUDY AREA AND DATA ACQUISITION	28
3.1 The Study Area	28
3.2 The Basin Topography	28
3.3 Rainfall Data	31

3.4	Methodology	37
CHAPTER 4 HYDROLOGIC AND HYDRAULIC MODELING USING WMS – RESULTS AND ANALYSIS		38
4.1	Hydrologic Model (HEC-HMS)	38
4.2	Hydraulic Model (HEC-RAS).....	49
4.3	Floodplain Delineation Model.....	59
4.4	Proposed Actions to Control Floods	65
4.4.1	The south channel	68
4.4.2	The north channel	68
4.4.3	Hafar Al-Batin retention pond	72
CHAPTER 5 SENSITIVITY ANALYSIS.....		77
5.1	Effect of Urbanization	78
5.2	Effect of Rainfall Storm	83
5.3	Effect of Rainfall Duration.....	88
CHAPTER 6 SUMMARY, CONCLUSION AND RECOMMENDATIONS.....		92
6.1	Summary and Conclusion.....	92
6.2	Recommendations	94
REFERENCES.....		96
APPENDICES		102
APPENDIX I		104
APPENDIX II		111
APPENDIX III		117

APPENDIX IV	123
APPENDIX V	125
VITAE	127

LIST OF TABLES

Table 1.1 Effects of flood events worldwide and other natural disasters	2
Table 1.2 The top ten natural catastrophic events in Saudi Arabia.....	5
Table 2.1 Summary of flood models.....	25
Table 3.1 Design storm for Hafar Al-Batin	36
Table 4.1 Runoff curve numbers for hydrologic soil group	46
Table 4.2 Peak discharge, runoff volume, and runoff coefficient of Hafar Al-Batin outlet	52
Table 4.3 The designed channels of Hafar Al-Batin watershed	73
Table 4.4 Elevation-area function for Hafar Al-Batin retention basin design analysis	74
Table 4.5 Design parameters for each detention basin design capacity	75
Table 5.1 Summary of the effect of urbanization on peak flow, runoff volume for different return periods	82
Table 5.2 Watershed peak discharge and volume for different design storm durations for a return period of 100 years.....	89

LIST OF FIGURES

Figure 2.1 Energy in open channel flow	14
Figure 2.2 Elementary control volume	18
Figure 3.1 Hafar Al-Batin catchment area: (a) Hafar Al-Batin boundary of the watershed and (b) Hafar Al-Batin city	29
Figure 3.2 Hafar Al-Batin topography: (a) Hafar Al-Batin contour map and (b) 3D contour map of Hafar Al-Batin watershed.....	30
Figure 3.3 Hafar Al-Batin digital elevation model (DEM).....	32
Figure 3.4 Hafar Al-Batin watershed.....	33
Figure 3.5 Annual rainfall distribution depth for Saudi Arabia [56]	35
Figure 4.1 Flow chart of the steps involved in floodplain analysis	39
Figure 4.2 Delineated Hafar Al-Batin watershed classified by the basin area	40
Figure 4.3 Hafar Al-Batin approximate streams [57]	41
Figure 4.4 Delineation of Hafar Al-Batin watershed.....	44
Figure 4.5 Hafar Al-Batin watershed classified by curve number.....	47
Figure 4.6 Rainfall hyetograph: (a) the 6-minute hyetograph of the 100-year storm (storm total is 79.34 mm) and (b) the 1-hour hyetograph of the 2, 5, 10, 25, 50, and 100-year storms.....	48
Figure 4.7 HEC-HMS basin model of Hafar Al-Batin watershed	50
Figure 4.8 Hafar Al-Batin outlet hydrograph: (a) for different return periods and (b) for 100-year storm runoff	51
Figure 4.9 TIN map for Hafar Al-Batin watershed.....	54

Figure 4.10 Main reaches and sections along the main reach of Hafar Al-Batin watershed	56
Figure 4.11 Water surface level across the main channel (a) longitudinal profile for different return periods and (b) perspective plot for 100 years	57
Figure 4.12 Water surface elevation at different cross sections along the main reach for different return periods: (a) city entrance, (b) middle of the city, and (c) end of the city (outlet).....	58
Figure 4.13 Perspective plot of Hafar Al-Batin city	60
Figure 4.14 The 100-year floodplain map from WMS: (a) floodplain depths and (b) water surface elevations	62
Figure 4.15 The 2-year floodplain map from WMS: (a) floodplain depths and (b) water surface elevations	63
Figure 4.16 Flood risk map: (a) 100-year flooded area and (b) flooded area developed by Hafar Al-Batin municipality	64
Figure 4.17 Hafar Al-Batin flood risk map.....	66
Figure 4.18 Hafar Al-Batin main streams.....	67
Figure 4.19 Proposed actions	69
Figure 4.20 The south channel.....	70
Figure 4.21 Details of the trapezoidal sections: (a) north channel and (b) east channel ..	71
Figure 4.22 Effect of constructing retention pond: (a) HEC-HMS output graph and (b) summary table	76
Figure 5.1 Effect of urbanization on the change in peak discharges for different return periods.....	79

Figure 5.2 Effect of urbanization on the change in runoff volume for different return periods.....	81
Figure 5.3 SCS rainfall distributions[70].....	84
Figure 5.4 The 100-year storm runoff hydrograph of Hafar Al-Batin watershed (frequency storm method).....	86
Figure 5.5 Frequency storm distribution hyetograph of the 100-year storm	87
Figure 5.6 Watershed hydrographs for different storm durations for 100-year storm.....	91

LIST OF ABBREVIATIONS

<i>A</i>	:	cross section area (m ²) / catchment area (ha)
<i>C</i>	:	runoff coefficient
CN	:	curve number
CNs	:	curve numbers
DEM	:	digital elevation model(s) / map
<i>g</i>	:	gravitational acceleration (m/s ²)
GIS	:	Geographic Information System
GP	:	Generalized Pareto
<i>h</i>	:	flow depth (m)
HEC-HMS	:	Hydrologic Engineering Center-Hydrologic Modeling System
HEC-RAS	:	Hydrologic Engineering Center-River Analysis System
<i>i</i>	:	rainfall intensity (mm/h)
<i>I</i>	:	inflow (m ³ /s)
IDF	:	intensity-duration-frequency
LIDAR	:	light detection and ranging
<i>m</i>	:	exponent of the kinematic wave

MTM	:	Modified Talbot Method
n	:	channel roughness
NRCS	:	Natural Resources Conservation Service
O	:	outflow (m^3/s)
P	:	rainfall (mm)
PRM	:	Probabilistic Rational Method
q	:	lateral inflow per unit area ($\text{m}^3/\text{s m}^2$)
Q	:	discharge / flow rate (m^3/s)
Q_p	:	rate of peak runoff (m^3/s)
Q_r	:	direct runoff (mm)
R	:	hydraulic radius (m)
RFFA	:	Regional Flood Frequency Analysis
RMSE	:	Root Mean Square Error
S	:	water storage volume (m^3)
SCS	:	Soil Conservation Service
SCS-CN	:	Soil Conservation Service-curve number
S_f	:	friction slope (energy gradient) (m/m)

S_o	:	bed slope / channel slope (m/m)
S_r	:	potential difference between direct runoff and rainfall (mm)
SWBM	:	Spatial Water Budget Model
t	:	time (s)
TINs	:	triangulated irregular networks
u	:	velocity of longitudinal flow (m/s)
USGS	:	United States Geological Survey
WMS	:	Watershed Modeling System
x	:	longitudinal distance (m)
α	:	kinematic wave parameter

ABSTRACT

Full Name : Ahmed Mohammed Ahmed Al-Areeq
Thesis Title : Flood Modeling & Risk Forecasting for Al-Batin Watershed, Saudi Arabia
Major Field : Civil Engineering
Date of Degree : April, 2016

The study of flood in arid and semi-arid regions is a challenging task for water resources engineers. In this research, the occurrence of flood in Hafar Al-Batin city will be investigated to identify the areas within the city with high risk of flooding. As a result of the limited data about the catchment of Hafar Al-Batin, Geographic Information System (GIS) has been used to obtain and prepare the input data prior to constructing and executing the hydrologic, hydraulic, and floodplain models. Moreover, Hafar Al-Batin intensity-duration-frequency (IDF) curves have been used in this study and two scenarios were applied to estimate the design storms. The first scenario was by using the Soil Conservation Service (SCS) hypothetical storm method while the second scenario was by using the frequency storm method. The catchment was divided into three main parts, and each part was divided into many sub-basins to run the hydrologic model in a semi-distributed mode. The effect of urbanization was investigated by simulating different urbanization scenarios to find its effect on peak discharge resulting from the design storms.

Flood modeling and simulation can help decision-makers to take the necessary actions to control or minimize the consequences of floods. To achieve the objectives of this research, Watershed Modeling System (WMS), Hydrological Modeling System (HEC-HMS), and River Analysis System (HEC-RAS) were used to construct the hydrologic, hydraulic, and

floodplain models, which were used to estimate the expected flow due to flood and identify the areas with high risk of flooding. Urbanization and rainfall characteristics were investigated and the results show their significant effects on the peak discharge and runoff volume. On the other side, it presents the estimated volume of water that can be collected during the design storm in the whole catchment area of 1,669.014 km², which can cause inundation of a wide portion of Hafar Al-Batin city. Accordingly, three proposed actions (retention pond at the entrance of the city, two trapezoidal channels at the south and north sides of the city) were suggested to reduce the risk of flood on the city of Hafr Al-Batin.

ملخص الرسالة

الاسم الكامل: أحمد محمد أحمد العريق

عنوان الرسالة: نمذجة الفيضانات والتنبؤ بالمخاطر لحوض حفر الباطن، المملكة العربية السعودية

التخصص: هندسة مدنية

تاريخ الدرجة العلمية: إبريل 2016

تعتبر دراسة الفيضانات في المناطق الجافة وشبه الجافة تحدياً كبيراً في هندسة مصادر المياه. في هذا البحث تم دراسة حدوث الفيضانات في مدينة حفر الباطن، الواقع في المنطقه الشرقيه من المملكة العربية السعودية، لتحديد المناطق ذات الخطورة العالية داخل المدينة. نتيجة لشحة البيانات في منطقة الدراسة فقد تم استخدام نظام المعلومات الجغرافية (GIS) للحصول على واعداد البيانات المدخلة قبل انشاء وتنفيذ النموذج الهيدرولوجي، الهيدرولوجي، والسهول الفيضيه. علاوة على ذلك، في هذه الدراسة تم استخدام منجنيات الشدة، الاستدامة و التكرار (IDF) لمحطة حفر الباطن وتم تطبيق سيناريوهين لتقدير العواصف التصميمية. تم استخدام طريقة مصلحة حماية التربة لعاصفة افتراضية SCS في السيناريو الاول بينما تم استخدام طريقة عاصفة التكرار في السيناريو الثاني. تم تقسيم المسقط المائي الى ثلاثة اجزاء رئيسية وكل جزء تم تقسيمه الى عدة اجزاء وذلك لتنفيذ النموذج الهيدرولوجي في نمط نصف موزع. تمت دراسة التمدد الحضري من خلال نمذجة سيناريوهات مختلفة للتمدد الحضري لايجاد الجريان الاقصى الناتج من العواصف التصميمية.

نمذجة ومحاكاة الفيضانات يمكن ان تساعد صناع القرار على اتخاذ الاجراءات اللازمة للسيطرة أو التقليل من اثار الفيضانات. لتحقيق اهداف هذه الدراسة، فقد تم استخدام برامج (WMS Watershed Modeling System, Hydrologic Modeling System HEC-HMS, and River Analysis System HEC-RAS)

لبناء النموذج الهيدرولوجي، والسهول الفيضيه التي تستخدم لتقدير الجريان المتوقع الناتج عن الفيضانات وتحديد المناطق ذات المخاطر العالية. أظهرت الدراسة بان التوسع العمراني وخصائص المطر لها تأثير واضح على التصريف الاقصى وحجم الفيضان. من ناحية اخرى، وبناء على نتائج الدراسة فقد تم تقدير حجم الفيضان الناتج عن سقوط الامطار ل 24ساعة وتكرار 100 عام بحوالي 13,016,600م³ مما يسبب باغراق جزء كبير من مدينة حفر

الباطن. ووفقا لذلك تم اقتراح بعض الاجراءات التي تساهم في تخفيف حدة السيول على مدينة حفر الباطن والتي من شأنها تقليل الخسائر والاضرار المتوقعه في حالة حدوث سيول على المدينة.

CHAPTER 1

INTRODUCTION

Floods are one of the dangerous natural catastrophes which hit many countries around the world every year, causing massive losses in human lives, property, and structures and affect millions of people. Moreover, huge amount of money is spent every year to avoid and protect the people and infrastructure from the effects of the floods.

Jonkman [1] mentioned that about 100,000 persons were killed and over 1.4 billion people were affected by floods during the last decade of the 20th century. Table 1.1 shows a comparison between the effects of flood events worldwide and other natural disasters. It can be noticed from the table that the floods are the most frequently occurring events, followed by the windstorm.

There are many types of floods which can be classified as [1]:

Flash floods: generally, this type of flood occurs in a mountainous region due to the rapid rise of water levels resulting from the high rainfall intensity.

River floods: caused by high precipitation levels either inside or outside the flooded region or due to melting snow, causing the river to overflow outside its normal boundaries.

Table 1.1 Effects of flood events worldwide and other natural disasters[1]

Disaster type	No. of events		Total killed		Total affected	
	<i>No.</i>	<i>%</i>	<i>No.</i>	<i>%</i>	<i>No.</i>	<i>%</i>
Earthquake	548	9	483,552	24	79,316,329	2
Drought	495	8	560,381	28	1,381,353,218	33
Famine	62	1	282,299	14	62,913,301	2
Epidemic	656	10	143,276	7	17,712,233	0
Windstorm	1741	28	279,894	14	462,772,019	11
Freshwater floods	1816	29	175,056	9	2,198,579,362	52
Others	969	15	65,892	3	19,484,370	1
TOTAL	6287		1,990,350		4,222,130,832	

Coastal floods: these occur along the big lakes and coasts of seas due to windstorms and low atmospheric pressure.

Drainage problems: these cannot be controlled by the normal drainage systems due to the high precipitation levels. However, the risk to life due to this type of flood is limited because of the limited water levels while it causes main economic damage.

Tsunamis (or seismic sea waves): caused by a submarine landslide, earthquake, or volcanic eruption resulting in generation of large waves, causing a destructive surge on reaching land.

1.1 Problem Definition

Flash floods are large events that happen in a relatively short duration due to excessive rainfall and form one of the most important challenges in the water science field. Floods in arid and semi-arid regions have specific characteristics, which makes them more hazardous than ordinary floods which occur in wet regions. Arid regions' floods occur fast and suddenly, so it is called flash floods. There are two main differences between ordinary flood and flash flood, which are the speed of occurrence and the time between the observed events and its flood occurrence. The hydrograph of flash flood distinguishes a single peak flood with a very short period in the time between the beginning of the flood event and its peak. Many researchers related to flood analysis, consider the usual duration of flash floods to be less than six hours, which is considered as an ideal value to distinguish between ordinary and flash floods [2].

In Saudi Arabia, floods may be the major catastrophic natural hazard as shown in Table 1.2. The table indicates that floods are the most frequently occurring disasters followed by epidemic. According to Momani and Fadil [4], more than 121 fatalities, around 20,000 sheltered families and billions of dollars in losses were due to the natural disasters in Saudi Arabia in 2009 in addition to the effects on human health as a result of flooding. Moreover, the amount of three billion riyals was the monetary loss. Maghrabi [5] stated that several fatalities and massive destruction in structures, properties, and highways occurred as a result of massive floods due to heavy rains, which affected Jeddah in 2009.

Hafar Al-Batin city, which is located in the eastern part of the Kingdom of Saudi Arabia, is also suffering from the occurrence of floods. In the past few years, flash floods hit the city many times and caused losses in economic and human life. The current study will focus on the effect of flash flood on Hafar Al-Batin by constructing a flood hazard map which will help the decision makers to adopt the appropriate plan to control and reduce the effect of floods.

1.2 Objectives of the Study

The aim of this study is to construct hydrologic, hydraulic and floodplain models that are capable of predicting the flood in the city of Hafar Al-Batin. The research objectives are as follows:

- Construct a flood model for Hafar Al-Batin watershed.
- Estimate the flood peak for the watershed using different methods.

Table 1.2 The top ten natural catastrophic events in Saudi Arabia[3]

Disaster	Date	No. of fatalities
Flood	24 Nov. 2009	163
Epidemic	11 Sep. 2000	76
Epidemic	Mar. 2000	57
Epidemic	9 Feb. 2001	35
Flood	28 Apr. 2005	34
Flood	24 Dec. 1985	32
Flood	22 Jan. 2005	29
Flood	4 Apr. 1964	20
Epidemic	8 Apr. 2002	19
Epidemic	11 Nov. 2003	12

- Run the constructed model for different scenarios to predict the risk of flood.
- Perform sensitivity analysis to study the influence of urbanization and storm durations.
- Propose appropriate actions to minimize the risk of flood.

CHAPTER 2

LITERATURE REVIEW

In general, flood hazard maps can help to provide geographical information on flood inundation such as predicted inundation depth and inundation area, as well as on evacuation (location of evacuation routes, dangerous spots on evacuation routes, evacuation refuges, etc.) in an easy format to understand. Flood hazard maps are the effective way to reduce the impact of floods on people and property. In many countries, particularly the developed countries, the authorities develop flood hazard maps of known return periods which are used as a guide for the flood protection and land development plans to specify areas prone to flooding. On the other hand, in ungauged basins, several approaches range from indirect peak discharge and simple empirical methods to sophisticated rainfall-runoff modeling developed by using hydrologic and hydraulic models that can be applied to produce such maps.

Generally, three steps are required to develop the floodplain mapping [6]:

- Estimating 100-year peak discharge based on hydrological models or flow data.
- Computing the elevation profiles associated with the 100-year flood using hydraulic modeling.
- Delineating the inundated area.

Flood hazard maps are developed based on rainfall-runoff modeling. The main objective of rainfall-runoff models is to understand the rainfall-runoff process and extend streamflow

time series in both time and space [7]. These models are not only used for hydrologic investigation, but are also used for many purposes in engineering and environmental sciences, which include calculations of design floods, catchment response to climatic events, estimation of the impact of land use change, management of water resources, streamflow prediction, and flood forecasting.

2.1 Rainfall-Runoff Processes

When precipitation exceeds losses such as infiltration, surface storage, interception, and evaporation, runoff is generated to become concentrated flow in valleys and stream channel. Two mechanisms are included in runoff generation, which are Hortonian overland flow and saturation overland flow [9]. A severe storm will lead to runoff generation when the soil is saturated, while Hortonain overland flow depends on the relationship between infiltration capacity versus rainfall intensity. This means that runoff is generated when rainfall intensity exceeds infiltration capacity.

The hydrologic cycle can be obviously represented by watershed hydrologic models in various and appropriate ways. The hydrologic system embodies all of the physical processes that are involved in the conversion of precipitation to runoff as well as physical characteristics of the watershed and atmosphere that influence runoff generation. There are many factors affecting rainfall-runoff processes, such as physical processes, storm characteristics, and watershed characteristics [10].

The hydrologic cycle comprises all of the physical processes that affect the movement of water in its various forms, from its occurrence as precipitation near the earth's surface to its discharge to the ocean. Such processes include interception, water storage in depressions

in lakes and reservoirs, snow accumulation and melt, if there is any, infiltration through the earth's surface, percolation to various depths in the subsurface, storage of water in the subsurface, the later movement of water in both unsaturated and saturated portions of the subsurface, evaporation from water bodies and moist soil, transpiration from vegetation, overland flow, and streamflow. These processes are very complex and some of them are more significant than others for particular types of analyses.

Precipitation is viewed as an input to a hydrologic system. The precipitation might be associated with a historical storm, a design storm, or may result from a stochastic generation procedure. Generally, precipitation is averaged spatially over a sub-basin, which affects the shape of the outlet hydrograph. Likewise, precipitation intensity is averaged over a time interval which is significant on a small watershed. Thus, precipitation input to the hydrologic system is commonly represented by hyetographs of spatially and temporally averaged precipitation.

Topography has an effect on collecting and conveying water for any catchment system. Area, width, length, shape, slope, drainage patterns, and linear measures are some of the important catchment characteristics. Watersheds are heterogeneous with respect to topography, geology, soils, land use, vegetation, drainage density, and river characteristics.

2.2 Hydrologic Models

Hydrologic model is a mathematical representation of hydrologic processes which divide precipitation into two main parts, namely losses and runoff. The hydrologic system includes physical processes (interception, depressions, infiltration, evaporation, and transpiration) that are involved in the conversion to streamflow. In addition, the physical

characteristics of the watershed and atmosphere influence the runoff generation. The use of computer models to simulate the hydrologic system is of a major significance in the performance of such flood-runoff analysis. The aim of hydrologic models is often to establish rainfall-runoff relationships [11].

Nowadays, various hydrologic and hydraulic models have been used to predict floods and the required actions to reduce their effects. Many of these models are site specific containing assumptions and simplifications, which exclude their universal use. So, it is very important to understand the candidate model clearly in order to use it appropriately. Some of the models use physically based governing equations having computationally intensive numerical solutions, while others are based on simple empirical relations having strong algorithms. Sometimes, the simple models are insufficient in giving appropriately detailed results, and the detailed models are inefficient and prohibitive for the large catchment. Therefore, it is quite a challenging task to find an appropriate model for a certain watershed.

Harsh climatic conditions and lack of high-quality observations in arid regions make the flood simulation, especially flash flood forecasting, more difficult and of a great challenge. Due to the wide range of variety in hydrologic models which have been developed over the years, the classification of these models according to their structures and approaches has become necessary. Rainfall-runoff models were divided into three categories by model developers, which are the most commonly used classifications. The classifications are as follows [12, 13, 14]:

- Metric or empirical models which are derived from data observations to characterize the response of the catchment system [13]. Observed data, including rainfall and runoff records, are used to derive the model parameters and structure. Metric models derived as spatially lumped are not suitable for ungauged catchments because they treat the catchment as a single unit [7]. Generally, these models are simple, widely used, and easy to understand. However, several important factors may not be accounted for, such as antecedent moisture conditions. The Unit Hydrograph and Artificial Neural Networks are two of the most popular models of this type.
- Conceptual or parametric models describe all of the component hydrological processes. These models have a structure that is defined a priori using mostly fluxes of water between various reservoirs [7]. Conceptual models treat the catchment as a single unit, so these types of models are considered as a lumped approach.
- Physically based or mechanistic models are mathematical models based on the energy, momentum, and conservation of mass [7]. The aim of developing these types of models is to obtain models that can be run without calibration step, which would be applicable to ungauged catchment or applicable to catchment where the available data is not enough to calibrate conceptually.

Distributed and lumped models are another classification where the lumped models are appropriate to simulate the catchment as a single unit. Many lumped models were developed, such as AWBM [15], IHACRES model [16], and GR4J [17]. On the other hand, the predictions in the distributed models are done by dividing the catchment area into a large number of grid squares [18]. This type of model includes HEC-HMS [19],

TOPMODEL [20], and USDA SWAT [21]. Hydrological processes can be described in details in the distributed models where parameter values must be determined for each element. On the other hand, the parameter average values can be used in lumped models, which makes them suitable for the catchments of limited data. The following considerations must be taken when selecting a hydrologic model:

- The quality and availability of hydrological data.
- Model's ability in regionalization and model structure, and
- Characteristics of the catchment area and homogeneity of flow.

In this study, HEC-HMS rainfall-runoff model will be used for the following reasons:

- Model structure and availability.
- Applicability of the model in arid catchments, and
- Data availability.

The HEC-HMS input requirements are the basin model, meteorological model, and control specifications. Then, several techniques can be used to model the rainfall-runoff process. The basin model can be used to store and define the physical parameters which describe the catchment area. Meteorological data, such as precipitation and evapotranspiration, can be defined in the meteorological model, while the control specifications control the time span of a simulation.

2.3 Hydraulic Models

The hydraulic models are used to compute and predict the floodplain water level after executing the hydrologic model. The final calculated flood depth must be calibrated to actual flood depths observed from previous flood events within 0.5 feet [22]. The hydraulics models developed based on the following equations:

1. Conservation of mass or continuity
2. Momentum
3. Energy

The flow depth and rate of discharge, or the flow depth and velocity, are sufficient to define the flow conditions at a channel cross section. Therefore, the combined application of two governing equations may be used to analyze a typical flow situation. The continuity equation and the energy or momentum equation are used for this purpose.

Steady flow

Water surface profile for steady gradually varied flow is computed for two adjacent cross-sections based on an iterative solution of the energy equation. Figures 2.1 shows open channel energy concepts and equation (2.1) is the energy equation [63]:

$$Z_2 + Y_2 + \frac{\alpha V_2^2}{2g} = Z_1 + Y_1 + \frac{\alpha V_1^2}{2g} + h_e \quad (2.1)$$

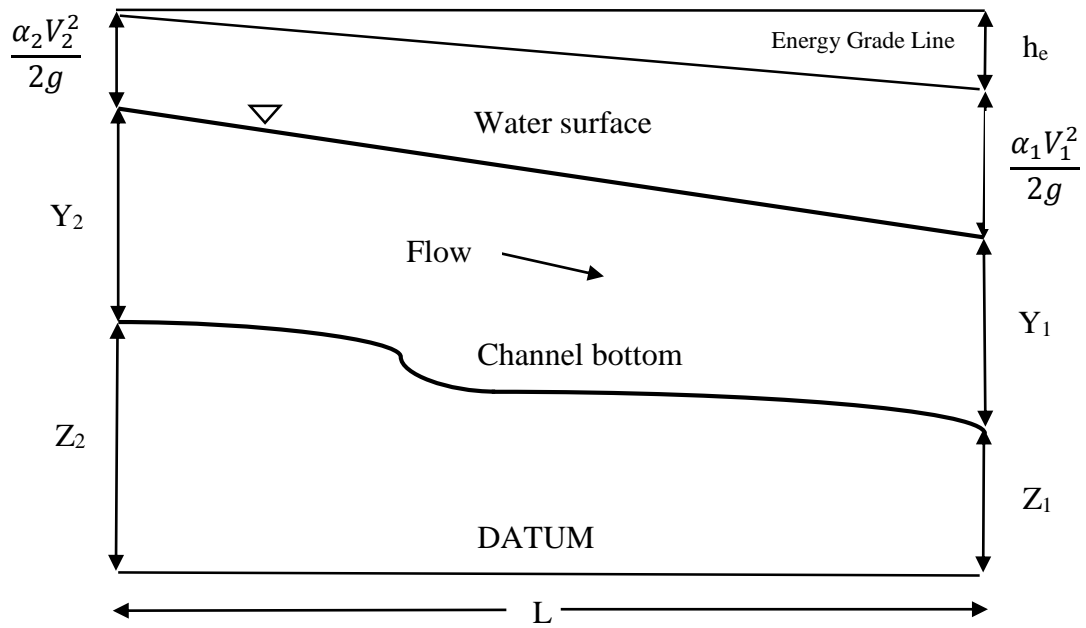


Figure 2.1 Energy in open channel flow

where Z_1, Z_2 = the main channel invert elevation(m), Y_1, Y_2 = water depth at cross sections(m), V_1, V_2 = velocity of longitudinal flow (m/s), α_1, α_2 = velocity weighting coefficients, g = gravitational acceleration (m/s²). The total head loss, h_e , is calculated as follows:

$$h_e = h_f + h_o \quad (2.2)$$

where h_f is the head loss due to friction and h_o is the minor losses due to the expansion or contraction of the channel. The head loss due to friction, h_f , is estimated by

$$h_f = \left(\frac{Q}{K}\right)^2 \quad (2.3)$$

where Q is the discharge and the loss coefficient K is calculated based on Manning's equation as follows:

$$K = \frac{1.486}{n} AR^{\frac{2}{3}} \quad (2.4)$$

where A_1, A_2 = upstream and downstream wetted area respectively of the cross-sections(m²), R_1, R_2 = downstream and upstream hydraulic radius(m), n = manning's roughness coefficient.

The minor losses due to contraction or expansion is estimated by the following equation:

$$h_o = C_L \left| \frac{\alpha_2 V_2^2}{2g} - \frac{\alpha_1 V_1^2}{2g} \right| \quad (2.5)$$

where C_L = loss coefficient for contraction and expansion.

For steady rapidly varied flow, the momentum equation (2.6) is used to compute the water surface profile. Momentum equation is applicable to rapidly varying flow situation transition from supercritical to subcritical or subcritical to supercritical such as bridge construction, significant change in channel slope, drop structure and weirs [63].

$$\frac{Q_2^2 \beta_2}{g A_2} + A_2 \bar{Y}_2 + \left(\frac{A_1 + A_2}{2} \right) L S_o - \left(\frac{A_1 + A_2}{2} \right) L S_f = \frac{Q_1^2 \beta_1}{g A_1} + A_1 \bar{Y}_1 \quad (2.6)$$

where Q_1, Q_2 = upstream and downstream discharge (m^3/s), β = momentum coefficient for a varying velocity distribution in irregular channels, \bar{Y}_1, \bar{Y}_2 = depths measured from the water surface to the centroid of the cross-sectional area (m), L = distance between sections along the channel (m), S_o = bed slope (m/m), and S_f = friction slope (energy gradient) (m/m).

Unsteady flow

The continuity and momentum equations are the physical laws which govern water flow in a stream. Broad assumptions are required to develop the governing equations of the hydraulic models when numerical methods are used to describe the natural physical phenomena.

Continuity equation

Consider an element of the fluid volume as shown in Figures 2.2. The rate of inflow to the control volume may be written as [63]:

$$Q + q \Delta x \quad (2.7)$$

The rate of outflow

$$Q + \frac{\partial Q}{\partial x} \Delta X \quad (2.8)$$

The rate of change in control volume

$$\frac{\partial A}{\partial t} \Delta X \quad (2.9)$$

According to the continuity equation:

$$\text{Inflow} - \text{outflow} = \text{rate of change in volume}$$

The change in mass in the control volume is equal to:

$$\frac{\partial A}{\partial t} + \frac{\partial Q}{\partial x} = q \quad (2.10)$$

Where q = the lateral inflow rate per unit length of channel ($\text{m}^3/\text{s m}^2$), x = longitudinal distance (m), t = time (s).

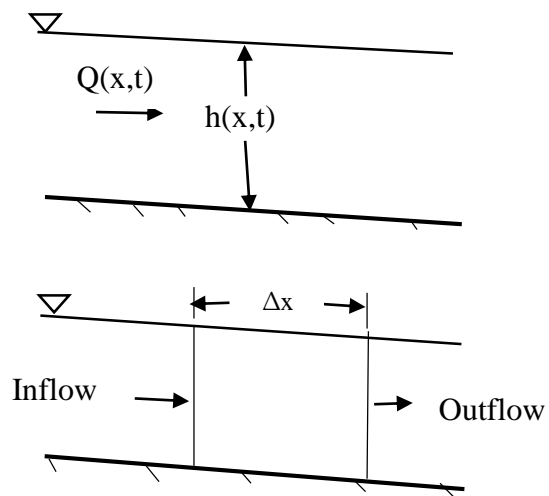


Figure 2.2 Elementary control volume

Momentum equation

The conservation of momentum states that the rate of change in momentum equal to the external forces (pressure, gravity, and friction force) acting on the system.

Pressure force:

$$F_{pn} = -\rho g A \frac{\partial h}{\partial x} \Delta x \quad (2.11)$$

where F_{pn} = the net pressure force, x = distance between two sections, A = cross section area, h = flow depth, ρ = water density.

Gravity force:

$$F_g = \rho g A \frac{\partial z}{\partial x} \Delta x \quad (2.12)$$

where F_g = gravity force, z = invert elevation.

Friction force:

$$F_f = \rho g A S_f \Delta x \quad (2.13)$$

where S_f = friction slope.

Momentum flux:

The net rate of momentum (momentum flux) entering the control volume can be written as:

$$-\rho \frac{\partial qv}{\partial x} \Delta x \quad (2.14)$$

The rate of accumulation of momentum may be written as:

$$\frac{\partial}{\partial t}(\rho Q \Delta x) = \rho \frac{\partial Q}{\partial t} \Delta x \quad (2.15)$$

From the principle of momentum conservation, the momentum flux plus the external forces = the rate of accumulation of momentum.

Therefore:

$$\frac{\partial z}{\partial x} = \frac{\partial h}{\partial x} = \frac{\partial z}{\partial x} \quad (2.16)$$

Where $\frac{\partial z}{\partial x}$ = water surface slope

Substituting (2.15) in (2.16) and dividing through by $\rho \Delta x$, the final form of momentum equation [63]:

$$\frac{\partial Q}{\partial t} + \frac{\partial QV}{\partial x} + g A \left(\frac{\partial z}{\partial x} + S_f \right) = 0 \quad (2.17)$$

The full Saint-Venant equations are the most widely used approach to model river hydraulics [23]. In differential form, Saint-Venant equations (the dynamic wave equations) consist of the equations of continuity and momentum for gradually varied unsteady flow are described in (2.10) and (2.17) [24]. Approximate numerical solutions have been used to solve these equations in stream flood routing models. Due to the computationally intensive numerical solutions of the dynamic wave equations (Saint-Venant equations), there used is limited in watershed models. Some models use approximation of these equations by ignores certain terms in the momentum equation (2.17).

The continuity and simplified momentum equations constitute the diffusive wave equations [24]:

$$\frac{\partial h}{\partial t} + \frac{\partial Q}{\partial x} = q \quad (2.18)$$

$$\frac{\partial h}{\partial x} = S_o - S_f \quad (2.19)$$

Similar to the Saint-Venant equations, the above equations can be solved numerically because there is no analytical solution of the diffusive wave equations [23].

The simplest form of the dynamic wave equations is the kinematic wave equations which can be expressed as:

$$S_o = S_f \quad (2.20)$$

$$\frac{\partial h}{\partial t} + \frac{\partial Q}{\partial x} = q \quad (2.21)$$

Equation (2.5), the momentum equation, assumes bed slope equals energy gradient and can be expressed as a parametric function of the stream hydraulic parameters by using any suitable law of flow resistance. A commonly used expression is:

$$Q = \alpha h^m \quad (2.22)$$

where α = kinematic wave parameter, and m = exponent of the kinematic wave. These two parameters (α and m) are related to geometry and plane (or channel) roughness and their values can be determined by using Manning's formula [25]. Therefore, kinematic wave equations consist of Equations (2.6) and (2.7). Some watershed models, such as KINEROS, DWWSM, and PRMS, were developed based on the kinematic wave equations. Accordingly,

the continuity equation and flow equation constitute the non-linear reservoir equations. Manning's equation as an example, is expressed below:

$$\frac{\partial s}{\partial t} = I - O \quad (2.23)$$

$$Q = \frac{1}{n} A R^{2/3} S_o^{1/2} \quad (2.24)$$

where S = water storage volume (m^3), I = inflow (m^3/s), O = outflow (m^3/s), Q = flow rate (m^3/s), n = channel roughness, S_o = channel slope, R = hydraulic radius (m), and A = cross section area (m^2). Equations (2.23) and (2.24) do not represent any waveforms and assume a leveled water surface throughout the overland plane or channel reach. Equation (2.23) is useful in reservoirs and lakes.

2.4 Modeling Flash Floods in Arid Zones

Several models have been applied to watershed analysis with different conditions (sizes, different climatic, hydrologic, and geologic conditions) to evaluate their suitability and performances. However, a limited number of hydrologic models have been developed in arid regions.

Lange et al. [26] concluded that the analysis of single events in arid regions is very important for better understanding of high magnitude floods. Abdulla et al. [27] used the water balance equation to develop their model for simulating the surface runoff hydrograph in the western part of Iraq, and they found that their model results show a good agreement between model output and observed data. Al-Abed et al. [28] studied the performance of HEC-HMS / HEC-GeoHMS extension model and the Spatial Water Budget Model

(SWBM) and found that the two models give satisfactory results. Al-Qurashi [29] applied distributed and lumped models for streamflow simulation in the Wadi Dhuliel arid catchment, north-east Jordan. They found that HEC-HMS results show a good agreement with the observed streamflow data, while IHACRES shows some weaknesses.

Al-Qurashi et al. [30] evaluated the distributed model (Kineros2) in application to an arid catchment in Oman where they conducted a series of three experiments with different calibration strategies. They found that the prediction performance was generally poor. They recommended that significant data collection and further research are required to realize the potential value of distributed physically-based models. McIntyre and Al-Qurashi [31] concluded that using parameters between 2 and 4 instead of a 9-parameter version of IHACRES (which was developed as an appropriate model for semi-arid and arid areas) produced simple models which gave the best performance for predicting flood peaks in Wadi Ahin, North-East of Oman. On the other hand, better results for predicting time to peak were achieved by using a 1-parameter model. However, uncertainty was very high in all predictions. Timpson [32] mentioned that there is no good method that can be used in Utah to estimate the peak flood discharge for rural watersheds with an area between 0.5 mi² and 30 mi². Accordingly, Timpson conducted the flood frequency analysis for small rural watersheds within the state of Utah to determine regression formulas in the style of the rational method for the desired area.

With reference to Zaman et al. [33], the partial duration series was found to be better than the annual maximum series in the arid regions of Australia, and based on this finding, data exponential and generalized Pareto were selected. They found that the generalized Pareto distribution is better than the exponential distribution to fit the partial duration series flood

data. Also, it was found that smaller runoff coefficient values and a higher loss were observed in semi-arid and arid catchments. Ghoneim and Foody [34] developed a hydrologic model for Wadi El-Alam, Egypt using HEC-HMS. They found that HEC-HMS is suitable for modeling the rainfall-runoff process in arid and semi-arid regions and it also gives satisfactory results in the absence of sufficient data for surface flow.

Mediero and Kjeldsen [35] used an extended generalized least squares model to investigate a semi-arid Ebro catchment in Spain. They found that their new model improved the existing ordinary least squares models. In addition, a suitable description of flood processes was obtained and more reliable flood predictions in ungauged catchments were achieved.

Table 2.1 summarizes some of the popular hydrologic and hydraulic models used worldwide.

2.5 Floods in Saudi Arabia

In recent years, there has been a considerable amount of attention to flooding in Saudi Arabia. Despite the proposed actions to avoid the effects of flooding, there is a lack of proper solutions in the flooded areas. Studies have been conducted in different regions of Saudi Arabia using different techniques. Following presents some studies which have been conducted in some regions of Saudi Arabia:

Table 2.1 Summary of flood models

Software	Study area	Country	Aim of study	Used tools / Method	Reference(s)
Excel and Matlab	Wadis Hali and Yibah	Saudi Arabia	flood inundation map	1/50,000 scale topographic map	[36]
Global mapper, Excel	Al-Kharj	Saudi Arabia	flood hazards	Soil Conservation Service (SCS) and Muskingum	[37]
WMS	Jeddah	Saudi Arabia	simulate the floods	HEC-HMS	[38]
WMS	Wadi Marwani basin	Saudi Arabia	The most accurate model for peak discharge estimation.	A regional flood frequency analysis (RFFA), the modified Talbot method (MTM), the probabilistic rational method (PRM), and the HEC-HMS program	[39]
WMS	Dez River basin	Iran	flood modeling	HEC-1, HEC-RAS	[40]
WMS	Midas Creek	Jordan	predict the area of flooding in the specified area, flood control	HEC-RAS	[41]
WMS	Koycegiz Lake-Dalyan Lagoon watershed	Turkey	delineation of boundaries	Rational method	[42]
WMS	Ciderewak River, west Java	Indonesia	flood risk reduction	HEC-1, HEC-HMS, HEC-RAS	[43]
HEC-RAS	Peace River, Alberta	Canada	flood routing and flood level forecasting		[44]
HEC-RAS and ArcView GIS	Waller Creek, Austin, Texas	USA	floodplain mapping		[45]
WMS	Mangla watershed	Pakistan	modeling flood conditions	Hydrological Simulation Program – FORTRAN (HSPF), HEC-RAS	[46]

Nouh [47] used three methods (region curves, common peak flow models, and duration reduction curves) to estimate the maximum flood in the southwest region of Saudi Arabia. Statistical measures were used to compare the accuracy of the three methods. The study concluded that the region curve method gives the best statistics. Al-Turbak [48] constructed a geomorphoclimatic model in three arid catchments in Saudi Arabia and found that the developed model is capable of predicting surface runoff hydrographs accurately when detailed and accurate data are available.

Subyani [49] studied flood probability and the hydrological characteristics in western Saudi Arabia of some main wadis, including Fatimah and Usfan, and found that Gumbel's extreme value distribution is the best fitting model for identifying and predicting future rainfall occurrence. Al-Shareef et al. [39] conducted a study on Wadi Marwani basin in Jeddah, Saudi Arabia and tried to find the best method that can be used to estimate the peak discharge. Four methods were tested, namely the Modified Talbot Method (MTM), the Hydrologic Engineering Center-Hydrologic Modeling System (HEC-HMS), the Regional Flood Frequency Analysis (RFFA) regression equations, and the Probabilistic Rational Method (PRM). The Root Mean Square Error (RMSE) was used to measure the accuracy of the four methods. The results indicate that the PRM is a more accurate model to compute the peak discharge compared to the others.

Dawod et al. [50] concluded that the most accurate national hydrological model for the Makkah area is the model developed based on actual precise field measurements in the southwest part of Saudi Arabia. However, they mentioned that the curve number method should be considered as the optimum flood modeling approach when the topography, land use, meteorological and geological datasets are available. Sharif et al. [51] produced a flood

hazard map for the rapidly urbanizing catchment of Al-Aysen in Riyadh, Saudi Arabia, using hydrologic/hydraulic model simulation. They also studied the impact of urbanization on the peak discharge and runoff volume resulting from different storms with various urbanization scenarios.

Hafar Al-Batin city, like many other cities in Saudi Arabia, has never had a comprehensive set of flood inundation maps. This study will investigate the risk of flood to the city of Hafar Al-Batin by constructing hydrologic, hydraulic and floodplain delineation models for the investigated region. Then, based on the constructed models, flood hazard maps will be generated to identify the areas within the city at high risk.

CHAPTER 3

STUDY AREA AND DATA ACQUISITION

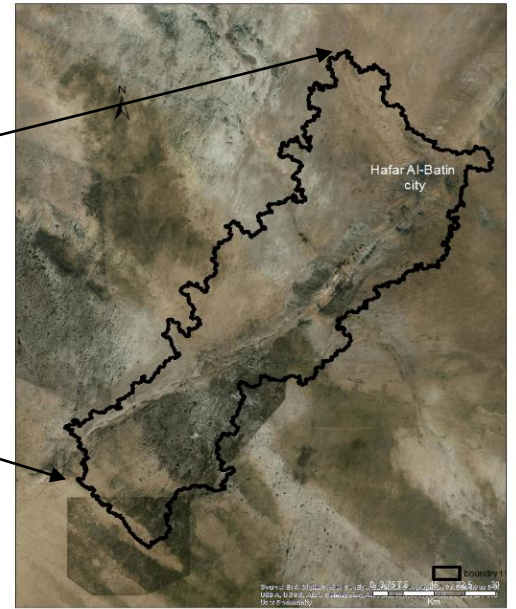
3.1 The Study Area

Hafar Al-Batin is one of many cities in Saudi Arabia, which were affected by flash floods. It is located in the northeast of Saudi Arabia, 430 km to the north of Riyadh, 74.3 km from the Iraq border, and 94.2 km from the Kuwait border. The city lies in the dry valley of Wadi Al-Batin, which is the main source of the flash flood. In 2003, the population of Hafar Al-Batin was estimated to be around 190,000 and reached 600,000 in 2010 [52]. Figure 3.1 shows the location of Hafar Al-Batin city and boundary of Hafar Al-Batin watershed.

The partially urbanized Wadi Al-Batin catchment was selected for this study with a drainage area of 1669.014 km² as shown in Figure 3.1b. The catchment drains in the dry valley of Wadi Al-Batin, which is part of the larger valley of the long, now-dry river Wadi Al-Rummah. The city of Hafar Al-Batin occupies approximately 3.6% of the catchment area.

3.2 The Basin Topography

Figure 3.2 shows Hafar Al-Batin contour map, which was developed from the 30-m resolution digital elevation models (DEM) by using global mapper and surfer programs.



(a)

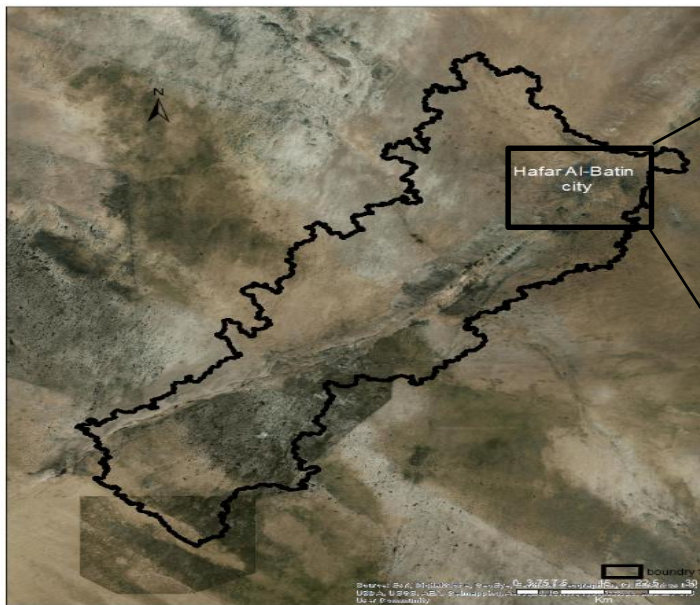
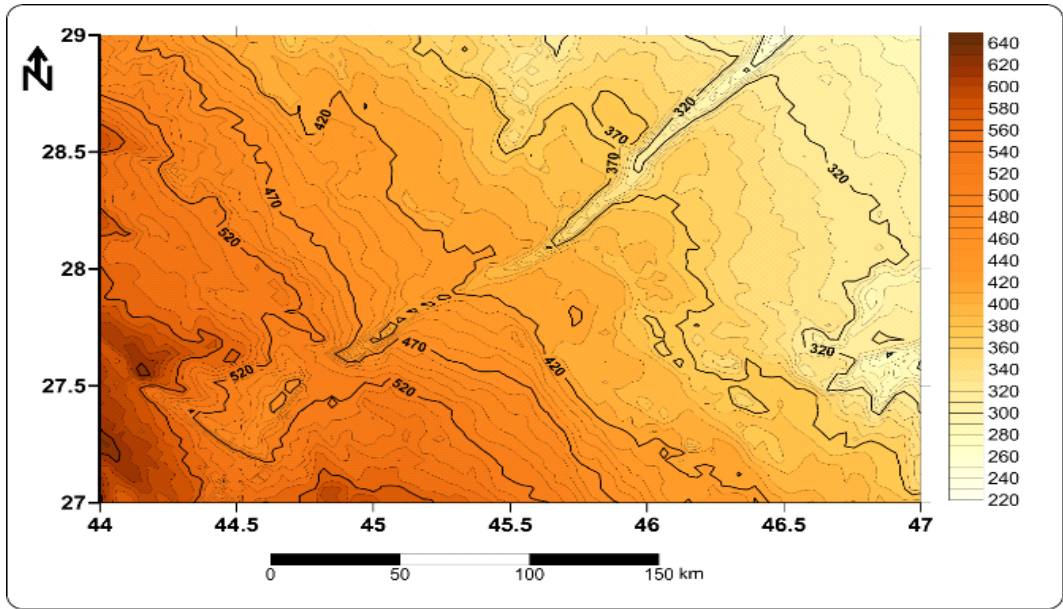
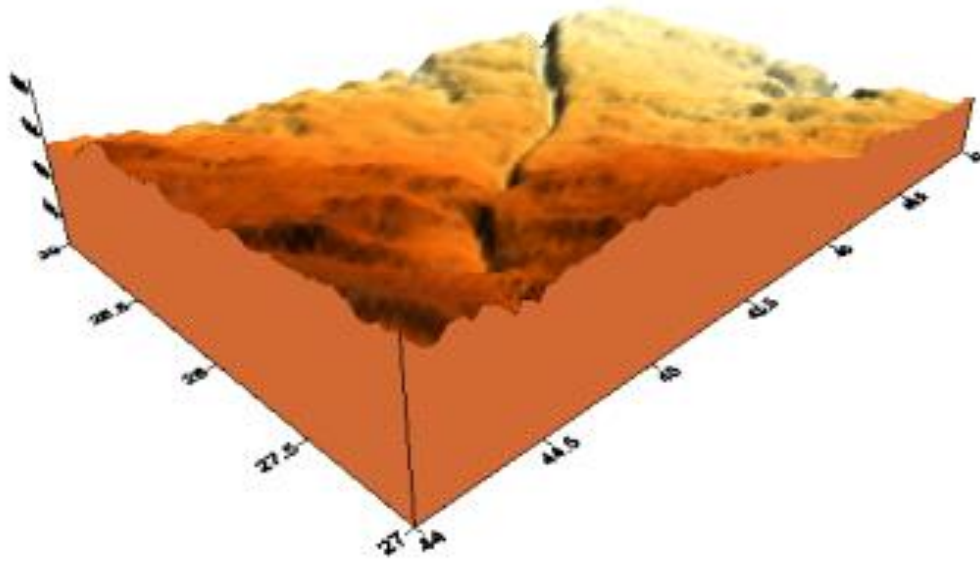


Figure 3.1 Hafar Al-Batin catchment area: (a) Hafar Al-Batin boundary of the watershed and (b) Hafar Al-Batin city



(a)



(b)

Figure 3.2 Hafar Al-Batin topography: (a) Hafar Al-Batin contour map and (b) 3D contour map of Hafar Al-Batin watershed

The lowest point above sea level, located at the northeast of the district, is approximately 200 m, while the highest point above sea level in the district reaches 640 m. The topography of Hafar Al-Batin can be divided into two parts: Al-Batin valley and the northeast slopes.

The 30-m resolution DEM, which was produced by the General Directorate of Military Survey (GDMS), was used to obtain topographic data for the study area (Figure 3.3). Four main streams are distinguished in Hafar Al-Batin district. The first stream runs from southeast to northwest and is called Al-Batin valley, which is the largest one. The second stream is north Fleaj stream which runs from north to south, the third stream is south Fleaj stream which runs from south to north, and the fourth stream is northwest Fleaj which run from northwest to the southeast. These four streams are considered as the main sources of runoff for Al-Batin valley as shown in Figure 3.4.

3.3 Rainfall Data

Precipitation is considered as one of the major input parameters required for hydrologic studies. In Saudi Arabia rainfall is the only form of precipitation. Precipitation data are essential and play an important role in the hydrologic model.

There are seven methods to define the meteorological model in HEC-HMS. One of these methods is the SCS hypothetical storm method which was used in this study for floodplain delineation, while the frequency storm method was used in the sensitivity analysis.

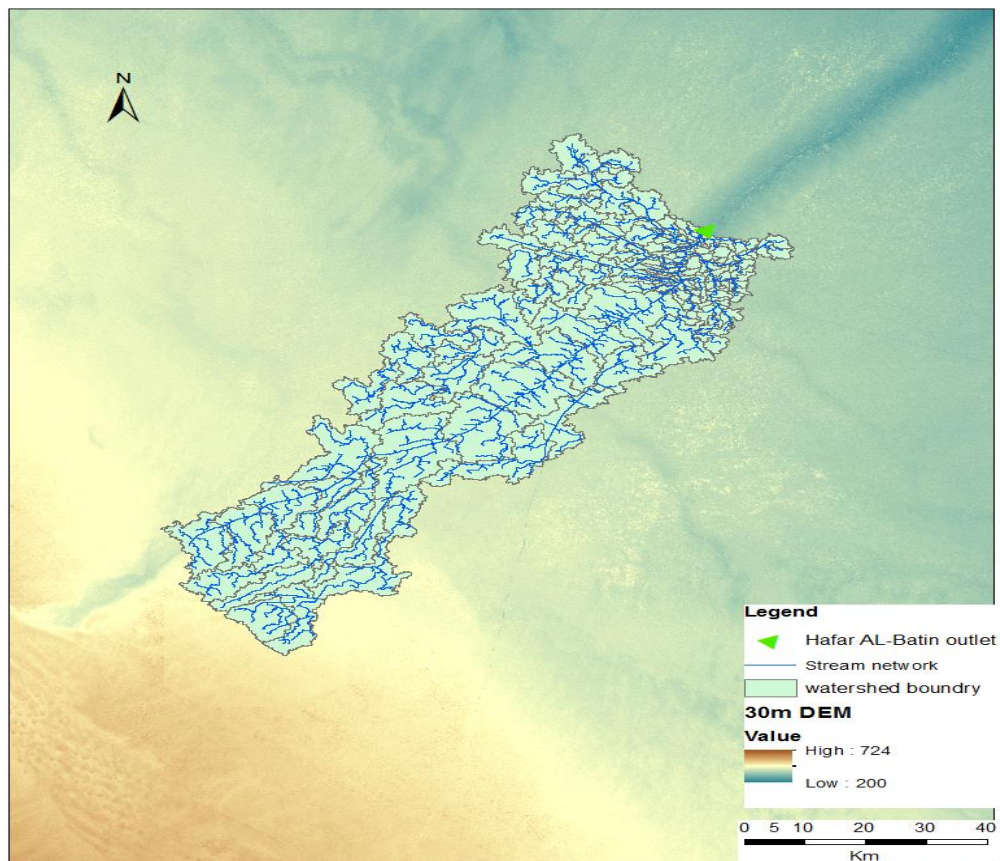


Figure 3.3 Hafar Al-Batin digital elevation model (DEM)

Usually, floods occur due to the extreme rainfall events, which are difficult to collect. Moreover, it is difficult to collect enough data to find the extreme values of rainfall events using the standard techniques of statistics, which makes the use of extreme distributions as the best choice.

The design return period for storm sewers can vary from 2 to 25 years, while for detention basin, it is 50 years, which is also the design value for major highway bridges. For floodplain delineation, a return period of 100 years is used [22].

Figure 3.5 shows the annual rainfall distribution in Saudi Arabia. The average rainfall ranges between 180 and 260 mm in various parts of Wadi Al-Batin and could reach over 240 mm in the study area [54]. In urban hydrology, two types of rainfall are usually required: actual hyetographs and processed data, which are usually frequency information. The 100, 50, 25, 10, 5, and 2-year events are the frequencies analyzed in this study. The 24 hours of the 100-year rainfall depth and a cumulative precipitation time series corresponding to the Soil Conservation Service (SCS) Type II dimensionless unit hydrograph were used in the model to estimate the rainfall events. Table 3.1 shows the design rainfall depths adopted in this study. These depths were estimated based on the IDF curves developed by Elsebaie [55]. Since an actual gauge rainfall was not available to work with, an artificial one was created to find the effectiveness of different storm durations on the peak discharge as will be described in Chapter 5.

2/18/2015

Map_of_Rainfall_Distribution_Saudi Arabia.jpg (1894x1640)

Distribution of Annual Rainfall in Saudi Arabia for a 50 year period (1950-2000)

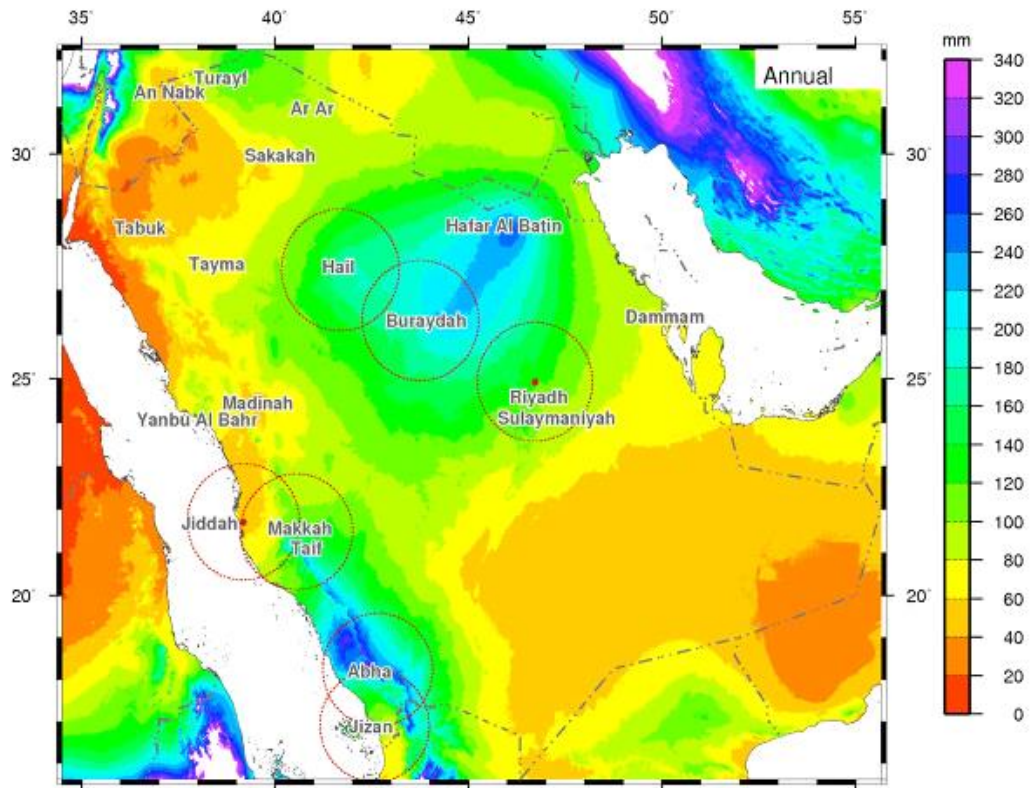


Figure 3.5 Annual rainfall distribution depth for Saudi Arabia [56]

Table 3.1 Design storm for Hafar Al-Batin [55]

Frequency (Years)	Depth (mm)
2	28.754
5	42.297
10	51.263
25	62.593
50	70.997
100	79.34

3.4 Methodology

In this study, Watershed Modeling System (WMS), Geographic Information System (GIS), AutoCAD, global mapper, Surfer-12, FlowMaster, HEC-HMS, and Hydrologic Engineering Center-River Analysis System (HEC-RAS) were used to construct the hydrologic, hydraulic and floodplain models.

The following steps summarize the methodology that was followed in this study:

1. Use the IDF curves for Hafar Al-Batin to determine the maximum rainfall intensity for specific return periods.
2. Generate Digital Elevation Map (DEM) for the study area.
3. Delineate the watershed, which depends on the generated flow directions and accumulation map.
4. Use an appropriate Hydrologic Modeling System (HEC-HMS) to establish a hydrologic model for Hafar Al-Batin.
5. Develop a hydraulic model for Hafar Al-Batin watershed using HEC-RAS.
6. Propose appropriate actions that can be taken to reduce the risk of flood.

CHAPTER 4

HYDROLOGIC AND HYDRAULIC MODELING

USING WMS – RESULTS AND ANALYSIS

Floodplain delineation is a difficult task because it involves an interaction of models and variables to determine a floodplain boundary for a specific return period. To delineate the floodplain, hydrologic, hydraulic and water surface interpolation models should be integrated. Figure 4.1 shows a summary of the steps involved in floodplain delineation. The delineated watershed of Hafar Al-Batin and the streams contributing to Hafar Al-Batin catchment are shown in Figures 4.2 and 4.3, respectively [57]. These streams will help as a guide to determine the boundary of the watershed. In this study, a hydrologic model using HEC-HMS, a hydraulic model using HEC-RAS, and a floodplain delineation model using WMS have been used to develop a flood hazard map for Hafar Al-Batin catchment area.

4.1 Hydrologic Model (HEC-HMS)

The HEC-HMS program was developed by the Hydrologic Engineering Center, U.S. Army Corps of Engineers to simulate precipitation-runoff processes with many choices of infiltration losses [58]. The USDA Soil Conservation Service runoff curve number method (SCS-CN) is used to compute peak flows based on the soil type, land use and

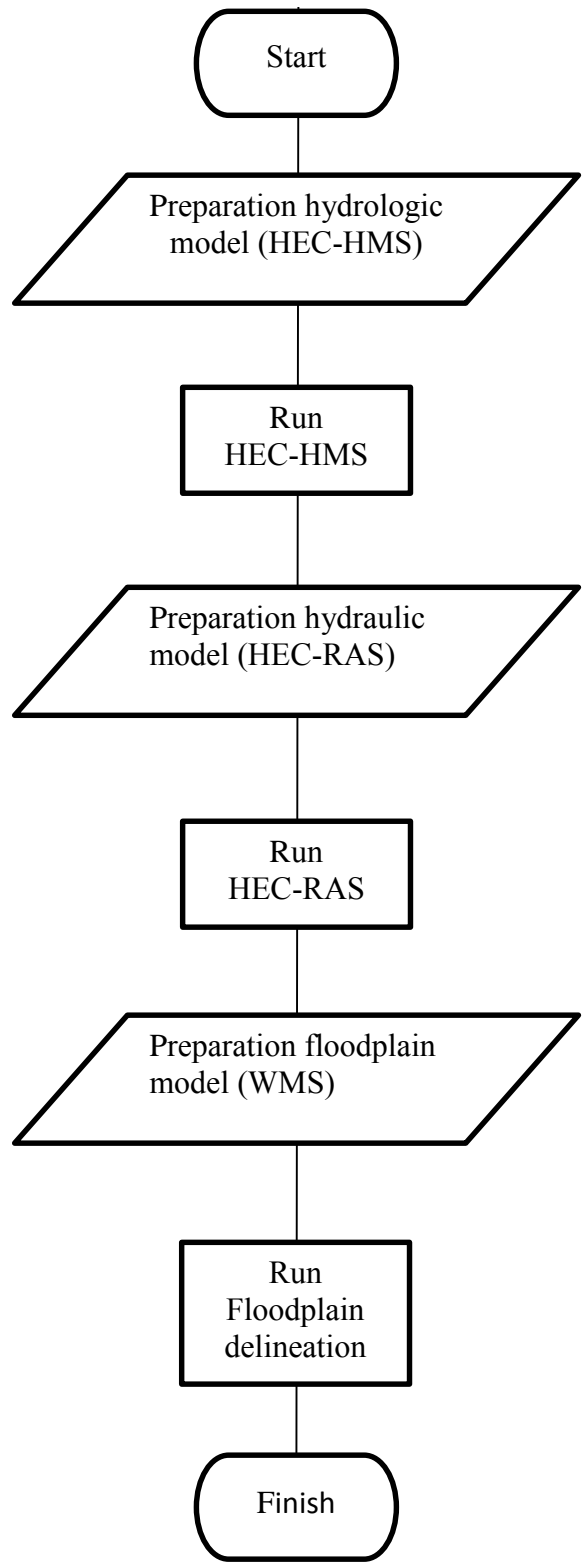


Figure 4.1 Flow chart of the steps involved in floodplain analysis

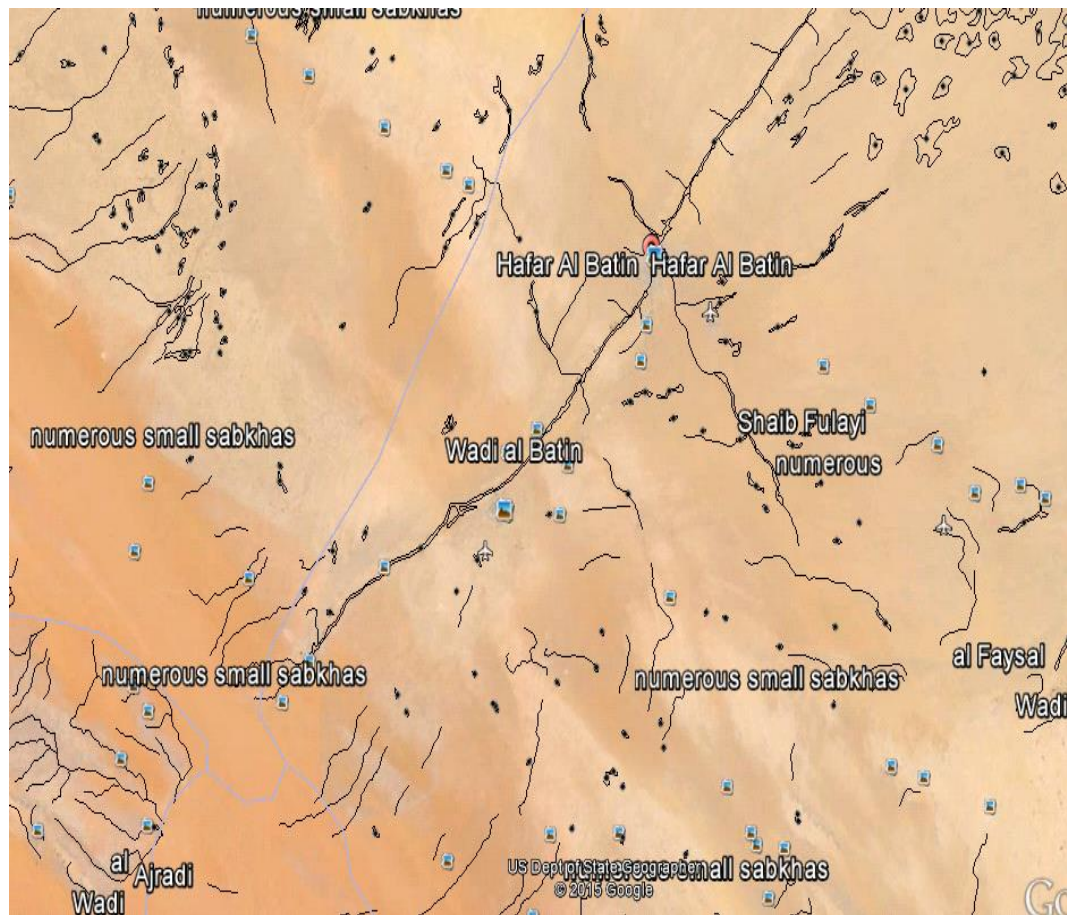


Figure 4.3 Hafar Al-Batin approximate streams [57]

hydrologic soil group [59]. The SCS-CN is widely used in arid regions and semi-arid regions. It has high accuracy in catchments where flood observations are not available, and it is also the most popular method to find the volumes of the runoff [60, 61].

The USDA Soil Conservation Service runoff curve number method is used by many models to find the volumes of the runoff peak flows [59], which can be expressed as:

$$Q_r = \frac{(P - 0.2S_r)^2}{P + 0.8S_r} \quad (4.1)$$

$$S_r = \frac{25400}{CN} - 254 \quad (4.2)$$

$$Q_p = 2.08 \frac{A}{T_p} \quad (4.3)$$

$$T_p = \frac{\Delta t}{2} + t_{lag} \quad (4.4)$$

where Q_r = direct runoff (mm), P = rainfall (mm), S_r = potential difference between direct runoff and rainfall (mm), CN = curve number, Q_p = the peak discharge for one unit of rainfall excess (m^3/s), A = the drainage area (km^2), T_p = the time of rise of the flood hydrograph (hours), Δt = the excess precipitation duration (hours), and t_{lag} = lag time (hours).

Obtaining the elevation data is the first step to develop the hydrologic model, which is very important in delineating the watershed and computing the basin parameters such as watershed area, concentration time, lag time, centroid, and slope. The 30-m resolution DEM was previously downloaded from the United States Geological Survey (USGS), which was then prepared by the Geographic Information System (GIS).

Due to the large size of the study area, about 1669.014 km², the catchment area was divided into three main parts, and each part was divided into sub-basins with different sizes. These three parts are upstream with large size sub-basins, middle with medium size sub-basins, and downstream, which includes Hafar Al-Batin city, with small size sub-basins to get more and accurate details due to the importance of this part.

The DEM was imported to the WMS after converting it to UTM coordinates to delineate the watershed and the sub-basin boundaries. TOPAZ software was run to compute flow directions and flow accumulations. After that, the stream network was computed. Next, the WMS delineated the watershed boundary after defining an outlet point at the required location of the stream network. To delineate the sub-basin boundaries, more outlet points, about 182, were defined, which takes into account the changes in the land use, soil type, and the catchment topography. This large number of sub-basin can help to estimate flooding over the whole catchment and not only at the catchment outlet. The WMS delineated the sub-basin boundaries from these outlet points and computed the geometric parameters (Appendix I), which were used as an input for the HEC-HMS model. Figure 4.4 shows Hafar Al-Batin watershed after delineation. The next step is to estimate the surface runoff due to a specified rainfall storm using the SCS method. Land use and soil data for the study area were extracted from the watershed modeling system (WMS), which were then prepared by the GIS program. Soil and land use data were imported to WMS, which combined them with a table relating land use and soil types to compute the curve numbers (CNs) for each sub-basin in the watershed. These CNs will be used as input in the SCS method to estimate the runoff.

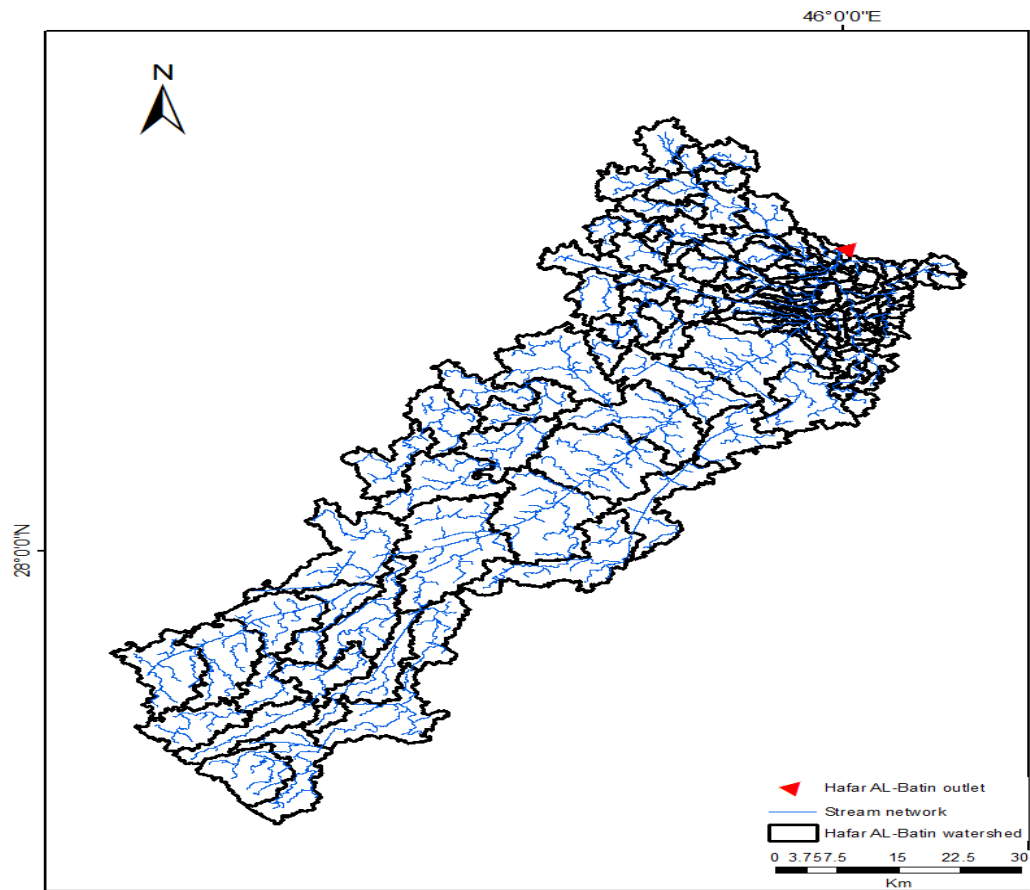


Figure 4.4 Delineation of Hafar Al-Batin watershed

Depending on the geometric parameters and the land use and soil type data, WMS and HEC-GeoHMS were integrated to compute the composite CNs, as shown in Table 4.1 and Figure 4.5, for HEC-HMS.

Appendix II summarizes the CN values for various combinations of hydrologic soil group and land use. Also, the table shows the area for each sub-basin, which was used by WMS to compute the lag time and the time of concentration for each sub-basin. The basin lag time for each sub-basin was calculated using SCS according to the following relation [62]:

$$L = \frac{2.587l^{0.8} \left(\frac{1000}{CN} - 9\right)^{0.7}}{1900y^{0.5}} \quad (4.5)$$

where L = lag time (hour), l = hydraulic length of catchment (m), CN = runoff curve number, and y = average watershed land slope (%).

The SCS hypothetical storm method implements four synthetic rainfall distributions developed by the Natural Resources Conservation Service (NRCS) based on the observed precipitation events. Each distribution contains rainfall intensities arranged to maximize the peak runoff for a given total storm depth. The four distributions correspond to different geographic regions [59]. The estimated discharges for Wadi Al-Batin were calculated for the following return periods: 100, 50, 25, 10, 5, and 2 years. Figure 4.6a shows the hourly distribution of 24 hours corresponding to a return period of 100 years for Hafar Al-Batin catchment area based on the Type II rainfall distribution of the Natural Resources Conservation Service (NRCS), which is suitable for arid and semi-arid regions. Figure 4.6b shows the 1-hour hyetograph of the 100, 50, 25, 10, 5, and 2-year return periods.

Table 4.1 Runoff curve numbers for hydrologic soil group [62]

Land use	Curve number for hydrologic soil group			
	A	B	C	D
Residential	75	80	85	90
Desert shrubs	55	68	80	86

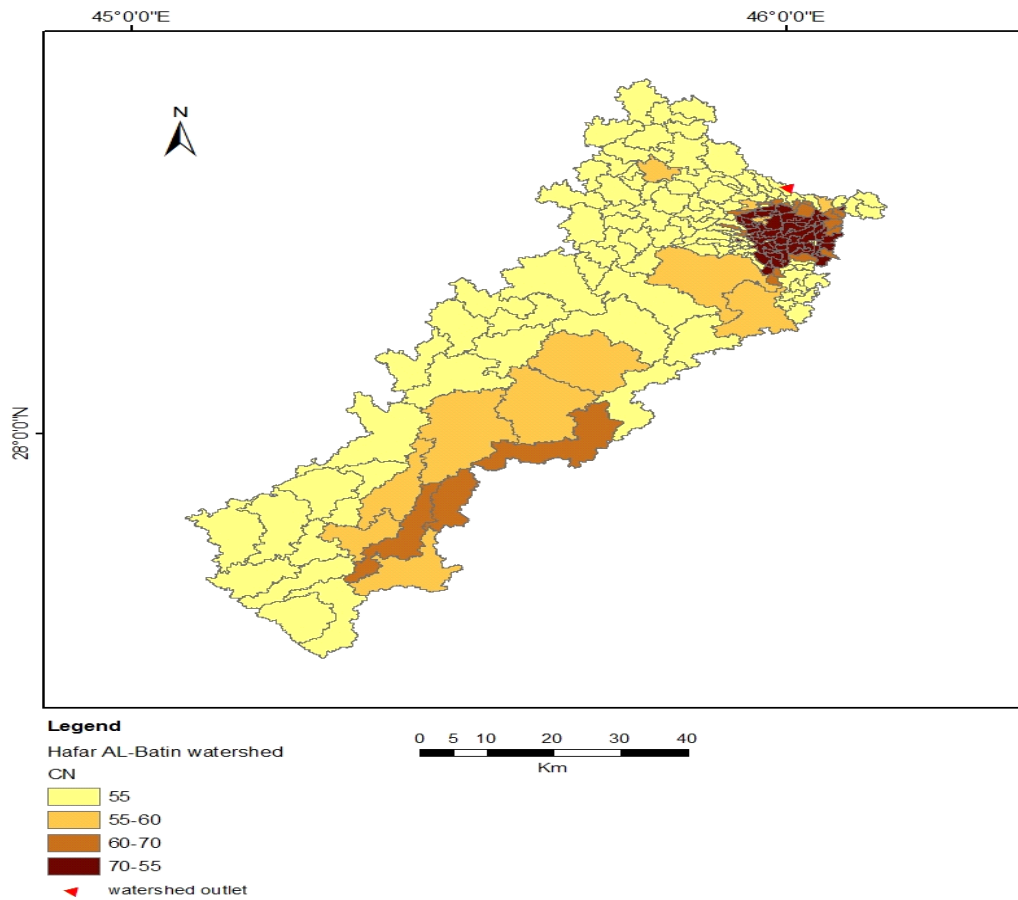
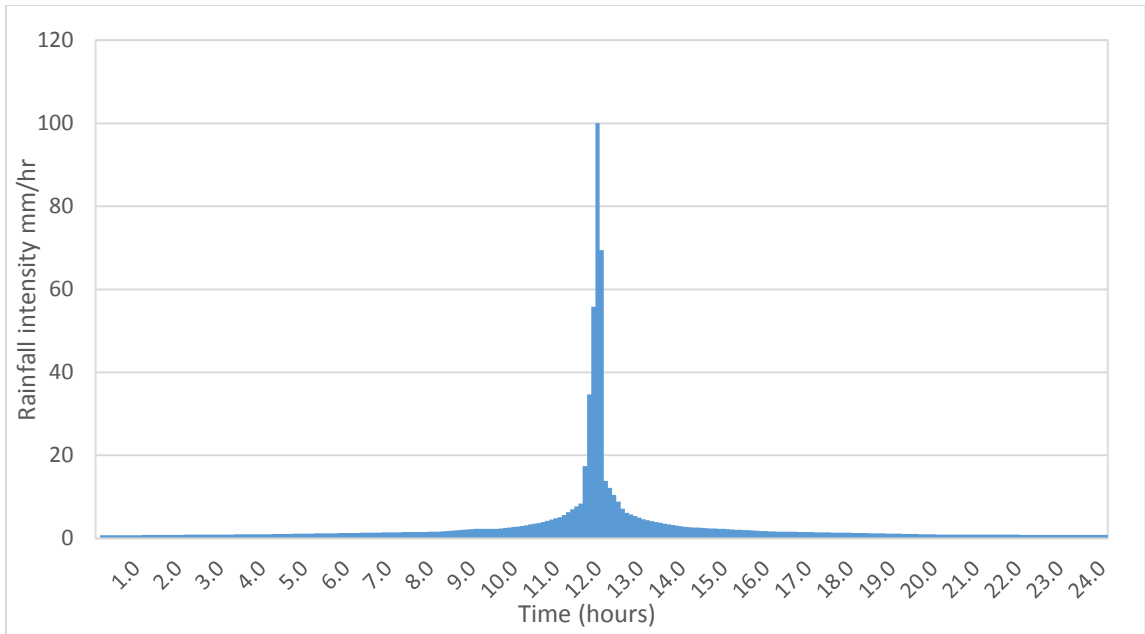
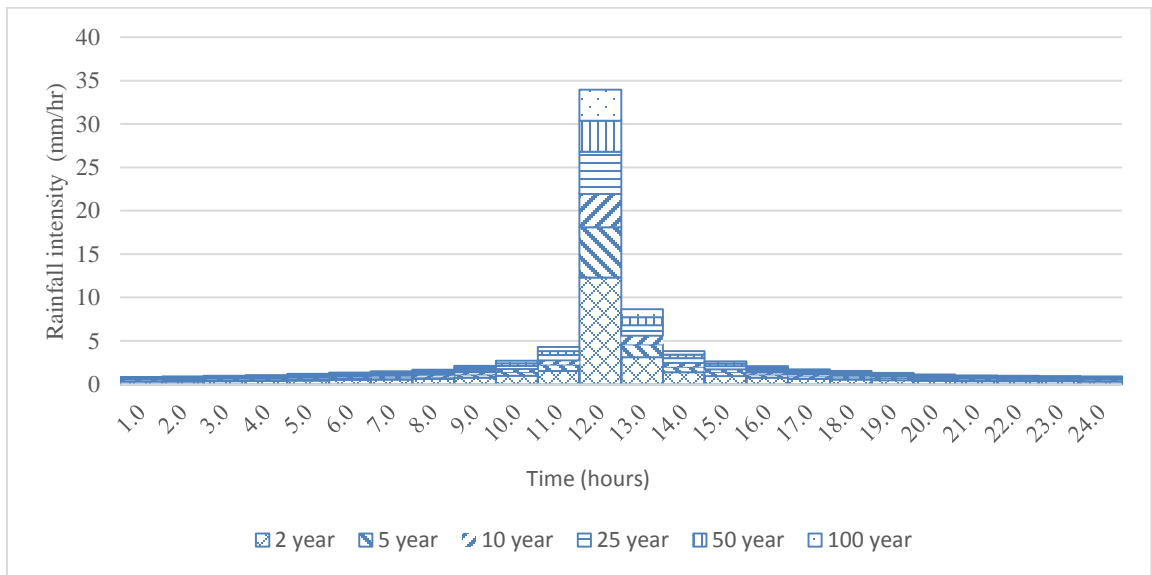


Figure 4.5 Hafar Al-Batin watershed classified by curve number



(a)



(b)

Figure 4.6 Rainfall hyetograph: (a) the 6-minute hyetograph of the 100-year storm (storm total is 79.34 mm) and (b) the 1-hour hyetograph of the 2, 5, 10, 25, 50, and 100-year storms

The 6-minute resolution of time intervals was used as rainfall input in HEC-HMS, which can give the highest possible level of accuracy.

All required data needed to run HEC-HMS were saved in a specific file. These data were imported by HEC-HMS as shown in Figure 4.7, and the model was run successfully. Appendix III shows the peak discharges for each sub-basin. Figure 4.8 shows the hydrograph at the outlet of Hafar Al-Batin watershed for 100, 50, 25, 10, 5, and 2-year return periods. From the figure, it can be noticed that the second peak is higher than the first peak in the 100-year return period, but in the remaining return periods, the first peak discharge is higher than the second peak. This is due to the amount of the rainfall for the 100-year return period, which is large enough to allow the whole catchment area to contribute to the outflow hydrograph. In other words, the infiltration in the upstream sub-basins, which are far from the watershed outlet, is higher than the rainfall for all the return periods except for 100 years. Table 4.2 shows the values of peak discharge and runoff volume for different return periods at Hafar Al-Batin watershed outlet.

4.2 Hydraulic Model (HEC-RAS)

HEC-RAS, which is considered as a powerful program, has been used widely in hydraulic simulation and floodplain studies [63]. It is also used to model one-dimensional steady and unsteady river flow and is capable of simulating many types of hydraulic structures. Three main equations (continuity, energy, and Manning equations) are used in HEC-RAS to determine water depths and water surface elevations, based on which flood mapping and floodplain delineation can be performed.

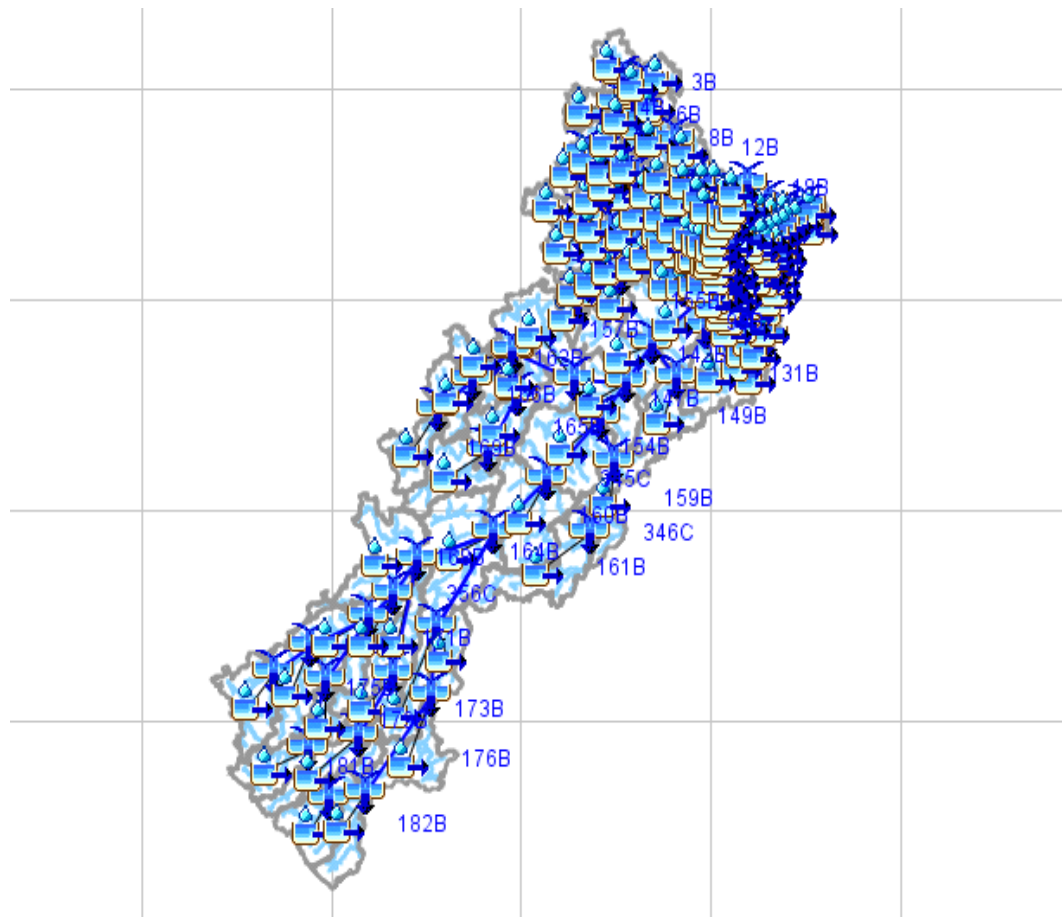
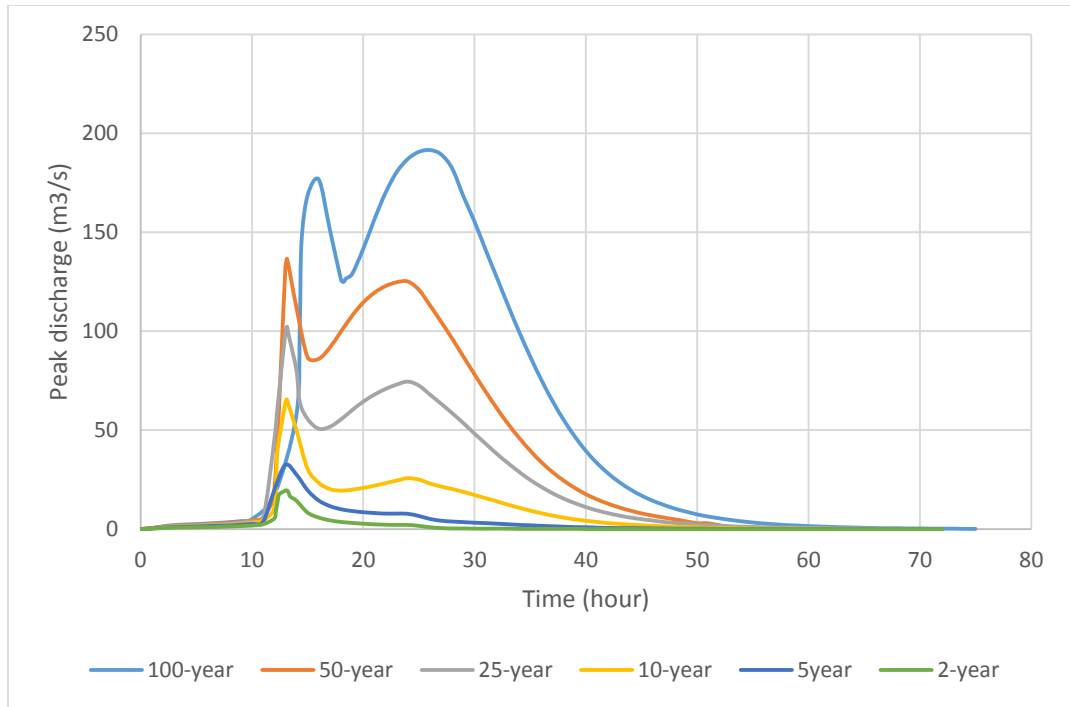
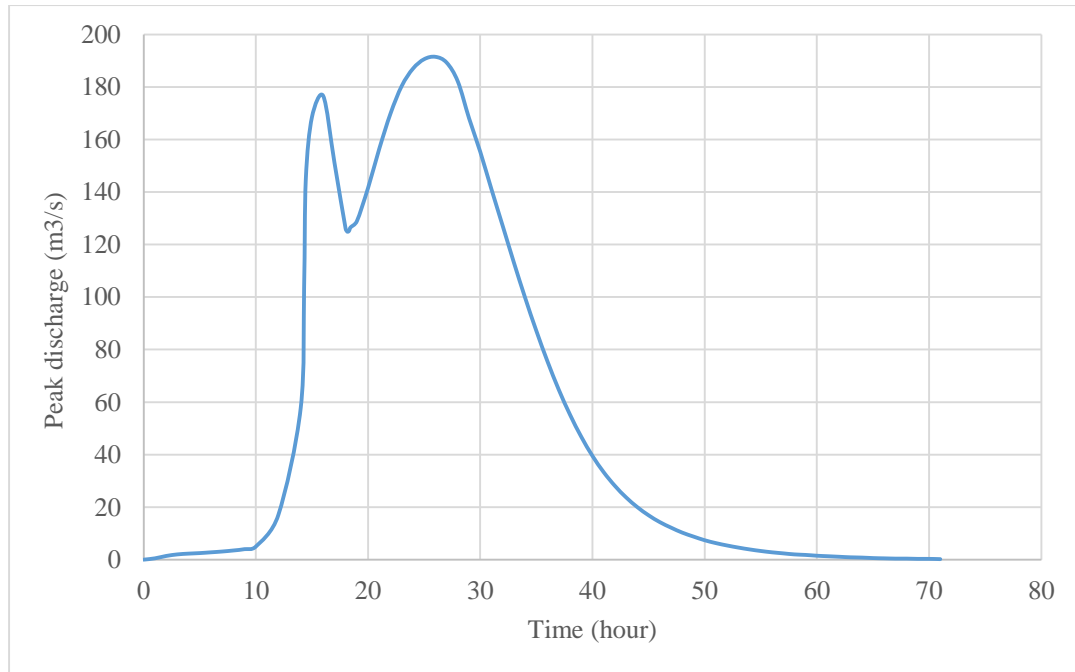


Figure 4.7 HEC-HMS basin model of Hafar Al-Batin watershed



(a)



(b)

Figure 4.8 Hafar Al-Batin outlet hydrograph: (a) for different return periods and (b) for 100-year storm runoff

Table 4.2 Peak discharge, runoff volume, and runoff coefficient of Hafar Al-Batin outlet

Item	Return period (year)					
	2	5	10	25	50	100
Peak discharge (m ³ /s)	19.6	42.7	65.6	102.3	136.7	191.5
Runoff volume (m ³)	329700	904900	2206900	5456400	8876700	13016600

Generally, water surface elevation at a location in a floodplain is a more direct interest for flood analysis than the magnitude of discharge. Water elevation is determined by a hydraulic analysis, which is often performed subsequent to a hydrologic analysis.

Hydraulic model (HEC-RAS) requires identification of watershed boundary and surface roughness values. For this purpose, HEC-RAS data were prepared using WMS and HEC-GeoRAS software. The first step in the hydraulic simulation is to get the watershed elevation data, which can be obtained from the digital elevation map (DEM). However, the resolution of the DEM used in this study is 30 m, which does not include bathymetry and may give an inaccurate hydraulic model. To overcome any expected missing data when using DEM, a new method called light detection and ranging (LIDAR)-survey triangulated irregular networks (TINs), developed by the researchers to provide data at a very high resolution, was used [64]. However, this method gives more points, more than what is required, which makes data filtering technique necessary. Omer et al. [65] used data filtering technique with a filter angle of 4 degrees, where they found that this value can be used without affecting the hydraulic or floodplain model results. In this study, a filter angle of 5 degrees was used, which does not affect the results of the floodplain model. The method generates too many triangles, approximately more than 1.5 million, which makes the contour lines impossible to be displayed and does not give a clear picture about the inundated area. This problem can be solved by using different values of filter angle until reaching a suitable value that makes the filled contours possible to be displayed and at the same time does not affect the output of the floodplain model. Figure 4.9 shows the final TIN network of the investigated catchment, which was used to extract the cross sections for the purpose of hydraulic simulation using HEC-RAS model.

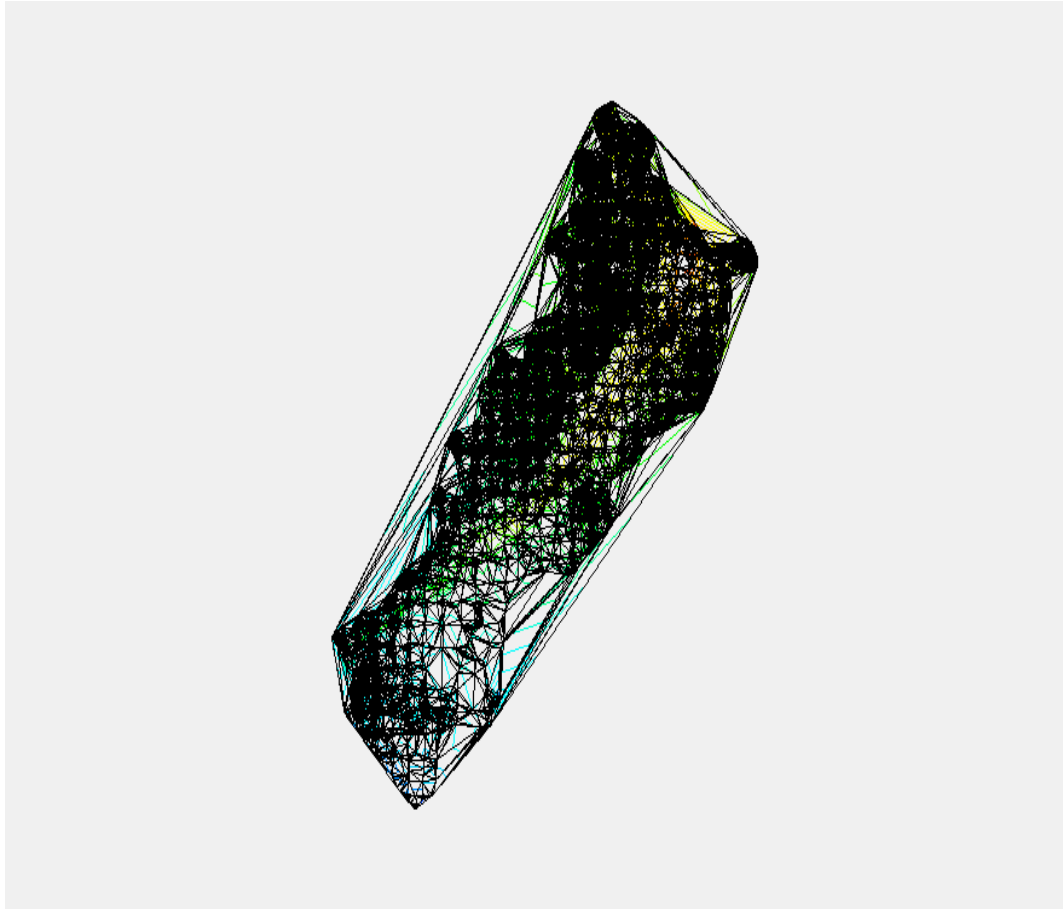


Figure 4.9 TIN map for Hafar Al-Batin watershed

Roughness values are one of the input requirements of HEC-RAS, so surface type was designated to different areas in the constructed model depending on the channel type and land use, and then each surface was assigned with the proper roughness value. The most important part of the map in HEC-RAS is the cross sections where most of the model input data are associated with. Moreover, at the cross sections, solutions or outputs are generated. At least two cross sections on each reach were considered. These cross sections should be perpendicular with the expected flow path and extend across the entire floodplain [63]. In this study, the AutoCAD program was used as the best choice to construct the cross sections at a specific distance, which can be considered much better than using WMS to develop the cross section manually and at an arbitrary distance. Figure 4.10 shows the geometry of the hydraulic model with the wadi reaches and cross sections.

Next, any required boundary condition should be entered to establish the starting water surface at the ends of the wadi channel. This starting water surface is used by HEC-RAS to start the calculation. In this study, the normal depth was assumed to be the boundary condition at the downstream of Hafar Al-Batin wadi. Then, the generated peak discharges using HEC-HMS (Appendix IV) were entered manually into HEC-RAS. The outputs of HEC-RAS simulations were extracted by WMS and used to determine the floodplain boundary. Figure 4.11 shows the water levels for return periods of 2, 5, 10, 25, 50, and 100 years, while Figure 4.12 represents water surface levels at different cross sections along the main channel. Water level analysis shows that the most affected reaches are those located inside the city.

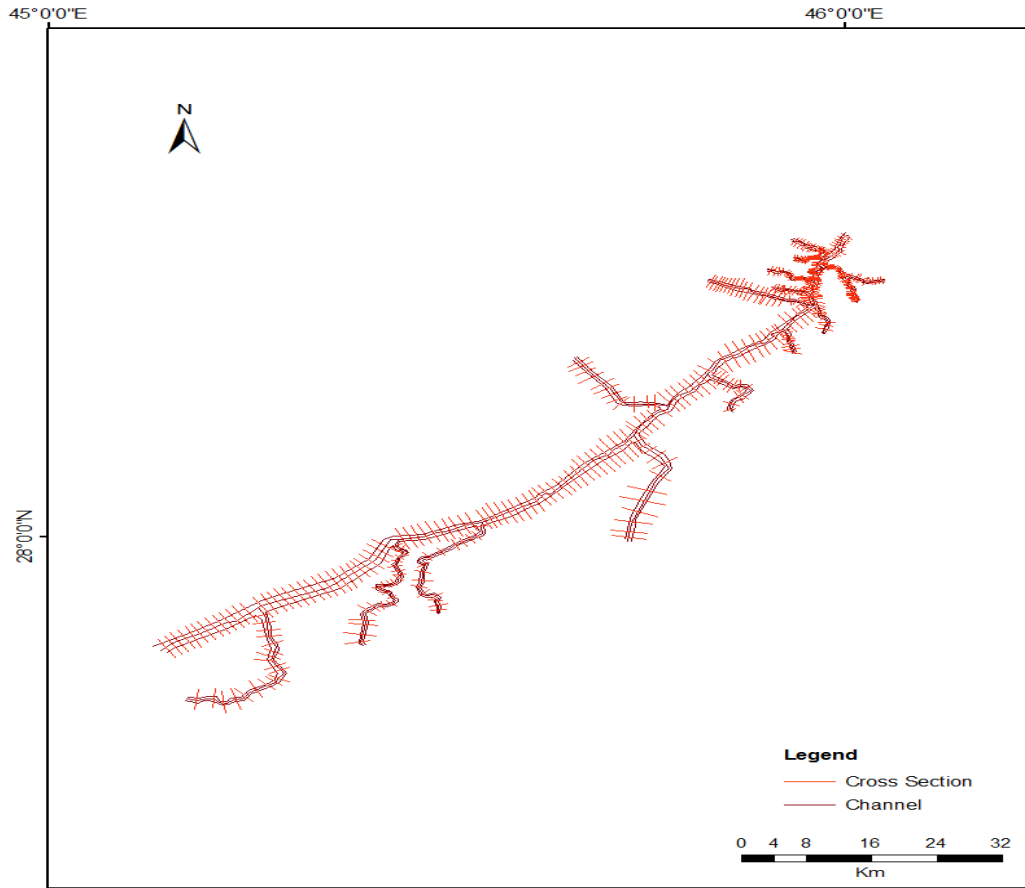
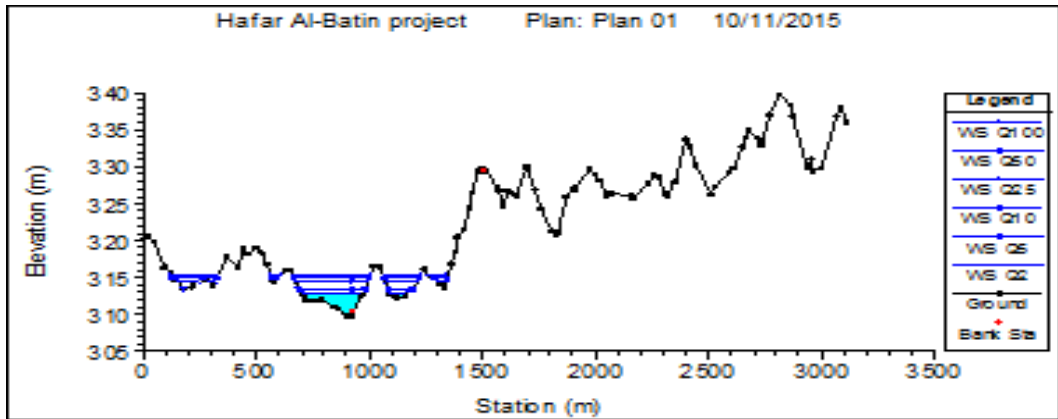
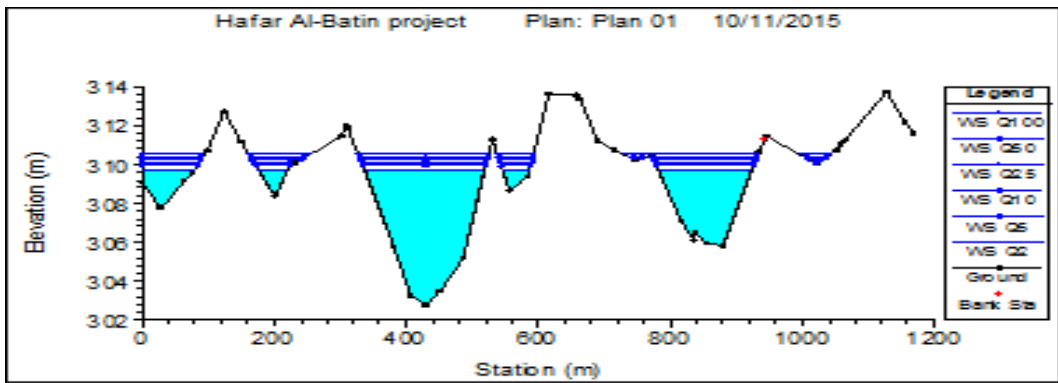


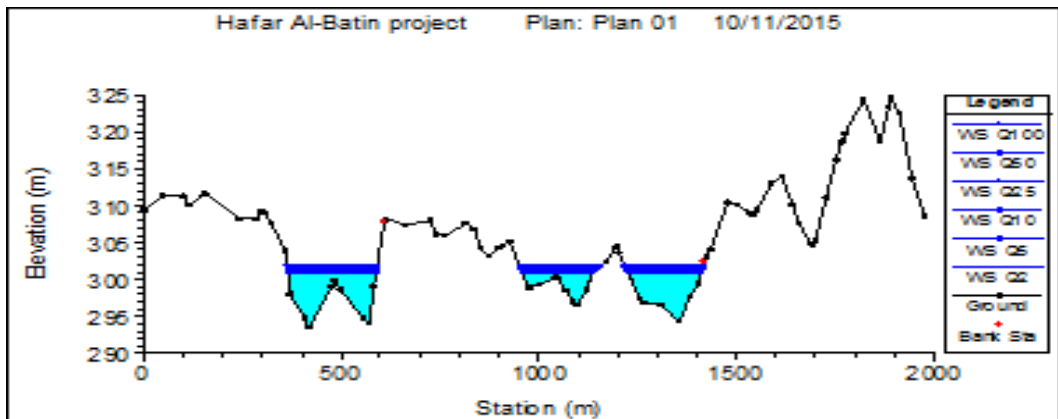
Figure 4.10 Main reaches and sections along the main reach of Hafar Al-Batin watershed



(a)



(b)



(c)

Figure 4.12 Water surface elevation at different cross sections along the main reach for different return periods: (a) city entrance, (b) middle of the city, and (c) end of the city (outlet)

Starting from the city entrance point to the outlet downstream, flood exceeds the bank levels of the existing channel for most of the return periods as shown in Figure 4.13.

4.3 Floodplain Delineation Model

Watershed Modeling System (WMS) is an integral program for developing watershed computer models that support 2D hydrologic modeling, regression, and lumped parameter of watersheds. It supports river hydraulic and storm drain models such as HEC-1, HEC-HMS, HEC-RAS, TR-55, TR-20, NFF, HSPF, Rational MODRAT, GSSHA, CE-QUAL-W2, EPA SWMM, SMPDBK, and other models [42, 66, 67, 68].

Floodplain delineation using WMS requires identification of the water depths at each section along the channel. For this purpose, a file containing the water depths resulting from HEC-RAS, needs to be imported to WMS. The scatter points which contain the water surface elevations were interpolated at a 60-m spacing along the wadi centerline and cross sections to achieve more accurate floodplain delineation. Then, the interpolated data was used as input data to the floodplain delineation models by switching to the terrain data module which has the floodplain process and delineation. For this purpose, 1000 m max search radius (the maximum search radius defines the limiting distance that will be used when collecting the nearest stage scatter points) and 4 numbers of stages (which were used for interpolation) were selected for the project, which have been used after many trials with different values.

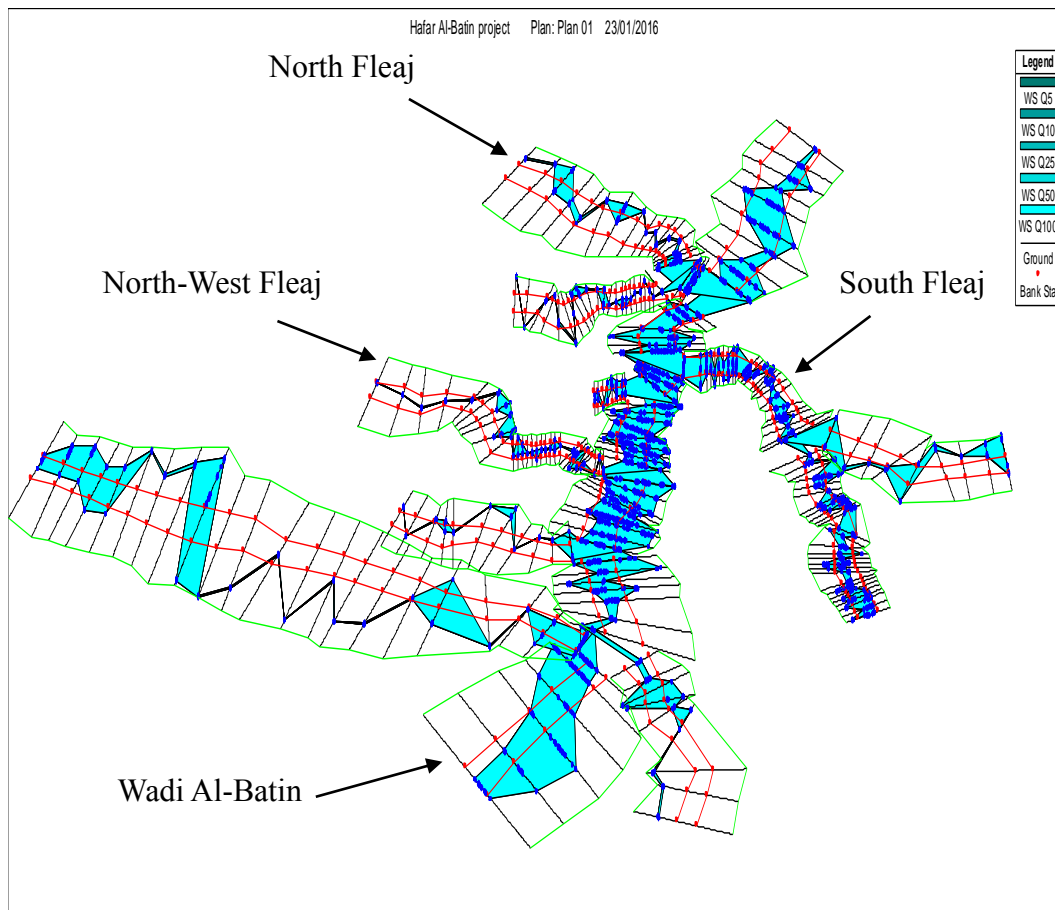
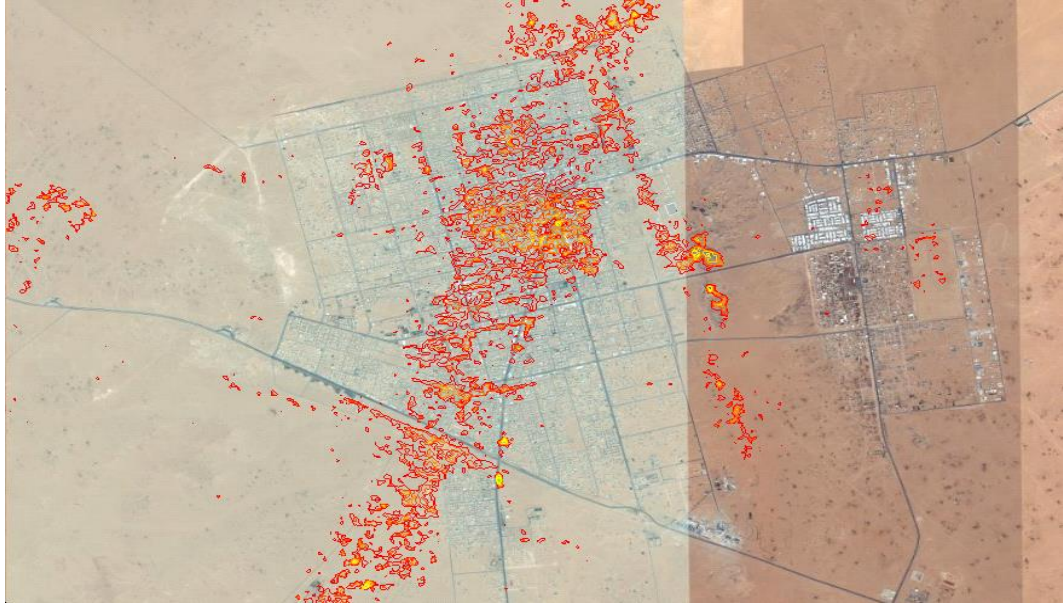


Figure 4.13 Perspective plot of Hafar Al-Batin city

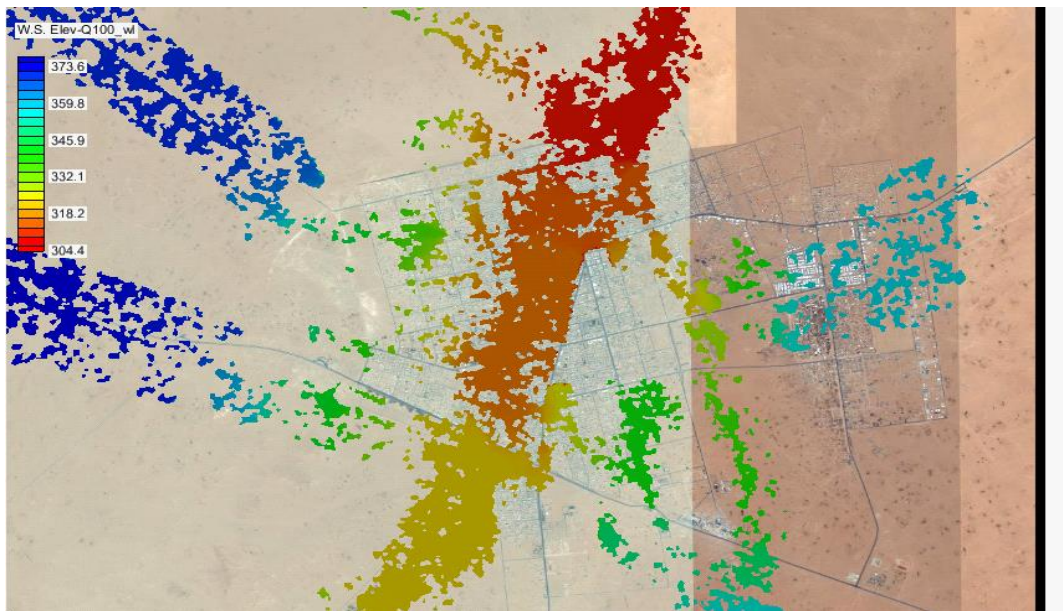
In this step, two new datasets which are water surface elevations and floodplain depths (flood depth and river bed elevation) were computed. These datasets are named W.S. Elev-PF 1 (fd) which represents the flood depth and W.S. Elev-PF 1 (wl) which represents the water surface elevation. Finally, the inundated areas were presented as flood polygons in a developed flood hazard map as shown in Figure 4.14, which represent the flood depth values and the water elevation values, respectively, for a return period of 100 years.

Figure 4.15 shows the flood depth values and the water elevation values, respectively, for a return period of 2 years. From Figures 4.14 and 4.15, the inundated areas in the case of 100-year storm are larger than those of 2 years because the amount of the 2-year storm is much less than that for 100 years.

The inundation area resulting from this study was compared with a study conducted by Hafar Al-Batin municipality as shown in Figure 4.16. The figure reveals that the model output based on WMS resulting from this study (Figure 4.16a) and the risk map constructed by Hafar Al-Batin municipality (Figure 4.16b) are matching. This proves the capability of WMS to model flood events and their expected risks to the city of Hafar Al-Batin.



(a)

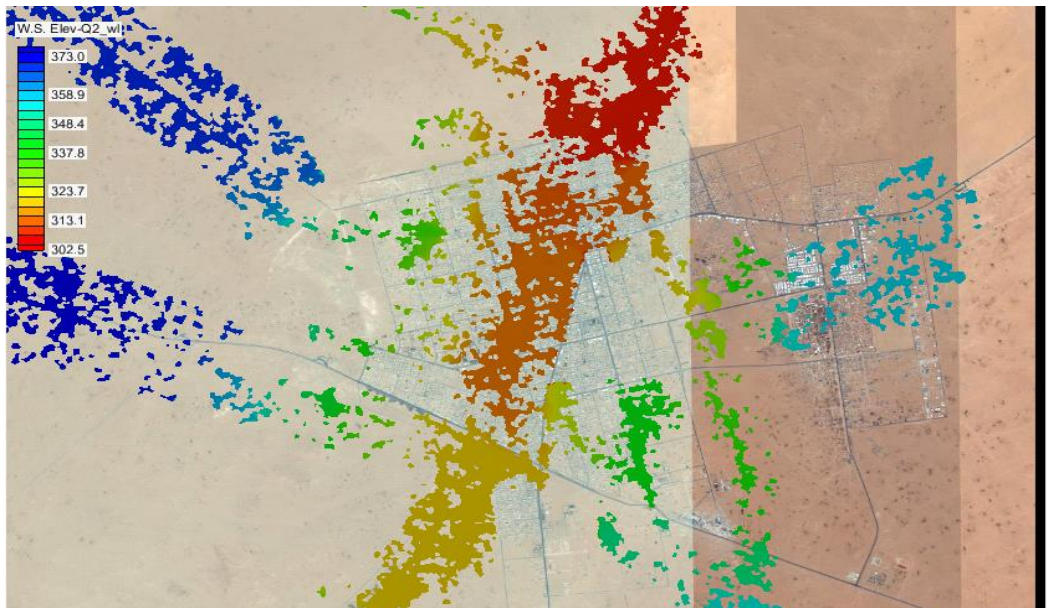


(b)

Figure 4.14 The 100-year floodplain map from WMS: (a) floodplain depths and (b) water surface elevations

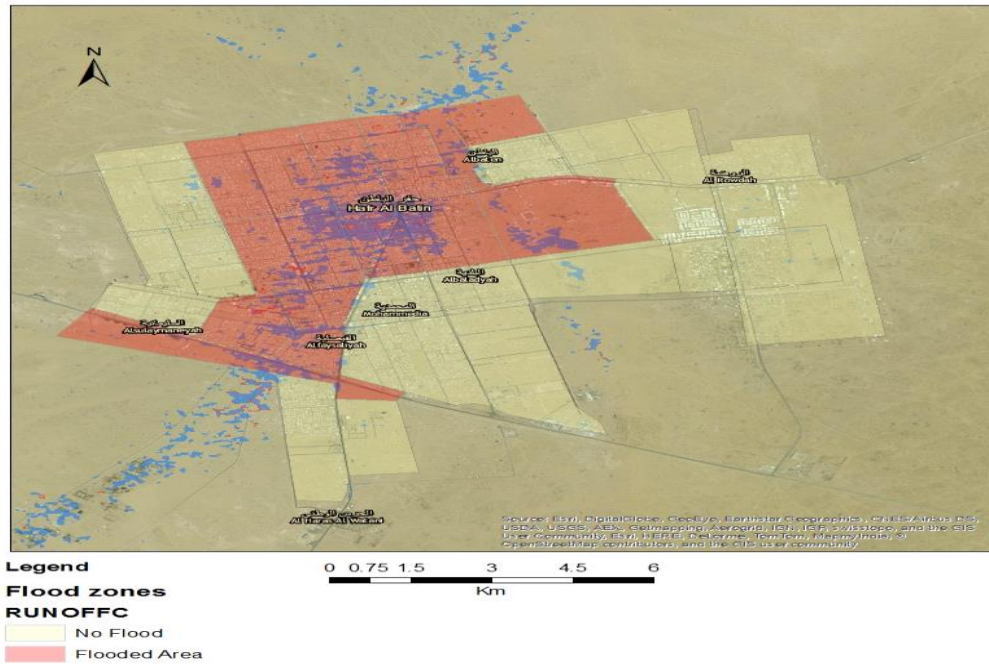


(a)

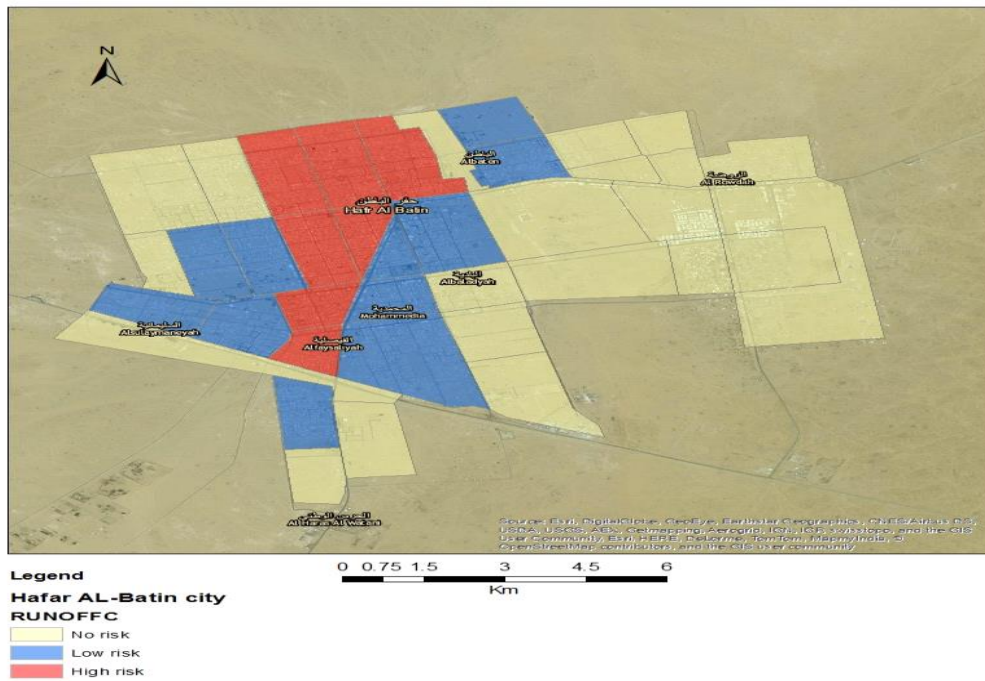


(b)

Figure 4.15 The 2-year floodplain map from WMS: (a) floodplain depths and (b) water surface elevations



(a)



(b)

Figure 4.16 Flood risk map: (a) 100-year flooded area and (b) flooded area developed by Hafar Al-Batin municipality

Geographic information system (GIS) is an effective tool in hazard assessment. In this study, four important factors, which are runoff depth, watershed slope, soil type, and land use, were taken into account to estimate the flood hazard map. Each parameter was valued and weighed according to its contribution in causing a flood. After that, the total sum of the three developed maps was determined to estimate the probability of flood occurrence in the studied area as shown in Figure 4.17. It is clear from the figure that the city of Hafar Al-Batin is located in the high risk regions, which reflects the bad location of the city. Obviously, the CN values, sub-basins slopes, and runoff depth have high values in the city, which makes it within the high risk region.

4.4 Proposed Actions to Control Floods

Recently, flood has become a very serious problem for Hafar Al-Batin city due to its effect on the property and infrastructure of the city in addition to the risk to human lives. Unfortunately, the existing measures to control and resolve the problems associated with flood occurrences adopted by Hafar Al-Batin municipality are not sufficient. This study proposes some actions, based on the output of the constructed models, to control and reduce the effects of floods on the city of Hafar Al-Batin.

According to this study, four main streams contribute to the runoff in the city of Hafar Al-Batin, which are north Fleaj, northwest Fleaj, south Fleaj, and Wadi Al-Batin as shown in Figure 4.18. The contribution of the north Fleaj stream is approximately $18.96 \text{ m}^3/\text{s}$, but as indicated in Figure 4.18, the streamflow does not have any influence on the city of Hafar Al-Batin since most of the runoff is collected outside the city. On the other

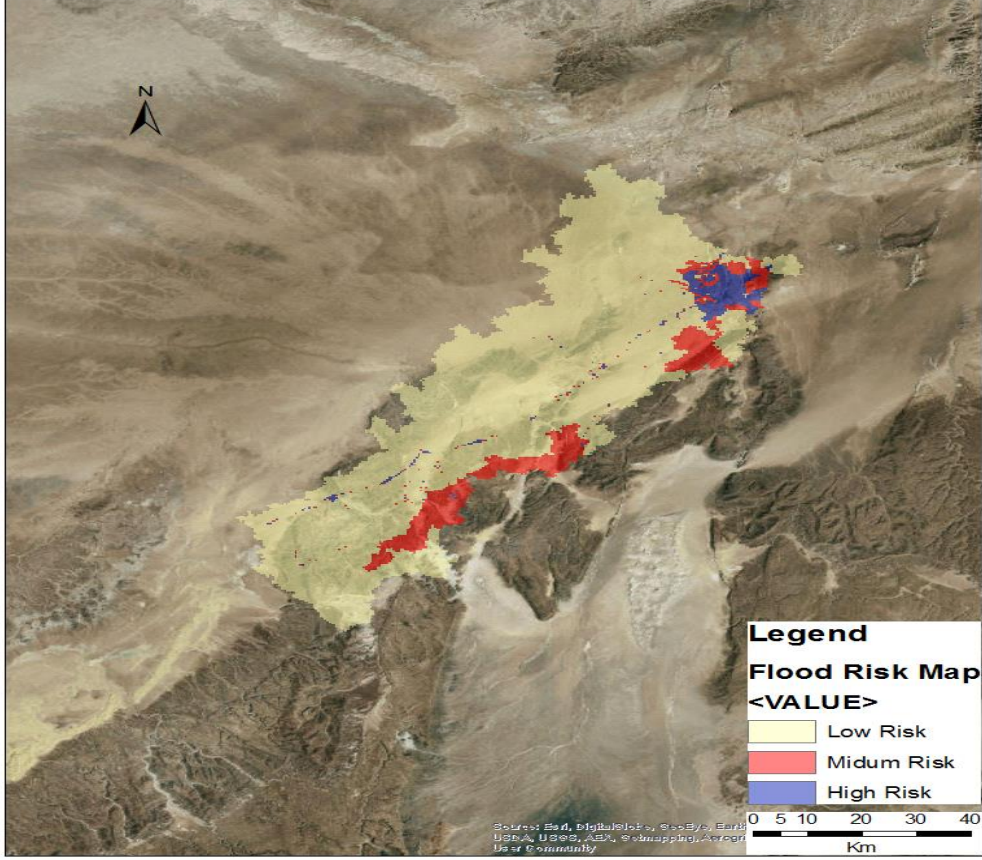


Figure 4.17 Hafar Al-Batin flood risk map

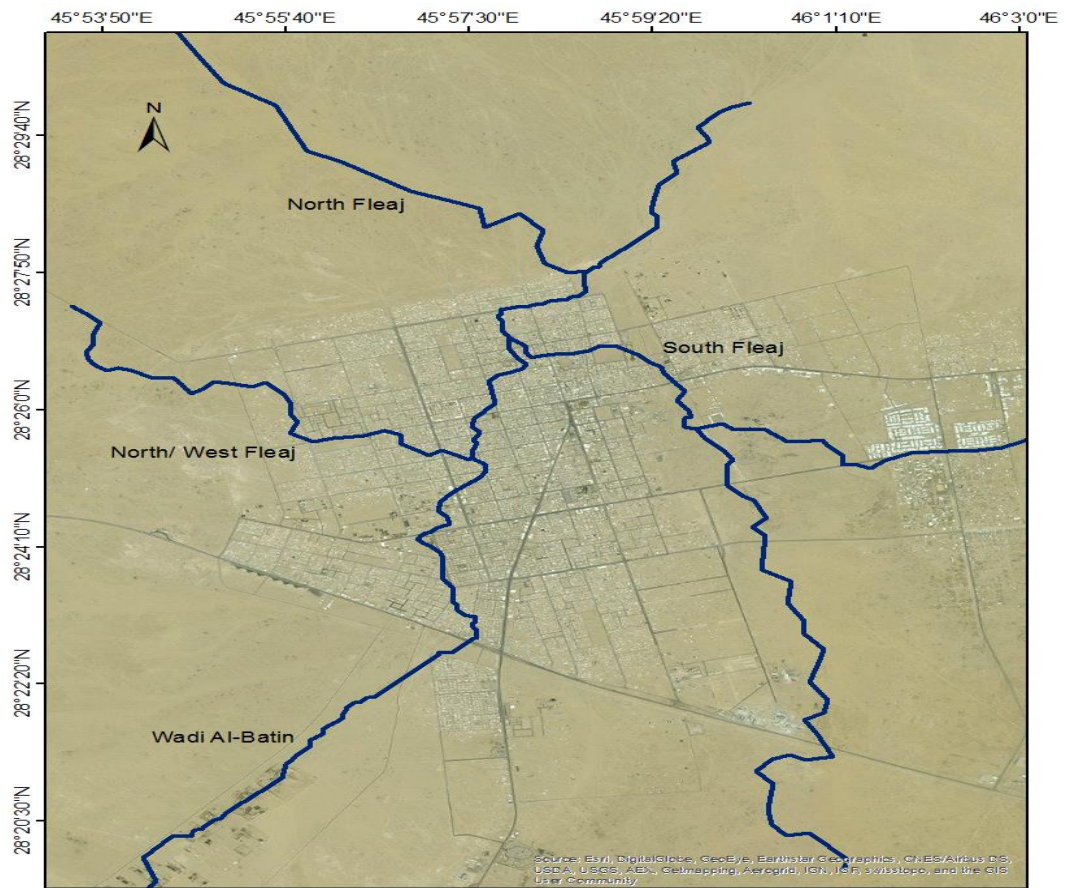


Figure 4.18 Hafar Al-Batin main streams

hand, the flows generated by the other streams will run through the city. The contributions of northwest Fleaj, south Fleaj, and Wadi Al-Batin are $12.16 \text{ m}^3/\text{s}$, $67.12 \text{ m}^3/\text{s}$, and $144 \text{ m}^3/\text{s}$, respectively. These three streams are the main sources of Hafar Al-Batin flood. Based on this summary, the study suggests constructing two trapezoidal channels and a retention pond. The first channel is called the south channel and is located at the south of the city. The second one is called the north channel and is divided into two parts. The first part is at the north of the city and the second is at the east of the city. The locations of the proposed actions are shown in Figure 4.19. The dimensions and characteristics of these channels are presented below.

4.4.1 The south channel

The south channel is a trapezoidal section with a length of 1600 m. FlowMaster software was used to design the channel to carry the discharge of south Fleaj, which is $67.12 \text{ m}^3/\text{s}$. Figure 4.20 shows the details of the proposed cross section.

4.4.2 The north channel

This channel is divided into two parts, the first part with a length of 1200 m and the second part with a length of 6500 m. Accordingly, two trapezoidal channels were designed in the north and east of the city to carry the discharge of north Fleaj, which is $12.16 \text{ m}^3/\text{s}$. Figure 4.21 shows the details of these sections.

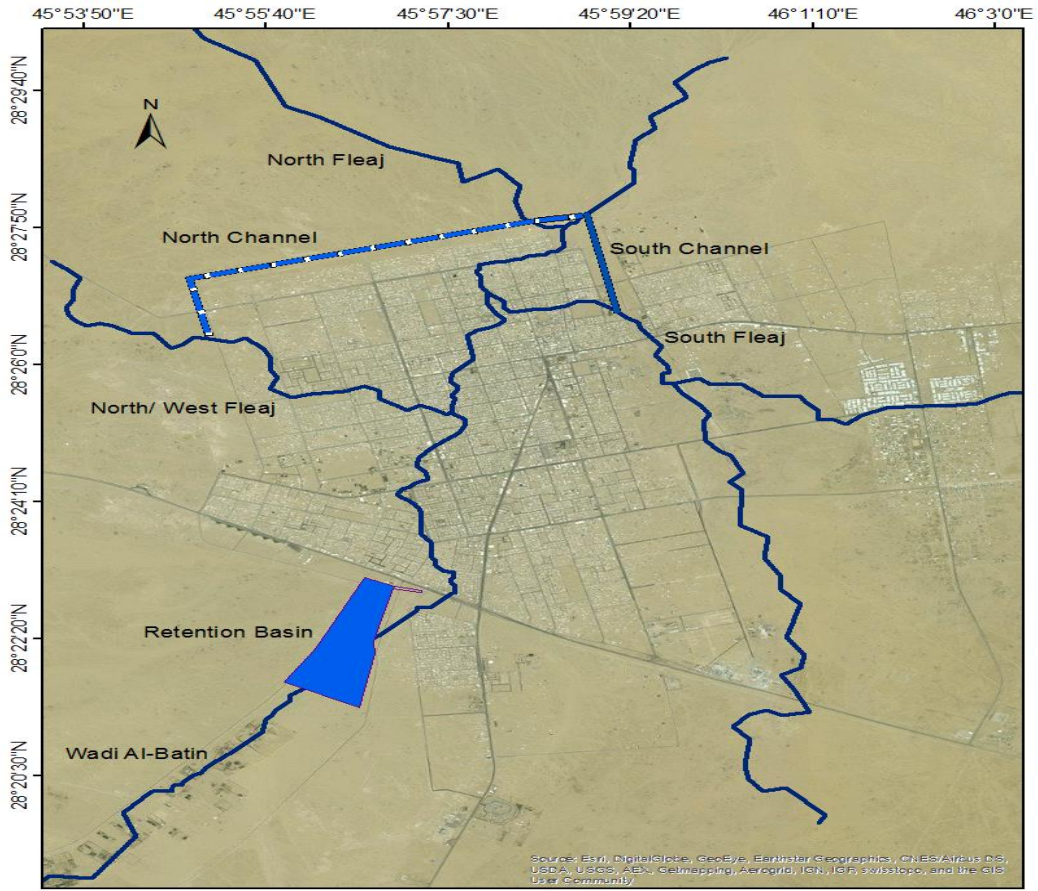


Figure 4.19 Proposed actions

Roughness Coefficient	0.015
Channel Slope	0.00534 m/m
Normal Depth	1.50 m
Left Side Slope	1.00 m/m (H:V)
Right Side Slope	1.00 m/m (H:V)
Bottom Width	6.96 m
Discharge	67.21 m ³ /s

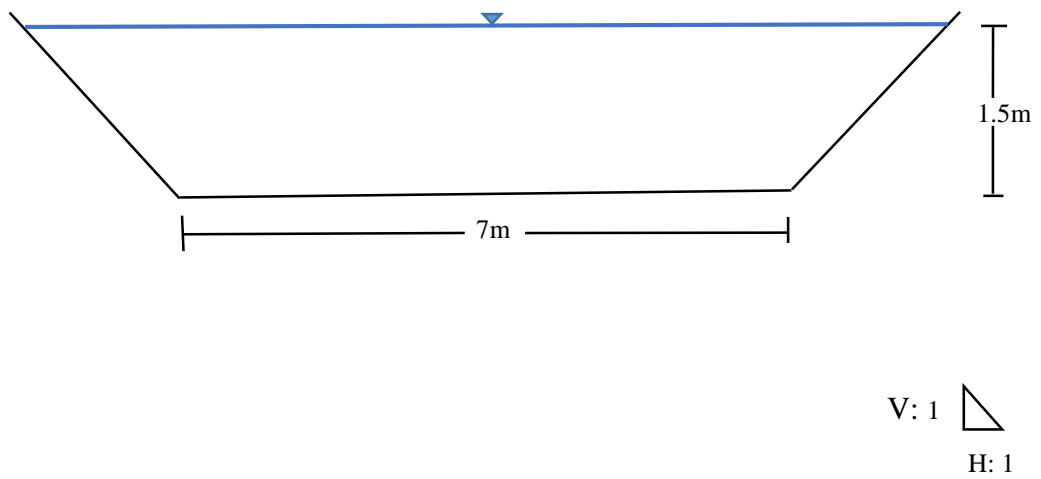
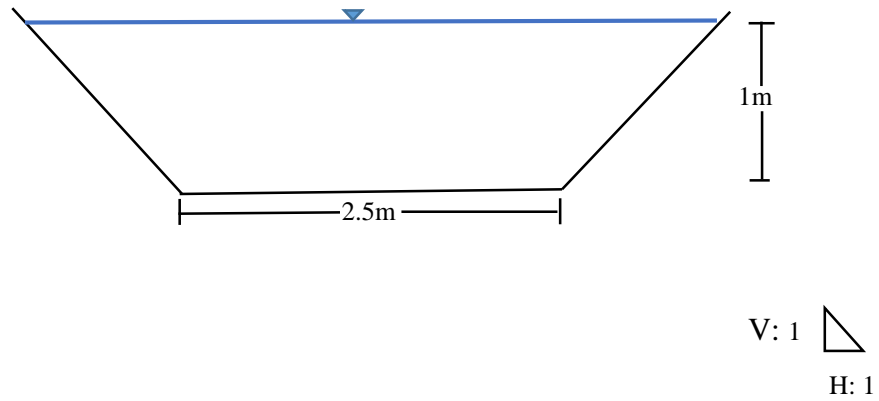


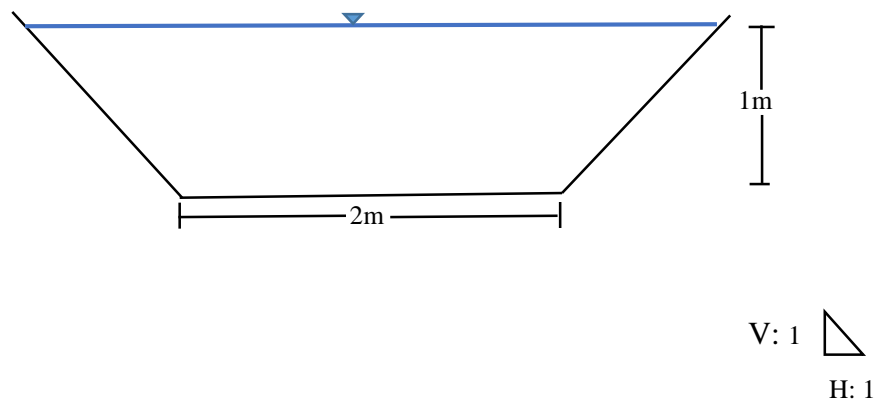
Figure 4.20 The south channel

Roughness Coefficient	0.015
Channel Slope	0.00500 m/m
Normal Depth	1.00 m
Left Side Slope	1.00 m/m (H:V)
Right Side Slope	1.00 m/m (H:V)
Bottom Width	2.43 m
Discharge	12.16 m ³ /s



(a)

Roughness Coefficient	0.015
Channel Slope	0.00739 m/m
Normal Depth	1.00 m
Left Side Slope	1.00 m/m (H:V)
Right Side Slope	1.00 m/m (H:V)
Bottom Width	1.93 m
Discharge	12.16 m ³ /s



(b)

Figure 4.21 Details of the trapezoidal sections: (a) north channel and (b) east channel

Table 4.3 summarizes the final dimensions of the proposed channels of Hafar Al-Batin watershed.

4.4.3 Hafar Al-Batin retention pond

Wadi Al-Batin is the main stream of Hafar Al-Batin watershed. It has a major contribution to the flood of Hafar Al-Batin city with a peak discharge of 144 m³/s and runoff volume of 8,456,700 m³. This study suggests a retention pond at the entrance of the city as shown in Figure 4.19. Retention pond is a natural measure that can be implemented in urban areas to reduce runoff and flood risks. Retention pond is a downstream control measure that can be implemented in urban areas to reduce the potentially dangerous impacts of high runoff volumes and high peak flow rates. Additionally, it provides a permeable area which allows more runoff to infiltrate into the ground. This study suggests implementing a retention pond to retain about 3,750,000 m³ of water. A retention pond was designed based on the 100-year rainfall storm and the area-elevation function for the retention pond as shown in Table 4.4. The design parameters for the retention pond are summarized in Table 4.5. Figure 4.22 shows the HEC-HMS output graph and summary table. As can be revealed from the summary table and Figure 4.22, the peak flow was reduced to 31.1 m³/s, which emphasizes the efficiency of the proposed retention pond.

Table 4.3 The designed channels of Hafar Al-Batin watershed

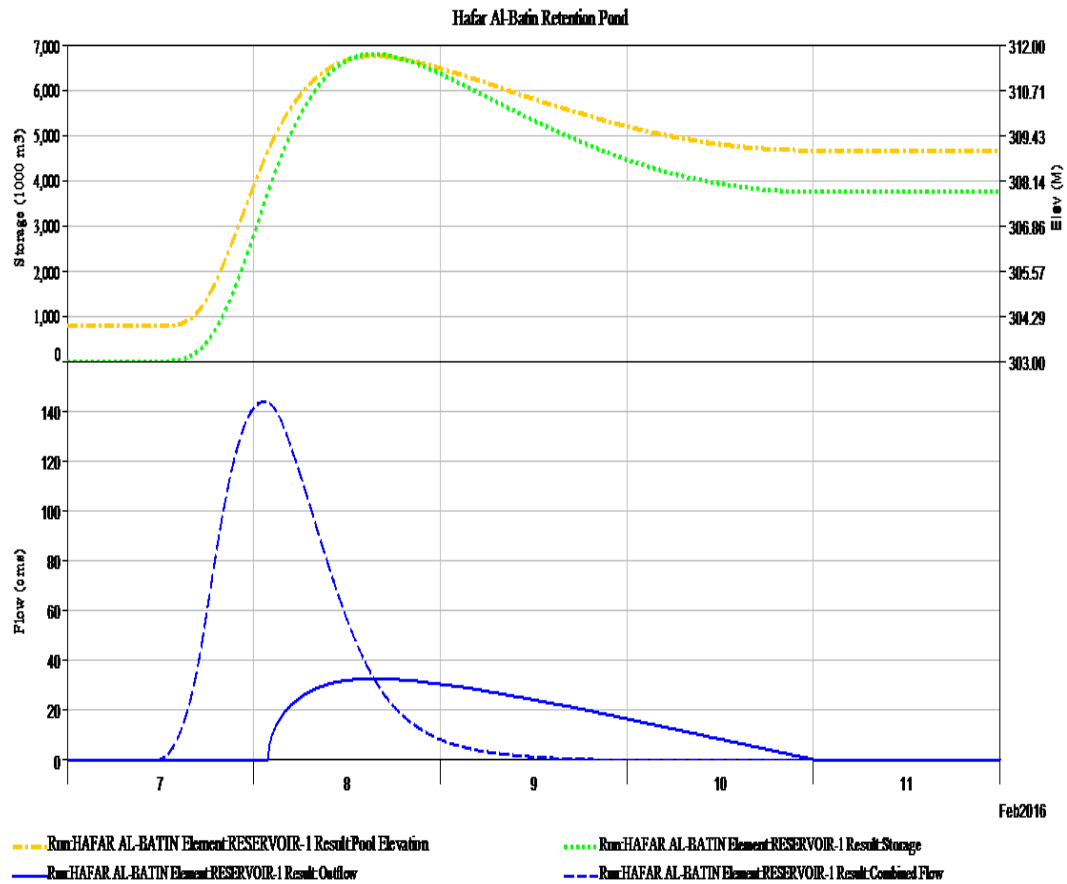
Channel name	Left side slope m/m (H:V)	Right side slope m/m (H:V)	Bottom width (m)	Normal water depth (m)	Total depth (m)
South channel	1	1	7	1.5	1.7
North channel	1	1	2.5	1	1.2

Table 4.4 Elevation-area function for Hafar Al-Batin retention basin design analysis

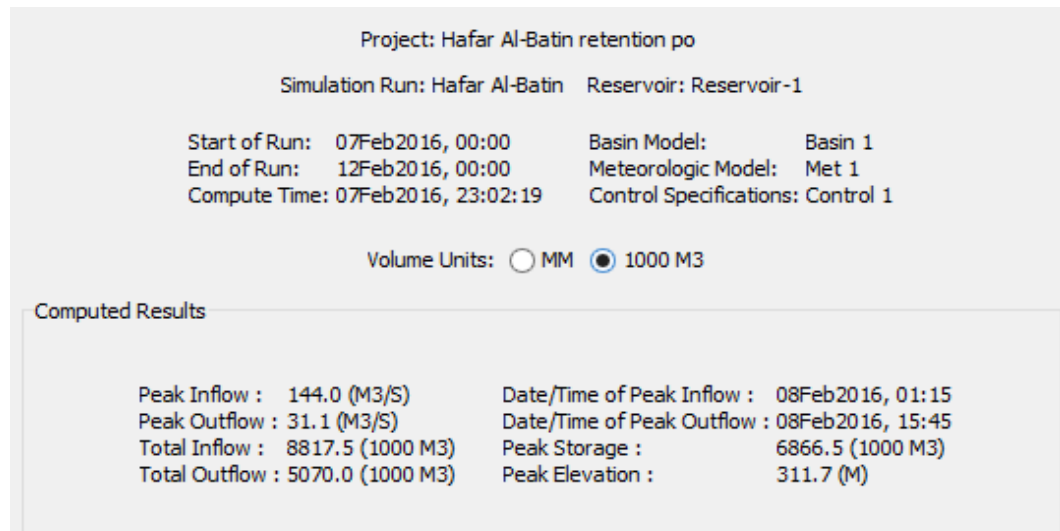
Elevation (m)	Area (km²)	Volume (1000 m³)
304	0.5	0.00
305	0.6	550000
306	0.7	1200000
307	0.8	1950000
308	0.9	2800000
309	1	3750000
310	1.1	4800000
311	1.2	5900000
312	1.3	7150000

Table 4.5 Design parameters for each detention basin design capacity

Outlet (Orifice) (m)	Outlet Area (m ²)	Total Runoff (m ³)	Basin Depth (m)	Basin Volume (m ³)	Volume Fraction %	Outlet Capacity (m ³ /s)
3	7.07	8456700	7.7	6866500	0.81	31.1



(a)



(b)

Figure 4.22 Effect of constructing retention pond: (a) HEC-HMS output graph and (b) summary table

CHAPTER 5

SENSITIVITY ANALYSIS

The models results should be compared with the real data and then the models calibration should be done to adjust the model parameters. The best values of the parameters which give the best agreement between the measured and modeled data will be considered as an input value of the models. However, this process needs detailed data which are available for the hydrologic and hydraulic models, while not available for floodplain model for this study. Sensitivity analysis will be the other choice in this study due to the lack of the detailed calibration data.

In this study, sensitivity analysis is performed to investigate the effects of the following factors:

- Urbanization
- Rainfall storm
- Rainfall duration

Sensitivity analysis is performed by changing one factor while keeping other parameters unchanged and assessing the change in the model output.

5.1 Effect of Urbanization

Urbanization (a population shift from rural to urban areas) has a greater effect on surface runoff in watersheds with soils having high infiltration rates (sands and gravels) than in watersheds predominantly composed of silts and clays, which generally have low infiltration rates. A watershed's response to precipitation is changed by urbanization, which significantly increases the runoff and peak discharges due to the decrease in travel time and reduction in infiltration. Another impact of urbanization is a reduction in lag time as water moves faster through the basin.

Hafar Al-Batin city like many cities in Saudi Arabia, faces a rapid rate of urbanization. This rapid change in urbanization affects the occurrence of flooding as a major factor. In this study, the urbanization impact was examined using different urbanization scenarios which represent possible development conditions (the past and future) of the study area to simulate the runoff generated in Hafar Al-Batin and the peak discharge at its outlet.

The future urbanization scenarios were generated using HEC-HMS where fractions of built area (ranging from 0% to 30%) were considered to run HEC-HMS simulations. For each scenario, the hydrographs for the outlet of Hafar Al-Batin were generated with different storm scenarios.

The results indicate that urbanization has a direct effect on outflow hydrograph. As the percentage of urbanization increases, an increase in excess precipitation as well as an increase in surface runoff were observed as shown in Figure 5.1.

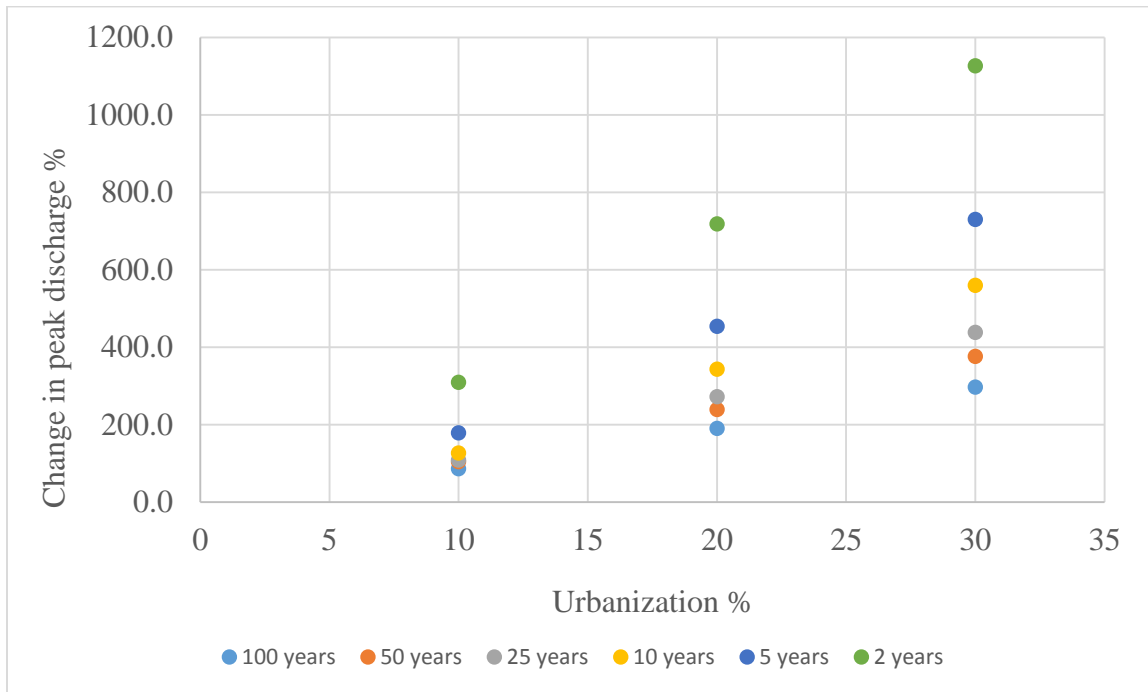


Figure 5.1 Effect of urbanization on the change in peak discharges for different return periods

Currently, the urban area (Hafar Al-Batin) represents approximately 3.6% of the total catchment area with urbanization ratio of 1.8%, which can be used as a reference for the urbanization level. In general, the results indicate that storms of short return period have more effect than larger events on the watershed response to the degree of urbanization as shown in Figure 5.1.

For instance, the peak discharge will be increased by 1126.5%, 729.5%, 559.3%, 437.7%, 375.9%, and 296.7% above the current value when the watershed becomes at 30% urbanization for the 2-year, 5-year, 10-year, 25-year, 50-year, and 100-year storms, respectively. Similar effects were found with the runoff volume when the watershed becomes at 30% urbanization; the runoff volume increased above its current value by 4236.2%, 2235.6%, 1087.9%, 518.5%, 351.1%, and 259.6% for the 2-year, 5-year, 10-year, 25-year, 50-year, and 100-year storms, respectively, as shown in Figure 5.2.

In general, urbanization tends to increase the peak discharge and runoff volume and, as a result, the flood inundation area is expected to increase within the catchment. Table 5.1 summarizes the effect of urbanization on the peak flow and runoff volume for different return periods. As shown in Table 5.1, the 100-year storm, at the current level of urbanization, would result in peak discharge and runoff volume lower than what will be caused by a 2-year storm at 30% urbanization. This change is due to the fact that a large fraction of the rainfall is infiltrated for the 2-year event, which makes it more sensitive to the urbanization level. Another impact of urbanization is a reduction in lag time as water moves faster through the basin. For the 100-year event, infiltration represents a much smaller fraction of the rainfall, which makes it less sensitive to the changes in the water losses.

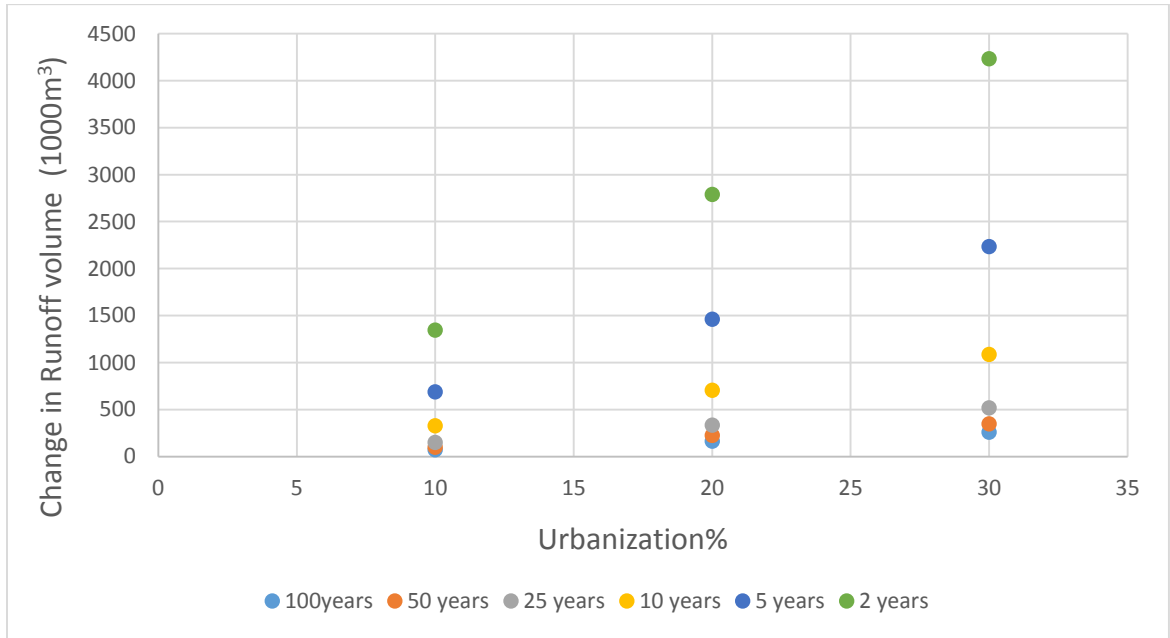


Figure 5.2 Effect of urbanization on the change in runoff volume for different return periods

Table 5.1 Summary of the effect of urbanization on peak flow, runoff volume for different return periods

	100YEAR (79.34mm)		50 YEAR (70.997 mm)		25YEAR (62.593 mm)		10YEAR (51.263mm)		5YEAR (42.297 mm)		2YEAR (28.754 mm)	
Urbanization (%)	Q (m ³ /S)	Runoff volume (1000m ³)	Q (m ³ /S)	Runoff volume (1000m ³)	Q (m ³ /S)	Runoff volume (1000m ³)	Q (M ³ /S)	Runoff volume (1000m ³)	Q (m ³ /S)	Runoff volume (1000m ³)	Q (m ³ /S)	Runoff volume (1000m ³)
Current case	191.5	13016	136.7	8877	102.3	5456	65.6	2207	42.7	905	19.6	330
10	355.6	22623	278.6	17869	213.3	13758	148.7	9437	118.7	7150	80.1	4769
20	555.6	34716	462.8	28954	380.6	23753	290.4	17826	236.4	14142	160.3	9533
30	759.7	46809	650.5	40039	550.1	33748	432.5	26215	354.2	21135	240.4	14296

According to the results of the study, it becomes very clear that urbanization (i.e. increase in impervious cover) tends to increase excess precipitation and surface runoff. In addition, the results show that urbanization has a direct impact on lag time. The increase in urbanization level will reduce lag time, causing the surface runoff to move faster over the catchment.

5.2 Effect of Rainfall Storm

This part describes a comparison of the calculated peak discharges with two kinds of rainfall data: design rainfall developed from the SCS hypothetical storm method and intensity-duration-frequency relationships. A simulation using HEC-HMS has been done to compare between these two approaches by finding the peak discharge for the study area. The design rainfalls have been used to simulate the peak discharge for a runoff area in Hafar Al-Batin, Saudi Arabia. The two methods used the 24-hour rainfall, which ensures that the distribution includes the maximum of any duration less than 24 hours.

The SCS storm distribution method identified as Type I, Type IA, Type II, and Type III, is used for different hydrologic studies (floodplain management studies, urban damage evaluations, flood insurance studies, flood routings, etc.) with a return period of 1 year up through the 500-year event. Selecting one of the four distributions depends on regions of the country. For example, Type II is appropriate for dried regions type thunderstorm. In Type II, 45 percent of the 24-hour rainfall are assumed to be distributed in the maximum 1 hour [69]. Mass curves are used to indicate what fraction of precipitation has fallen at any time of the total 24 hours (Figure 5.3). The same data for IDF curves were used to develop these mass curves.

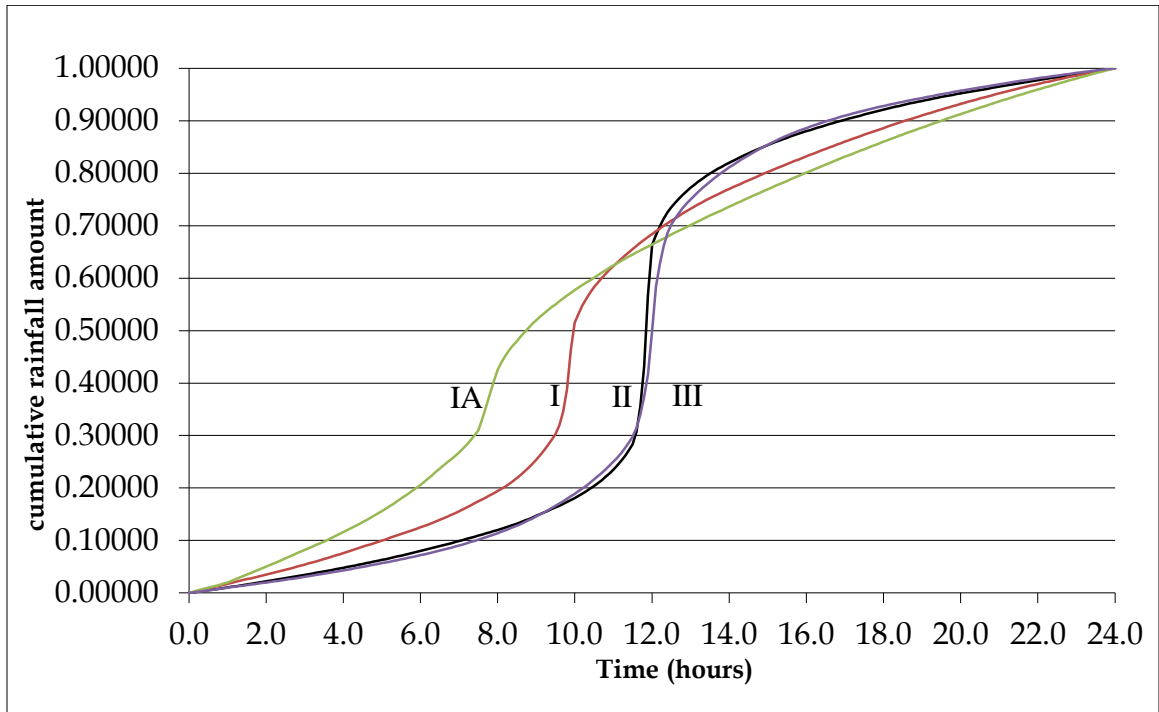


Figure 5.3 SCS rainfall distributions [70]

Type II distribution is arranged so that the greatest 30-minute depth occurs at the middle of the 24-hour storm, the second largest in the next 30-minutes, while the third largest depth in the preceding 30 minutes. The entire 24-hour distribution is developed by repeating this process up to 24 hours [70]. The SCS hyetograph distribution for Hafar Al-Batin watershed is shown in Figure 4.6. The frequency storm method can be used to create a balanced, synthetic storm with a known exceedance probability. Automatic adjustments for storm area and series type are based on the exceedance probability. Depth-duration data were obtained from Hafar Al-Batin IDF curves developed by Elsbaie [55] as shown in Appendix V. Figure 5.4 shows the maximum peak discharge at the watershed outlet. By comparing Figure 5.4 with Figure 4.8, it can be noticed that the calculated peak discharge based on SCS method is 27.7% higher than the one obtained when using the frequency storm method. By comparing Figure 5.5 with Figure 4.6, it can be found that the reason for this difference is related to the rainfall distribution estimated by each method. Appendix III shows the peak discharge for each sub-basin based on the two methods of rainfall, and according to these results, the SCS hypothetical storm method was used to produce Hafar Al-Batin hazard map, which gives the worst case.

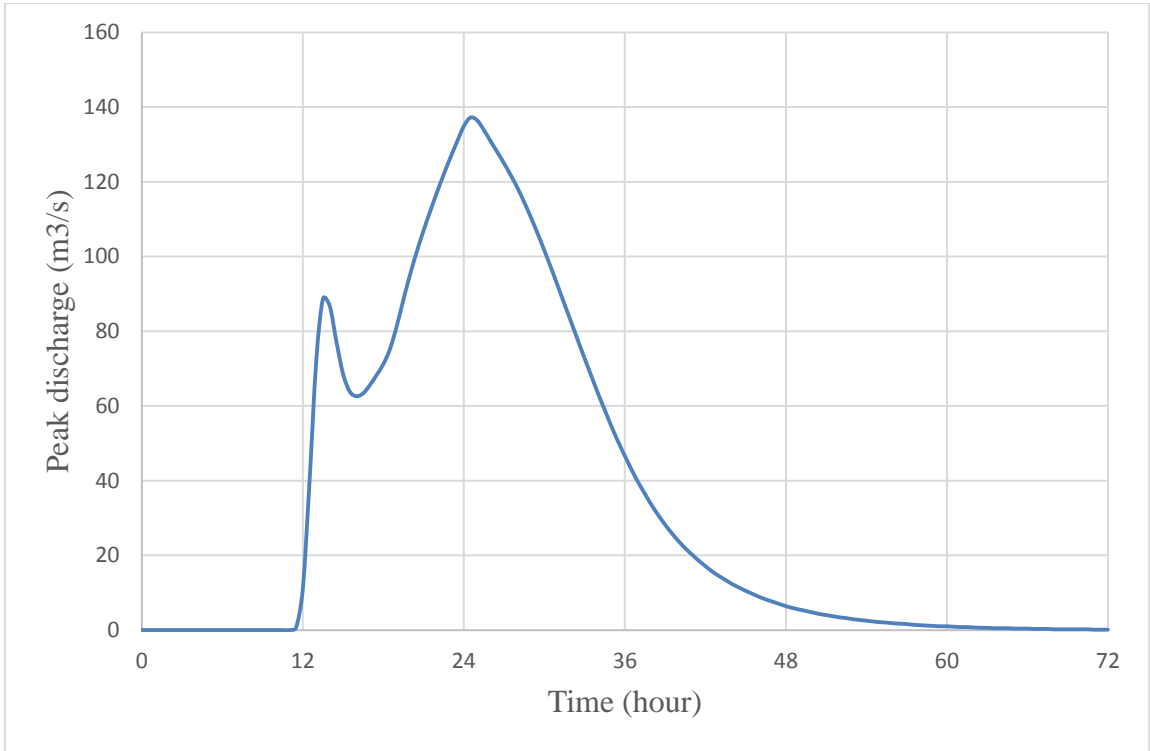


Figure 5.4 The 100-year storm runoff hydrograph of Hafar Al-Batin watershed (frequency storm method)

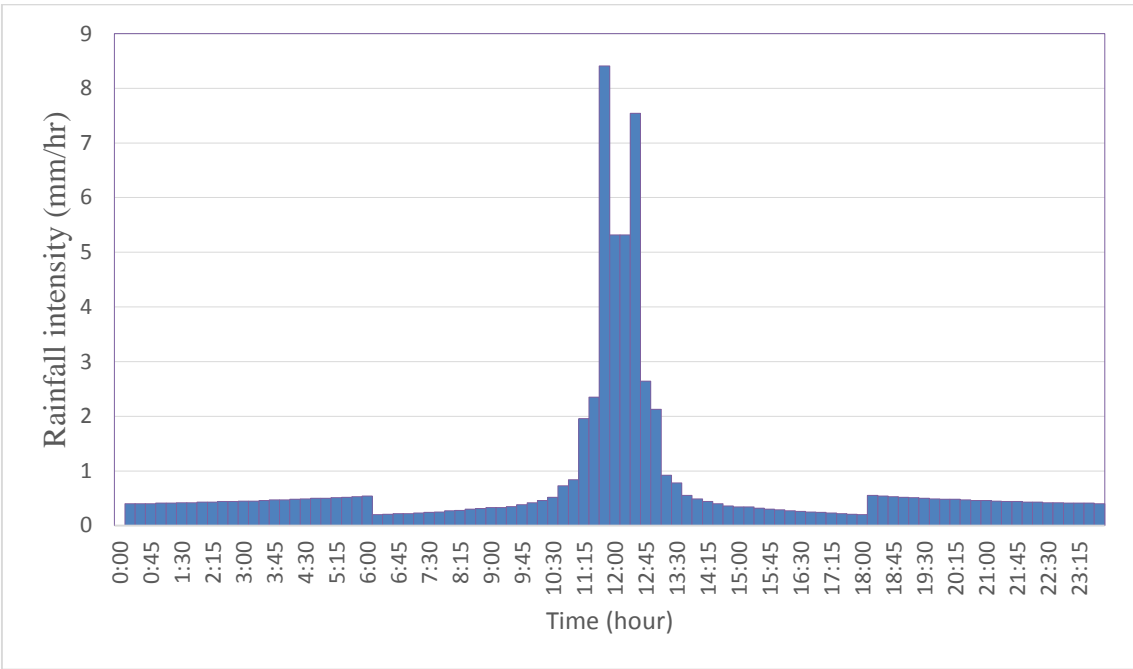


Figure 5.5 Frequency storm distribution hyetograph of the 100-year storm

5.3 Effect of Rainfall Duration

The duration of the design storm is usually selected based on the catchment response time, which is a function of the time of concentration. The time of concentration represents the time the flow will take to move from the most remote point of the watershed to the watershed outlet. In general, the design duration of a storm used in water control system design must be equal or exceed the time of concentration of the catchment area. The duration of the design storm is selected equal to the time of concentration for small urban catchment ($< 1 \text{ km}^2$), which leads to the peak discharge for a given return period. However, the duration which causes the largest detention volume is the design rainfall duration for the design of the detention basins [71]. On the other side, the critical design-storm duration for the catchment with high infiltration losses may be less than the time of concentration [72]. Typically, for large watersheds with a long time of concentration, the storm duration should exceed the time of concentration to achieve the maximum hydrological response [69].

In this study, different rainfall durations (1, 2, 3, 6, 12, and 24 hours) have been used to find the design rainfall duration which causes the peak discharge. Table 5.2 shows the values of the peak discharge and runoff volume for each duration. The 2-hour duration gave a peak discharge higher than 1, 3, 6, and 12 hours but less than 24 hours. The peak discharge for 1 hour, 3 hours, 6 hours, and 12 hours represents 35.2%, 1.4%, 7.9%, and 7.8%, respectively, lower than that for 2-hour duration. However, the peak discharge for 2 hours is lower than that for the 24-hour duration by 158.8%. On the other hand, the change in the runoff volume increases for the storms of high return period as shown in Table 5.2.

Table 5.2 Watershed peak discharge and volume for different design storm durations for a return period of 100 years

Time (hour)	1	2	3	6	12	24
Peak discharge (m³/s)	47.6	73.5	72.5	67.7	67.8	191.5
Runoff volume (1000 m³)	500	1290.6	1583.1	2205.8	3342.2	13016.6

By close inspection of Figure 5.6, it can be observed that the double peak discharges were obtained for storm durations of 24, 12, and 6 hours, while the second peak is not clear for the remaining durations. The reason for this is that the whole watershed does not contribute to the outlet flow, especially that is far from the watershed outlet. In other words, the time of concentration for some sub-basins is much higher than the storm durations, which means that these basins do not contribute to the outlet flow. On the other side, the second peak for the 24-hour duration is higher than the first peak because the whole catchment contributes to the outlet flow. The runoff from the sub-basins with a high CN value flows faster than that having low values. On the other hand, the differences in the time of peak for each duration are related to the hyetograph distribution for these durations, which are concentrated in the middle half of each duration.

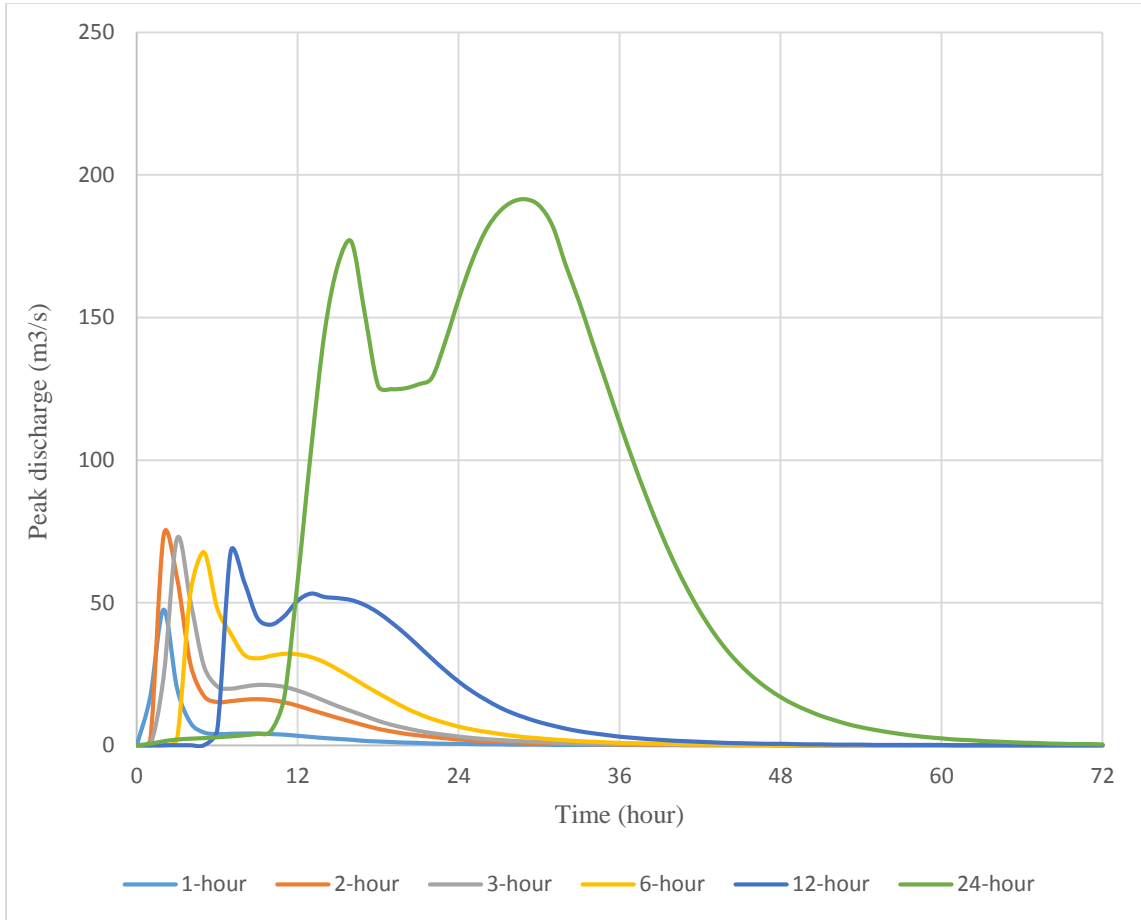


Figure 5.6 Watershed hydrographs for different storm durations for 100-year storm

CHAPTER 6

SUMMARY, CONCLUSION AND

RECOMMENDATIONS

6.1 Summary and Conclusion

In this study, a flood model was constructed for Hafar Al-Batin watershed located in the eastern part of Saudi Arabia. The model integrates a hydrologic model (HEC-HMS), a hydraulic model (HEC-RAS), and a floodplain delineation model (WMS) and (GIS). First, HEC-HMS was applied to Wadi Al-Batin arid watershed to simulate the wadi flow by dividing the catchment area into many sub-basin areas. The peak discharge and the flow volume were estimated for different return periods. Next, the flow depths were calculated by HEC-RAS, then the flood depth maps were delineated using WMS and, finally, the flood risk maps were generated using GIS.

For various magnitudes of rainfall storms and different urbanization scenarios, the effect of urbanization on peak discharge and runoff volume was investigated. The results indicate that the flood depth and flood hazard area can significantly be increased as a result of the urbanization on the peak discharge and runoff volume resulting from a given storm. This is due to the decreased infiltration and obstruction of natural runoff. Therefore, the whole city, including properties, critical facilities, and people, will be significantly exposed to the

risk of flooding. Also, the results indicate that storms of short return period have more effect than larger events on the watershed response to the degree of urbanization. This is due to the high impermeability where most of the rainfall is infiltrated for 2 years. However, for 100 years, the amount of rainfall is much more than that for 2 years, which makes 100 years less sensitive to urbanization. But when the ratio of urbanization increases, the impermeability will decrease and the runoff will increase. Unfortunately, Hafar Al-Batin city is located in the downstream of the watershed, which makes it more affected by any changes within the watershed. In addition, the hydrograph at the outlet has two peaks, which means that the flood will hit the city two times during the same storm in contrast if the city is located in the upstream.

The response of the watershed was also examined for the effect of the storm distribution using two methods, frequency storm and SCS. The results show that the SCS is more appropriate with dried regions type thunderstorm due to its distribution, which assumes the rainfall to be distributed in the maximum 1 hour. In addition, the change of the outlet peak discharge and runoff volume due to the change in storm duration was examined. The result shows that the 24-hour duration is suitable for floodplain simulation. This is due to the big difference in the peak discharge values between 24 hours and the other durations. This big difference is attributed to the size of the catchment area and the big difference in the amount of rainfall.

A good understanding of the watershed response to storm events will lead to a good successful flood hazard management. In addition, floods impact the road networks, creating hazards for drivers, so decision makers must protect drivers by taking the necessary precautions. Reliable hydrologic, hydraulic, and floodplain models will be required in

addition to the effect of the future urbanization for creating successful planning studies. Data management and spatial analysis tool's capabilities in GIS make flood hazard studies easier. The city's vulnerability to flood impact could be reduced by using wisely managed development. The large catchment area, which included Hafar Al-Batin city, was used to perform this study. The outflow from Hafar Al-Batin watershed will be useful for flood analysis at the downstream watershed, while for flood analysis in HafarAl-Batin city, the peak discharge at the entrance of the city should be considered. The expected volume of water that can be collected during the design storm from the whole area of Hafar Al-Batin is 13,016,600 m³ and the peak discharge reached 191.5 m³/s for 100 years, which caused inundation of the widest parts of Hafar Al-Batin city. For planning purposes, such as flood control structures and the design of drainage, design storms will be helpful. However, high temporal and spatial resolutions of actual storms should be involved in detailed flood risk assessment due to their significant influence on the watershed response.

6.2 Recommendations

Based on the findings of this study, the following recommendations are suggested:

- The results of this study can be used to understand and manage the flood in Hafar Al-Batin watershed.
- Flow measuring devices should be installed at the outlet of Hafar Al-Batin to get high-quality data and, thus, to examine the applicability of the developed models. Also, the availability of real storms can help in this evaluation.

- More metrological stations should be installed at different locations of the catchment to record hydrological parameters which can be used in any future studies.
- Filed data related to channel roughness coefficient need to be collected which can help to get better results of the hydraulic model.
- Evaluate the existing flood protection works in the study area to specify the efficiency of these structures.
- Early warning networks should be constructed in the city for the people to take the necessary precaution to avoid the damage resulting from the flood.
- Preventing any new residential structures in the areas with high risk of flood.
- Construct a stormwater drainage system that covers all parts of Hafar Al-Batin city to collect and transport stormwater outside the city.
- Explore the consequences of the occurrences of flood events on the economy of Hafr Al-Batin city
- Investigate input parameters uncertainties on hydrologic and hydraulic models outputs.

References

- [1] S. N. Jonkman, “Global perspectives on loss of human life caused by floods,” *Natural Hazards*, Vol. 34, pp. 151–175, 2005.
- [2] X. Lin, “Flash floods in arid and semi-arid zones,” *Technical Documents in Hydrology*, No. 23, p. 65, 1999.
- [3] Y. A. Alamri, “Rains and floods in Saudi Arabia. Crying of the sky or of the people,” *Saudi Medical Journal*, Vol. 32, No. 3, pp. 311–313, 2011.
- [4] N. Momani and A. Fadil, “Changing public policy due to Saudi City of Jeddah flood disaster,” *Journal of Social Sciences*, Vol. 6, No. 3, pp. 424–428, 2010.
- [5] K. Maghrabi, “Impact of flood disaster on the mental health of residents in the eastern region of Jeddah Governorate, 2010: A study in medical geography,” *Life Science Journal*, Vol. 9, No. 1, pp. 95–110, 2012.
- [6] J. Jones and T. Haluska, “Updating flood maps efficiently: building on existing hydraulic information and modern elevation data with a GIS,” *US Geological Survey*, pp. 1–12, 1998.
- [7] T. Wagener and H. S. Wheater, “A comparison of metric and conceptual approaches in rainfall-runoff modeling and its implications,” Imperial College Press, London, England, p. 306, 2004.
- [8] T. Wagener and M. J. Lees, “Incorporating predictive uncertainty into a rainfall-runoff modeling system,” In *Proceedings of Hydroinformatics Conference*, 2000.
- [9] T. H. M. Rientjes, “Inverse modelling of the rainfall-runoff relation: a multi-objective model calibration approach,” Dissertation, Delft University of Technology, 2004.
- [10] A. Y. Saad, *Manual of Applied Hydrology for Dams*, 1st ed., Ministry of Agriculture & Irrigation, Yemen, 2003.
- [11] S. M. S. Shah, P. E. O’Connell, and J. R. M. Hosking, “Modelling the effects of spatial variability in rainfall on catchment response. 1. Formulation and calibration of a stochastic rainfall field model,” *Journal of Hydrology*, Vol. 175, No. 1–4, pp. 67–88, Feb. 1996.
- [12] B. F. W. Croke, F. Andrews, A. J. Jakeman, S. M. Cuddy, and A. Luddy, “IHACRES Classic Plus: A redesign of the IHACRES rainfall-runoff model,” *Environmental Modelling & Software*, Vol. 21, No. 3, pp. 426–427, 2006.

- [13] T. S. Kokkonen and A. J. Jakeman, “A comparison of metric and conceptual approaches in rainfall-runoff modeling and its implications,” *Water Resources Research*, Vol. 37, No. 9, pp. 2345–2352, 2001.
- [14] M. B. Beck, “Forecasting environmental change: a prospectus,” *Journal of Forecasting*, Vol. 10, No. 1, pp. 3–19, 1991.
- [15] W. Boughton and F. Chiew, “Estimating runoff in ungauged catchments from rainfall, PET and the AWBM model,” *Environmental Modelling & Software*, Vol. 22, No. 4, pp. 476–487, 2007.
- [16] A. J. Jakeman and G. M. Hornberger, “How much complexity is warranted in a rainfall-runoff model,” *Water Resources Research*, Vol. 29, No. 8, pp. 2637–2649, 1993.
- [17] C. Perrin, C. Michel, and V. Andréassian, “Improvement of a parsimonious model for streamflow simulation,” *Journal of Hydrology*, Vol. 279, No. 1–4, pp. 275–289, 2003.
- [18] K. Beven, *Rainfall-Runoff Modelling: The Primer*, John Wiley & Sons, 2011.
- [19] W. Scharffenberg and M. Fleming, “Hydrologic modeling system HEC-HMS V32 User’s Manual,” USACE-HEC, Davis, USA, 2010.
- [20] K. Beven, “Linking parameters across scales: subgrid parameterizations and scale dependent hydrological models,” *Hydrological Processes*, Vol. 9, No. 5–6, pp. 507–525, 1995.
- [21] J. Arnold, R. Srinivasan, R. Muttiah, and J. Williams, “Large area hydrologic modeling and assessment Part I: Model development,” *Journal of American Water Resources Association (JAWRA)*, Vol. 34, No. 1, pp. 73–89, 1998.
- [22] FEMA, “National Flood Insurance Program: Flood Hazard Mapping,” 2001. [Online]. Available: <http://www.fema.gov/national-flood-insurance-program-flood-hazard-mapping>. [Accessed: 06-Sep-2015].
- [23] P. D. Bates and A. P. J. De Roo, “A simple raster-based model for flood inundation simulation,” *Journal of Hydrology*, Vol. 236, No. 1–2, pp. 54–77, 2000.
- [24] V. P. Singh, *Kinematic Wave Modeling in Water Resources, Surface-water Hydrology*, John Wiley & Sons, 1996.
- [25] D. K. Borah, “Runoff simulation model for small watersheds,” *Transactions of the ASAE*, Vol. 32, No. 3, pp. 881–886, 1989.
- [26] J. Lange, C. Liebundgut, and A. Schick, “The importance of single events in arid zone rainfall-runoff modelling,” *Physics and Chemistry of the Earth, Part B: Hydrology, Oceans and Atmosphere*, Vol. 25, pp. 673–677, 2000.

- [27] F. Abdulla, J. Amayreh, and A. Hossain, "Single event watershed model for simulating runoff hydrograph in desert regions," *Water Resources Management*, vol. 16, pp. 221–238, 2002.
- [28] N. Al-Abed, F. Abdulla, and A. Khyarah, "GIS-hydrological models for managing water resources in the Zarqa River basin," *Environmental Geology* 2005, Vol. 47, pp. 405–411, 2005.
- [29] A. M. A.-S. H. Al-Qurashi, "Rainfall-runoff modelling in arid areas," Dissertation, Imperial College, London, 2008.
- [30] A. Al-Qurashi, N. McIntyre, H. Wheeler, and C. Unkrich, "Application of the Kinos2 rainfall-runoff model to an arid catchment in Oman," *Journal of Hydrology*, Vol. 355, pp. 91–105, 2008.
- [31] N. McIntyre and A. Al-Qurashi, "Performance of ten rainfall-runoff models applied to an arid catchment in Oman," *Environmental Modelling & Software*, Vol. 24, No. 6, pp. 726–738, 2009.
- [32] A. J. Timpson, "Small watershed flood frequency analysis for Utah," The University of Utah, USA, 2012.
- [33] M. A. Zaman, A. Rahman, and K. Haddad, "Regional flood frequency analysis in arid regions: A case study for Australia," *Journal of Hydrology*, Vol. 475, pp. 74–83, 2012.
- [34] E. Ghoneim and G. M. Foody, "Assessing flash flood hazard in an arid mountainous region," *Arabian Journal of Geosciences*, Vol. 6, No. 4, pp. 1191–1202, 2013.
- [35] L. Mediero and T. R. Kjeldsen, "Regional flood hydrology in a semi-arid catchment using a GLS regression model," *Journal of Hydrology*, Vol. 514, pp. 158–171, 2014.
- [36] Z. Şen, H. A. Khiyami, S. G. Al-Harthy, F. A. Al-Ammawi, A. B. Al-Balkhi, M. I. Al-Zahrani, and H. M. Al-Hawsawy, "Flash flood inundation map preparation for wadis in arid regions," *Arabian Journal of Geosciences*, pp. 3563–3572, 2012.
- [37] M. A. Hagra, A. M. Elmoustafa, and A. Kotb, "Flood plain mitigation in arid regions case study: South of Al-Kharj city, Saudi Arabia," *International Journal of Recent Research and Applied Studies (Ijrras)*, Vol. 16, pp. 147–157, July 2013.
- [38] S. Ismail, "Influence of deficit irrigation on water use efficiency and bird pepper production (*Capsicum annum L.*)," *Journal of King Abdulaziz University: Meteorology, Environment and Arid Land Agriculture Sciences*, Vol. 21, No. 1, pp. 29–43, 2010.
- [39] O. H. Al-Shareef, M. Ezzeldin, and S. A. Gutub, "Comparison of peak discharge estimation methods in northern Jeddah in western Saudi Arabia," *Journal of Environmental Hydrology*, Vol. 21, 2013.

- [40] S. S. Sadrolashrafi, A. Samadi, M. A. Rodzi, and A. M. Thamer, "Flood modeling using WMS Software : A case study of the Dez River Basin, Iran," *River Flow 2008*, pp. 1735–1744, 2008.
- [41] L. Ekstrom, D. Palmer, and B. Hargis, "Inundation mapping initiatives of the Iowa flood center," Brigham Young University, 2013.
- [42] A. Erturk, M. Gurel, M. A. Baloch, T. Dikerler, E. Varol, N. Akbulut, and A. Tanik, "Application of watershed modeling system (WMS) for integrated management of a watershed in Turkey," *Journal of Environmental Science and Health Part A. Toxic/Hazardous Substances and Environmental Engineering*, Vol. 41, No. 9, pp. 2045–2056, February 2006.
- [43] A. Sarminingsih, "Floodplain mapping using HEC-RAS and ArcView GIS," In *Proceedings, the 6th Civil Engineering Conference in Asia Region: Embracing the Future through Sustainability*, 2001, pp. 1–12.
- [44] F. E. Hicks and T. Peacock, "Influence of deficit irrigation on water use efficiency and bird pepper production," *Canadian Water Resources Journal*, Vol. 30, pp. 159–174, December 2005.
- [45] E. Tate and D. Maidment, "Floodplain Mapping Using HEC-RAS and ArcView GIS," MS Thesis. University of Texas at Austin, 1999.
- [46] R. Siddiqui, H. Maqsood, and S. Ahmed, "Modeling flood assessment for a northern watershed in Pakistan," *45th IEP Convention*, pp. 1–24, 2012.
- [47] M. Nouh, "A comparison of three methods for regional flood frequency analysis in Saudi Arabia," *Advanced Water Resources*, Vol. 10, pp. 212–219, 1987.
- [48] A. Al-Turbak, "Geomorphoclimatic peak discharge model with a physically based infiltration component," *Journal of Hydrology*, pp. 1–12, 1996.
- [49] A. M. Subyani, "Hydrologic behavior and flood probability for selected arid basins in Makkah area, western Saudi Arabia," *Arabian Journal of Geosciences*, Vol. 4, No. 5, pp. 817–824, 2011.
- [50] G. M. Dawod, M. N. Mirza, and K. A. Al-Ghamdi, "Assessment of several flood estimation methodologies in Makkah metropolitan area, Saudi Arabia," *Arabian Journal of Geosciences*, Vol. 6, No. 4, pp. 985–993, 2013.
- [51] H. O. Sharif, F. H. Al-Juaidi, A. Al-Othman, I. Al-Dousary, E. Fadda, S. Jamal-Uddeen, and A. Elhassan, "Flood hazards in an urbanizing watershed in Riyadh, Saudi Arabia," *Natural Hazards and Risk*, Vol. 7, No. 2, pp. 702–720, 2016.
- [52] "Climate: Hafar Al-Batin - Climate graph, Temperature graph, Climate table," Climate-Data.org. [Online]. Available: <http://en.climate-data.org/location/53359/>. [Accessed: 14-Nov-2015].

- [53] R. Linsley, *Hydrology for Engineers*, SI metric edition, McGraw-Hill, London, 1988.
- [54] “Hafar Al-Batin average precipitation,” 2015.
- [55] I. H. Elsebaie, “Developing rainfall intensity-duration-frequency relationship for two regions in Saudi Arabia,” *Journal of King Saud University – Engineering Sciences*, Vol. 24, pp. 131–140, 2012.
- [56] Research Applications Laboratory (RAL), “Improve understanding of the atmosphere, earth system, and sun,” 2008.
- [57] “Saudi Arabia – Nationwide Data,” 2015. [Online]. Available: <http://data.geocomm.com/catalog/SA/datalist.html>.
- [58] W. A. Scharffenberg, “Hydrologic Modeling System HEC-HMS – User’s Manual,” p. 442, December 2013.
- [59] Soil Conservation Service, “Urban Hydrology for Small Watersheds (Technical Release 55),” US Department of Agriculture, Washington, 1986.
- [60] V. M. Ponce and R. Hawkins, “Runoff curve number: has it reached maturity?,” *Journal of Hydrologic Engineering, ASCE*, Vol. 1, No. 1, pp. 11–19, 1996.
- [61] M. N. Shrestha, “Spatially distributed hydrological modelling considering land-use changes using remote sensing and GIS,” In *Proceedings, Map Asia Conference*, Kuala Lumpur, Malaysia, pp. 13–15, October 2003.
- [62] “Watershed Modeling System, Version 9.1, Reference Manual,” Engineering Computer Graphics Laboratory, Brigham Young University, Provo, Utah, 2012.
- [63] USACE, “HEC River Analysis System (HEC-RAS) User’s Manual 4.1,” USACE Hydrologic Engineering Center, Davis, CA, 2010.
- [64] D. Gilles, N. Young, H. Schroeder, J. Piotrowski, and Y.-J. Chang, “Inundation mapping initiatives of the Iowa flood center: Statewide coverage and detailed urban flooding analysis,” *Water*, Vol. 4, No. 4, pp. 85–106, 2012.
- [65] C. R. Omer, E. J. Nelson, and A. K. Zundel, “Impact of varied data resolution on hydraulic modeling and floodplain delineation,” *Journal of American Water Resources Association (JAWRA)*, Vol. 39, No. 2, pp. 467–475, 2003.
- [66] C. Smemoe, E. Nelson, A. Zundel, and A. Miller, “Demonstrating floodplain uncertainty using flood probability maps,” *Journal of American Water Resources Association (JAWRA)*, Vol. 43, No. 2, pp. 359–371, 2007.

- [67] N. Noman, E. Nelson, and A. Zundel, “Improved process for floodplain delineation from digital terrain models,” *Journal of Water Resources Planning and Management*, Vol. 129, No. 5, pp. 427–436, 2003.
- [68] E. Nelson, “Watershed Modeling System Help File, Version 8.0,” 2007.
- [69] J. N. Moore, C. Engineer, R. C. Riley, and W. P. Specialist, “Comparison of temporal rainfall distributions for near probable maximum precipitation storm events for dam design,” In *Proceedings of the 1993 Annual Conference of the Association of State Dam Safety Officials*, Minneapolis, MN, 1993.
- [70] HydroCAD Software Solutions LLC. (2011). *HydroCAD® Owner’s Manual*.
- [71] M. M. Soliman, *Engineering Hydrology of Arid and Semi-arid Regions*, CRC Press, 2011.
- [72] C. Chen and T. S. W. Wong, “Climate: Hafar Al-Batin – Climate graph,” *Journal of Hydraulic Engineering*, Vol. 119, No. 9, pp. 1040–1045, Sep. 1993.

APPENDICES

List of Appendices

- Appendix I : The morphology characteristics of the basins of Hafar Al-Batin
- Appendix II : The curve numbers for each sub-basin and SCS Lag Time
- Appendix III : The peak discharge for each sub-basin for the two method of rainfall
- Appendix IV : Peak discharge used in HEC-RAS
- Appendix V : Rainfall intensity for different duration and return period

APPENDIX I

The morphology characteristics of the basins of Hafar Al-Batin

Basin ID	Basin Area (Km2)	Basin Slope	Basin Length (m)	Perimeter (m)	Mean Elevation (m)
178	37.82210	0.0768265500	14343.97611	115104.90685	436.28877
178	37.82210	0.0768265500	14343.97611	115104.90685	436.28877
181	27.46860	0.0677157400	13546.03625	86123.10939	461.20587
178	37.82210	0.0768265500	14343.97611	115104.90685	436.28877
181	27.46860	0.0677157400	13546.03625	86123.10939	461.20587
175	39.61700	0.0642785300	17079.21260	105580.32949	437.88644
180	26.64370	0.0575125000	20038.73592	91592.21419	458.03467
183	30.15520	0.0446432400	10462.02253	63316.80327	469.49844
174	31.82710	0.0571187000	13822.33184	75669.61442	423.03052
182	34.42720	0.0467252000	15414.77355	112841.79959	465.76300
179	18.95380	0.0510745300	11092.84766	74050.05049	447.14035
182	34.42720	0.0467252000	15414.77355	112841.79959	465.76300
168	55.77980	0.0617610400	20319.91457	136229.12045	415.50612
177	23.32980	0.0358592100	12220.50063	84246.27888	437.42235
171	25.66240	0.0473858000	17183.38665	93090.33179	419.97146
182	34.42720	0.0467252000	15414.77355	112841.79959	465.76300
173	33.84570	0.0395554700	26318.56781	125304.07105	434.90258
176	39.26190	0.0464234700	18796.98013	116775.48708	443.79752
167	35.18400	0.0389558900	22551.81727	111609.45735	419.28584
169	25.51970	0.0629347700	14414.42332	90061.48623	416.81097
170	40.12620	0.0627513800	16736.79445	106768.84369	414.08436
164	77.80970	0.0494605500	19359.90820	135066.90156	402.76702
172	24.30780	0.0335114800	11254.75650	76305.88636	419.39670
166	25.86280	0.0632528200	10829.63563	72442.82314	406.98810
162	21.16430	0.0738980400	11942.45789	76795.87762	401.09520
165	30.47920	0.0692627800	13066.56549	91045.51631	404.39760
165	30.47920	0.0692627800	13066.56549	91045.51631	404.39760
161	49.00230	0.0500585900	23618.67595	134123.45148	408.53017
163	21.36920	0.0718959100	10662.63400	84038.33107	398.46497
160	63.71790	0.0563518000	15759.08963	112256.71614	395.68214
157	49.36780	0.0750052500	17194.57225	114505.17152	390.83486
154	62.68030	0.0596608100	15405.44024	104159.60424	376.27449
150	14.00980	0.0830435000	10345.85846	60808.55564	382.89702
147	49.04820	0.0588382000	16003.48172	113948.91789	371.19054
151	17.31460	0.0712572400	8602.48043	56200.36021	384.13920
161	49.00230	0.0500585900	23618.67595	134123.45148	408.53017
9	8.37520	0.0812954400	6888.99066	39719.18612	382.51194

158	8.61510	0.0829610600	6541.41045	42903.02025	390.39438
156	8.03410	0.0741098700	5315.21309	39502.69352	385.30065
0	0.00000	0.0000000000	0.00000	0.00000	0.00000
4	14.14830	0.0793526200	9472.84071	53934.37684	377.73683
142	43.19660	0.0673732100	13749.16488	119013.29809	370.18953
10	5.97870	0.0732697800	6270.44426	37542.14961	379.23655
159	33.04380	0.0671369000	16153.50825	114136.00584	397.38351
16	11.93340	0.0804375700	6186.38953	47054.72751	381.03372
153	9.11050	0.0769722000	8472.52356	46687.84178	384.39017
144	5.15850	0.0813162200	6070.56571	36156.21489	380.70070
160	63.71790	0.0563518000	15759.08963	112256.71614	395.68214
7	11.76290	0.0706533700	10630.30205	59106.95847	375.34451
145	7.10770	0.0850198100	5958.19278	35020.27228	382.32200
1	16.16980	0.0773739600	7533.54216	60285.96713	367.96559
153	9.11050	0.0769722000	8472.52356	46687.84178	384.39017
11	2.42550	0.0660209400	4341.23784	21754.63233	376.95826
152	7.02150	0.0779984900	6027.28359	35491.79641	385.19504
15	3.39990	0.0714280300	3751.59232	24382.75912	376.94462
155	8.79480	0.0855218100	7818.31830	41248.77264	388.78815
6	10.86530	0.0615943500	7672.74068	43106.33286	368.52218
141	8.49700	0.0702213800	6830.50285	43600.82368	378.88580
14	8.60580	0.0615238000	5799.17596	41734.65309	373.86596
17	3.61870	0.0792819700	5563.67344	23589.44391	377.18866
145	7.10770	0.0850198100	5958.19278	35020.27228	382.32200
152	7.02150	0.0779984900	6027.28359	35491.79641	385.19504
99	59.89970	0.0668015600	15780.54443	130767.04635	357.75100
3	7.57030	0.0720939000	5886.35823	44155.42276	369.70332
140	6.63740	0.0760668600	5613.49701	32808.74974	383.58129
129	9.14970	0.0736765400	6267.28952	34933.71443	375.98344
8	15.92220	0.0657772500	7909.31390	69818.14002	367.45428
127	5.09350	0.0723676500	6005.55220	28597.97869	373.54705
149	28.19900	0.0615936000	12994.85536	86062.40875	388.41006
5	7.15870	0.0761792700	6297.69970	36020.71247	372.95041
2	9.37680	0.0830394300	6641.09996	40725.44921	375.72968
136	4.66720	0.0681978000	4972.13488	33709.07464	379.28775
7	11.76290	0.0706533700	10630.30205	59106.95847	375.34451
13	6.73190	0.0784453700	8107.17368	42838.13916	372.39582
102	3.73580	0.0701731500	5914.83851	26729.30924	374.64764
109	5.50990	0.0631570700	8397.67568	35409.72844	370.33398

93	3.04090	0.0586716300	5958.21294	27097.13943	374.44867
123	3.82180	0.0672529000	5321.31989	20882.17251	367.56217
116	2.66200	0.0784349900	3216.81976	20333.30340	373.95970
12	14.81990	0.0765600800	8502.29550	48200.00178	369.79608
108	2.22040	0.0655815500	5311.40001	20029.45059	359.67857
48	7.73550	0.0743500800	6645.98792	30564.12175	364.92567
80	3.68400	0.0700098100	4866.72224	31131.79886	369.08754
74	1.45450	0.0523152300	4279.94247	15634.76405	362.63961
47	2.67910	0.0839018400	5569.37760	22408.70550	355.18011
131	36.06010	0.0705079200	13808.49656	99131.04559	380.73449
110	1.92100	0.0628579900	3226.90497	16985.55498	346.28675
58	1.93060	0.0528252200	5225.28105	19581.76643	348.90552
66	0.98810	0.0515998000	4133.86854	16351.60111	343.95594
42	2.64770	0.0578990700	4561.00980	18875.10041	354.30573
65	1.37220	0.0510724900	4832.77725	21926.77218	341.12715
85	0.86350	0.0600113200	4589.39210	16007.21946	334.80568
71	0.81970	0.0521038300	2347.41477	10344.96072	351.84608
39	1.67000	0.0861260300	4678.39476	19835.51673	338.02103
35	1.17510	0.0538551000	4184.09233	14149.32957	341.03222
97	0.57780	0.0607699200	1962.14101	9605.83653	337.89097
98	0.55630	0.0537824100	2184.50824	9978.94544	334.32194
73	1.61120	0.0561602100	4289.30572	18730.77453	323.23997
104	0.23700	0.0574174900	937.43595	4907.49469	339.04255
28	3.04840	0.0651843500	5547.46088	24294.62429	331.09302
40	4.08390	0.0785064100	6225.92366	26638.72039	353.99446
61	0.53300	0.0548748900	1992.46893	7052.97154	338.42913
94	0.22220	0.0620706800	1176.37334	4729.30113	332.31829
31	1.93390	0.0569783200	3668.60550	19842.82374	330.89976
55	0.85550	0.0578700100	2283.61219	11110.61875	328.96189
84	0.57700	0.0519718700	1770.60794	7945.86112	325.45817
43	1.16190	0.0561404900	3007.94260	11634.78476	326.15413
83	0.31390	0.0474212200	1484.61885	6171.18810	322.97019
91	0.27430	0.0671237700	1575.28783	6444.27260	319.83674
50	0.57860	0.0552364100	2315.32799	8077.20977	323.96210
56	0.56280	0.0576095600	2173.95443	10012.46758	317.77611
86	1.36830	0.0633787500	4452.61353	16115.31276	341.22722
59	0.12980	0.0662678500	1129.91784	4203.25363	321.62131
51	1.09430	0.0517979500	2268.20694	13801.10467	316.26055
69	2.16160	0.0498087600	3129.45967	26284.69656	326.04382

77	0.33750	0.0302835800	1371.12343	5566.21833	317.39437
23	2.46330	0.0645037300	5901.09316	22510.53189	349.01078
63	1.20020	0.0620956500	2824.55116	14974.66643	323.09725
41	1.12120	0.0411272600	1900.20236	14184.51000	314.03281
39	1.67000	0.0861260300	4678.39476	19835.51673	338.02103
49	0.23670	0.0507955800	1158.25150	5319.79440	318.00511
89	1.75700	0.0668239700	3454.45986	13596.60171	340.67848
32	1.25200	0.0443912900	1771.44012	12933.12406	313.08332
46	0.96010	0.0459605200	2437.03345	14854.14018	313.39123
33	0.25360	0.0588566400	1081.88166	4807.74261	317.86976
26	0.39500	0.0501556300	2496.09819	8710.32274	312.58207
19	2.00210	0.0709455600	3918.43450	19662.92141	319.51371
21	1.61330	0.0471115200	3677.56448	25250.94765	310.81725
21	1.61330	0.0471115200	3677.56448	25250.94765	310.81725
25	0.88760	0.0464860400	2618.97003	11218.96706	311.33460
117	1.09580	0.0602977000	2221.75929	10168.38122	367.17275
57	1.45870	0.0646908300	3227.57584	14376.00415	326.41655
72	0.04580	0.1245788700	636.55367	2263.57796	318.93846
76	0.58710	0.0595550400	2419.17916	10156.32136	336.25929
67	0.16080	0.0625259700	1546.69911	4826.94810	327.83851
44	2.60420	0.0478501600	3254.27967	17269.30487	317.67752
87	1.07980	0.0654831900	2825.22403	11531.23554	348.19461
27	0.48670	0.0574635700	2206.70594	9890.49561	310.66946
130	1.47090	0.0693821600	2959.17639	13403.19979	373.05942
111	0.34210	0.0576765300	1253.14315	6018.65893	360.44691
18	2.58660	0.0709723100	4015.57057	22204.20372	318.99661
75	0.51620	0.0685025300	1664.24934	7187.55331	334.67016
101	1.34600	0.0605549000	2888.32277	13427.42409	360.28275
36	0.00280	0.0314111100	108.19180	443.87905	310.69565
37	0.37500	0.0533695000	1597.37958	6624.64028	312.98172
122	0.96970	0.0683505800	2546.51077	10751.27402	368.66091
24	1.49600	0.0597965800	2770.07360	13571.61398	320.52777
79	1.16210	0.0528541900	2201.72182	10577.74334	340.84041
146	2.27010	0.0792961100	3454.50255	22541.33551	378.37601
103	0.79230	0.0597526300	1392.03441	8811.97596	345.13839
64	2.57340	0.0605717900	3243.03083	27061.59680	345.44177
20	0.68060	0.0450877100	2704.82101	11237.94656	307.10774
132	4.96760	0.0816367100	5623.60562	36427.54806	367.36361
113	1.51310	0.0655576400	4052.78435	18207.25731	357.20852

126	2.35040	0.0727009700	3188.28423	24192.27817	362.15191
143	1.95910	0.0765223000	3702.98142	17959.71457	376.42236
45	1.89090	0.0602870900	3747.99894	17361.51512	331.20963
53	2.12090	0.0571846700	3266.27068	18636.47757	335.29071
148	4.80490	0.0841802900	4667.48448	25898.52145	380.23289
22	1.68270	0.0774928800	2914.44598	16755.58864	322.34269
54	1.20360	0.0555306100	4035.67111	16366.35483	345.28683
60	0.21860	0.0513710900	1187.09018	6080.51698	330.47248
82	1.85570	0.0665512600	2741.13630	19151.69959	348.48842
70	0.90880	0.0716101700	2230.46074	10505.84343	341.29866
120	1.27480	0.0785410800	3477.09428	15699.28911	359.76381
112	2.25590	0.0745319800	3223.40203	17202.12383	357.32404
92	1.08340	0.0688533600	2823.97685	15314.74868	352.61159
138	1.87830	0.0774858000	3642.77969	18021.79749	371.93963
30	1.33280	0.0637630200	3036.83130	19544.92301	335.68703
139	2.66330	0.0852448900	4402.95688	23857.87398	375.12977
18	2.58660	0.0709723100	4015.57057	22204.20372	318.99661
34	2.64570	0.0599977500	3112.04605	15901.78803	346.93194
62	0.56690	0.0576377300	2147.07509	8486.65020	349.88042
81	1.62550	0.0594750500	3290.49951	13918.25207	351.50196
29	1.86560	0.0643250000	4267.38802	18911.33279	341.81523
95	0.87180	0.0623710800	2322.20263	10900.69158	355.71429
137	3.71710	0.0857263900	4012.55012	26537.96742	369.37248
68	1.50660	0.0536786200	4112.71661	17261.88201	360.06994
95	0.87180	0.0623710800	2322.20263	10900.69158	355.71429
106	0.29730	0.0580375500	1176.76167	7024.55725	359.39154
133	1.72750	0.0774878400	2401.34656	16293.02014	365.61552
115	0.72420	0.0697401200	3079.22846	11953.87247	362.75564
88	0.79050	0.0465029800	2240.72215	9425.91707	359.62784
38	2.48330	0.0726210900	4121.83408	20036.52440	357.43130
96	1.14890	0.0436738300	2876.31442	13287.52483	360.59173
78	0.39240	0.0524758800	1638.02661	7315.83047	360.00917
114	1.76460	0.0647501900	4099.54772	17879.45673	362.91897
128	0.31420	0.0876933900	1356.96564	6134.98625	363.17496
100	0.70860	0.0765893200	1972.45227	8616.18197	361.67167
119	1.25100	0.0708316900	2616.72285	12372.61297	363.44301
124	1.30410	0.0736494600	3782.74179	14320.10043	365.29810
90	1.90340	0.0703939600	3335.39602	14953.99062	361.94606
107	1.24220	0.0775915800	2942.42991	14224.85906	363.71836

105	1.23590	0.0654081400	3304.11843	13737.62720	363.69349
118	1.07380	0.0673085100	2213.13784	12404.15411	365.06095
52	1.74490	0.0968907000	2618.97003	13486.29408	362.68838
121	0.29780	0.0746881200	1592.62260	6311.33980	365.16868
125	3.04090	0.0814972100	3192.69972	23664.15440	366.13571
134	3.66560	0.0844584500	4346.23009	22259.49413	364.14746
135	3.83500	0.0954325100	4713.96512	25985.70647	366.53429

APPENDIX II

**The curve numbers for each sub-basin
and SCS Lag Time**

sub-Basin name	Area km2	SCS Curve number	SCS Lag Time (hours)
100B	0.71	75.00	0.75
101B	1.35	75.00	1.03
102B	3.74	55.00	3.04
103B	0.79	75.00	0.67
104B	0.24	55.00	0.72
105B	1.24	65.00	1.65
106B	0.30	53.00	1.21
107B	1.24	65.00	1.41
108B	2.22	55.00	2.93
109B	5.51	55.00	4.81
10B	5.98	55.00	3.27
110B	1.92	55.00	2.25
111B	0.34	75.00	0.68
112B	2.26	68.33	1.39
113B	1.51	75.00	1.41
114B	1.76	75.00	1.52
115B	0.72	75.00	1.17
116B	2.66	55.00	2.39
117B	1.10	75.00	1.11
118B	1.07	61.67	1.37
119B	1.25	75.00	1.12
11B	2.43	55.00	2.59
120B	1.27	55.00	2.07
121B	0.30	75.00	0.59
122B	0.97	68.33	1.12
123B	3.82	55.00	3.40
124B	1.30	68.33	1.46
125B	3.04	55.00	2.45
126B	2.35	55.00	1.84
127B	5.09	55.00	3.34
128B	0.31	75.00	0.54
129B	9.15	55.00	3.58
12B	14.82	55.00	4.32
130B	1.47	61.67	1.58
131B	36.06	60.18	6.73
132B	4.97	55.00	3.27
133B	1.73	75.00	1.20
134B	3.67	55.00	2.33
135B	3.84	55.00	2.52
136B	4.67	55.00	3.15
137B	3.72	55.00	2.34

138B	1.88	55.00	2.18
139B	2.66	55.00	2.77
13B	6.73	55.00	3.90
140B	6.64	55.00	3.91
141B	8.50	55.00	3.62
142B	43.20	55.00	7.00
143B	1.96	55.00	2.10
144B	5.16	55.00	3.05
145B	7.11	55.00	3.81
146B	2.27	55.00	2.48
147B	49.05	55.00	8.59
148B	4.80	55.00	2.91
149B	28.20	55.00	7.53
14B	8.61	56.00	3.72
150B	14.01	55.00	4.39
151B	17.31	55.00	5.51
152B	7.02	55.00	3.65
153B	9.11	55.00	4.95
154B	62.68	55.41	9.33
155B	8.79	55.00	3.72
156B	8.03	55.00	4.46
157B	49.37	55.00	9.09
158B	8.62	55.00	4.04
159B	33.04	55.00	8.42
15B	3.40	55.00	2.15
160B	63.72	56.17	9.83
161B	49.00	66.24	9.84
162B	21.16	55.00	6.88
163B	21.37	55.00	7.17
164B	77.81	58.17	10.22
165B	30.48	55.00	6.90
166B	25.86	55.00	7.37
167B	35.18	56.79	15.52
168B	55.78	55.00	9.65
169B	25.52	55.00	9.07
16B	11.93	55.00	3.74
170B	40.13	55.00	8.58
171B	25.66	55.00	10.15
172B	24.31	69.73	6.98
173B	33.85	61.25	11.57
174B	31.83	55.00	7.88
175B	39.62	55.00	8.57
176B	39.26	55.53	12.35

177B	23.33	56.82	9.92
178B	37.82	55.00	7.02
179B	18.95	55.00	7.35
17B	3.62	55.00	2.94
180B	26.64	55.00	9.50
181B	27.47	55.00	7.84
182B	34.43	55.00	10.29
183B	30.16	55.00	8.90
18B	2.59	55.00	3.24
19B	2.00	55.00	2.62
1B	16.17	55.00	3.72
20B	0.68	55.00	2.06
21B	1.61	65.00	1.94
22B	1.68	55.00	1.76
23B	2.46	55.00	3.58
24B	1.50	75.00	1.30
25B	0.89	75.00	1.28
26B	0.40	55.00	1.78
27B	0.49	55.00	1.47
28B	3.05	55.00	3.84
29B	1.87	55.00	2.82
2B	9.38	55.00	3.86
30B	1.33	65.00	1.57
31B	1.93	60.00	2.01
32B	1.25	75.00	1.40
33B	0.25	75.00	0.50
34B	2.65	70.00	1.56
35B	1.18	68.33	1.81
36B	0.00	57.00	0.15
37B	0.38	75.00	0.69
38B	2.48	59.00	2.29
39B	1.67	55.00	2.13
3B	7.57	55.00	3.66
40B	4.08	55.00	3.55
41B	1.12	57.00	1.89
42B	2.65	55.00	2.78
43B	1.16	75.00	1.17
44B	2.60	75.00	1.38
45B	1.89	75.00	1.48
46B	0.96	75.00	1.43
47B	2.68	55.00	3.02
48B	7.74	55.00	4.65
49B	0.24	75.00	0.58

4B	14.15	55.00	4.88
50B	0.58	75.00	0.94
51B	1.09	75.00	1.05
52B	1.74	55.00	1.41
53B	2.12	75.00	1.41
54B	1.20	75.00	1.44
55B	0.86	75.00	0.95
56B	0.56	75.00	0.96
57B	1.46	75.00	1.04
58B	1.93	55.00	3.55
59B	0.13	57.00	0.76
5B	7.16	55.00	3.61
60B	0.22	75.00	0.73
61B	0.53	75.00	0.91
62B	0.57	75.00	0.91
63B	1.20	75.00	1.15
64B	2.57	75.00	1.76
65B	1.37	68.33	2.15
66B	0.99	55.00	2.52
67B	0.16	50.00	1.14
68B	1.51	75.00	1.66
69B	2.16	75.00	1.18
6B	10.87	55.00	4.77
70B	0.91	75.00	0.96
71B	0.82	55.00	1.81
72B	0.05	57.00	0.34
73B	1.61	55.00	2.67
74B	1.45	55.00	2.78
75B	0.52	75.00	0.67
76B	0.59	75.00	1.13
77B	0.34	55.00	1.34
78B	0.39	75.00	0.67
79B	1.16	75.00	1.24
7B	11.76	55.00	5.41
80B	3.68	55.00	2.89
81B	1.63	75.00	1.22
82B	1.86	75.00	1.17
83B	0.31	55.00	1.23
84B	0.58	55.00	1.34
85B	0.86	55.00	2.38
86B	1.37	55.00	2.57
87B	1.08	75.00	1.19
88B	0.79	75.00	0.99

89B	1.76	75.00	1.35
8B	15.92	55.00	4.48
90B	1.90	68.33	1.46
91B	0.27	55.00	1.01
92B	1.08	75.00	1.12
93B	3.04	55.00	4.22
94B	0.22	75.00	0.55
95B	0.87	75.00	1.10
96B	1.15	75.00	1.38
97B	0.58	55.00	1.45
98B	0.56	55.00	1.55
99B	59.90	56.13	7.90
9B	8.38	55.00	4.13

APPENDIX III

**The peak discharge for each sub-basin for
the two method of rainfal**

Hydrologic Element	Drainage Area (Km ²)	Peak Discharge (M3/S)											
		SCS						Frequency Storm					
		2 Year	5 Year	10 Year	25 Year	50 Year	100 Year	2 Year	5 Year	10 Year	25 Year	50 Year	100 Year
23B	2.4633	0	0	0.43	1.93	3.65	5.81	0	0	0.12	1.06	2.3	3.94
19B	2.0021	0	0	0.43	1.93	3.65	5.81	0	0	0.12	1.06	2.3	3.94
52B	1.7449	0	0	0.43	1.93	3.65	5.81	0	0	0.12	1.06	2.3	3.94
38B	2.4833	0	0.27	1.32	3.65	6.01	8.79	0	0.06	0.69	2.37	4.17	6.38
29B	1.8656	0	0	0.43	1.93	3.65	5.81	0	0	0.12	1.06	2.3	3.94
34B	2.6457	1.13	4.23	7.41	12.42	16.72	21.4	0.17	2.23	4.63	8.59	12.1	15.97
30B	1.3328	0.59	2.29	4.51	8.33	11.77	15.62	0	0.84	2.39	5.27	7.98	11.07
22B	1.6827	0	0	0.43	1.93	3.65	5.81	0	0	0.12	1.06	2.3	3.94
42B	2.6477	0	0	0.43	1.93	3.65	5.81	0	0	0.12	1.06	2.3	3.94
31B	1.9339	0.43	1.03	2.37	5.04	7.64	10.67	0	0.12	0.9	2.77	4.72	7.08
26B	0.395	1.8	2.65	3.61	5.72	7.86	10.41	0	0	0.12	1.06	2.3	3.94
24B	1.496	7.18	13.5	18.59	25.78	31.56	37.58	0.91	4.38	7.72	12.85	17.18	21.83
35B	1.1751	2.65	5.95	9.19	14.22	18.51	23.16	0.06	1.68	3.79	7.39	10.62	14.23
33B	0.2536	8.27	14.96	20.24	27.65	33.55	39.7	0.91	4.38	7.72	12.85	17.18	21.83
148B	4.8049	0	0	0.43	1.93	3.65	5.81	0	0	0.12	1.06	2.3	3.94
146B	2.2701	0	0	0.43	1.93	3.65	5.81	0	0	0.12	1.06	2.3	3.94
143B	1.9591	0	0	0.43	1.93	3.65	5.81	0	0	0.12	1.06	2.3	3.94
138B	1.8783	0	0	0.43	1.93	3.65	5.81	0	0	0.12	1.06	2.3	3.94
139B	2.6633	0	0	0.43	1.93	3.65	5.81	0	0	0.12	1.06	2.3	3.94
137B	3.7171	0	0	0.43	1.93	3.65	5.81	0	0	0.12	1.06	2.3	3.94
132B	4.9676	0	0	0.43	1.93	3.65	5.81	0	0	0.12	1.06	2.3	3.94
126B	2.3504	0	0	0.43	1.93	3.65	5.81	0	0	0.12	1.06	2.3	3.94
120B	1.2748	0	0	0.43	1.93	3.65	5.81	0	0	0.12	1.06	2.3	3.94
112B	2.2559	0.22	2.58	5.28	9.73	13.63	17.94	0.06	1.68	3.79	7.39	10.62	14.23
92B	1.0834	1.45	5.85	9.9	16	21.07	26.48	0.91	4.38	7.72	12.85	17.18	21.83
82B	1.8557	1.45	5.85	9.9	16	21.07	26.48	0.91	4.38	7.72	12.85	17.18	21.83
133B	1.7275	1.52	5.94	10.01	16.11	21.2	26.61	0.91	4.38	7.72	12.85	17.18	21.83
128B	0.3142	1.45	5.85	9.9	16	21.07	26.48	0.91	4.38	7.72	12.85	17.18	21.83
124B	1.3041	0.22	2.58	5.28	9.73	13.63	17.94	0.06	1.68	3.79	7.39	10.62	14.23
119B	1.251	1.45	5.85	9.9	16	21.07	26.48	0.91	4.38	7.72	12.85	17.18	21.83
115B	0.7242	1.45	5.85	9.9	16	21.07	26.48	0.91	4.38	7.72	12.85	17.18	21.83
114B	1.7646	2.27	6.94	11.14	17.39	22.57	28.07	0.91	4.38	7.72	12.85	17.18	21.83
106B	0.2973	0.09	0.13	0.32	1.45	2.89	4.76	0	0	0.01	0.6	1.56	2.92
95B	0.8718	1.45	5.85	9.9	16	21.07	26.48	0.91	4.38	7.72	12.85	17.18	21.83

81B	1.6255	2.81	7.67	11.97	18.33	23.57	29.12	0.91	4.38	7.72	12.85	17.18	21.83
70B	0.9088	1.45	5.85	9.9	16	21.07	26.48	0.91	4.38	7.72	12.85	17.18	21.83
64B	2.5734	3.09	8.03	12.39	18.79	24.07	29.65	0.91	4.38	7.72	12.85	17.18	21.83
60B	0.2186	1.45	5.85	9.9	16	21.07	26.48	0.91	4.38	7.72	12.85	17.18	21.83
53B	2.1209	1.99	6.58	10.73	16.93	22.07	27.54	0.91	4.38	7.72	12.85	17.18	21.83
135B	3.835	0	0	0.43	1.93	3.65	5.81	0	0	0.12	1.06	2.3	3.94
134B	3.6656	0	0	0.43	1.93	3.65	5.81	0	0	0.12	1.06	2.3	3.94
125B	3.0409	0	0	0.43	1.93	3.65	5.81	0	0	0.12	1.06	2.3	3.94
121B	0.2978	1.45	5.85	9.9	16	21.07	26.48	0.91	4.38	7.72	12.85	17.18	21.83
118B	1.0738	0	0.68	2.18	5.09	7.88	11.1	0	0.29	1.31	3.52	5.72	8.31
107B	1.2422	0.01	1.47	3.56	7.22	10.56	14.32	0	0.84	2.39	5.27	7.98	11.07
100B	0.7086	3.36	8.4	12.8	19.26	24.57	30.18	0.91	4.38	7.72	12.85	17.18	21.83
90B	1.9034	0.36	2.78	5.51	9.99	13.92	18.25	0.06	1.68	3.79	7.39	10.62	14.23
105B	1.2359	0.3	1.88	4.03	7.77	11.16	14.97	0	0.84	2.39	5.27	7.98	11.07
96B	1.1489	2.81	7.67	11.97	18.33	23.57	29.12	0.91	4.38	7.72	12.85	17.18	21.83
88B	0.7905	1.45	5.85	9.9	16	21.07	26.48	0.91	4.38	7.72	12.85	17.18	21.83
78B	0.3924	8	14.59	19.83	27.18	33.05	39.17	0.91	4.38	7.72	12.85	17.18	21.83
68B	1.5066	6.91	13.14	18.18	25.32	31.06	37.05	0.91	4.38	7.72	12.85	17.18	21.83
62B	0.5669	4.18	9.49	14.04	20.66	26.06	31.77	0.91	4.38	7.72	12.85	17.18	21.83
54B	1.2036	4.18	9.49	14.04	20.66	26.06	31.77	0.91	4.38	7.72	12.85	17.18	21.83
45B	1.8909	3.5	8.58	13.01	19.49	24.82	30.45	0.91	4.38	7.72	12.85	17.18	21.83
37B	0.375	1.45	5.85	9.9	16	21.07	26.48	0.91	4.38	7.72	12.85	17.18	21.83
36B	0.0028	15.81	23.3	28.56	35.65	41.19	46.89	0	0	0.35	1.65	3.17	5.09
43B	1.1619	9.09	16.05	21.48	29.04	35.05	41.28	0.91	4.38	7.72	12.85	17.18	21.83
44B	2.6042	15.1	24.07	30.58	39.29	46.04	52.91	0.91	4.38	7.72	12.85	17.18	21.83
58B	1.9306	0.29	0.43	0.94	2.54	4.33	6.55	0	0	0.12	1.06	2.3	3.94
50B	0.5786	8.27	14.96	20.24	27.65	33.55	39.7	0.91	4.38	7.72	12.85	17.18	21.83
113B	1.5131	1.45	5.85	9.9	16	21.07	26.48	0.91	4.38	7.72	12.85	17.18	21.83
103B	0.7923	6.23	12.23	17.14	24.15	29.81	35.73	0.91	4.38	7.72	12.85	17.18	21.83
79B	1.1621	8.14	14.78	20.04	27.41	33.3	39.43	0.91	4.38	7.72	12.85	17.18	21.83
75B	0.5162	10.19	17.51	23.14	30.91	37.05	43.4	0.91	4.38	7.72	12.85	17.18	21.83
67B	0.1608	10.06	14.8	17.94	22.25	25.82	29.64	0	0	0	0.15	0.71	1.66
130B	1.4709	0	0.68	2.18	5.09	7.88	11.1	0	0.29	1.31	3.52	5.72	8.31
122B	0.9697	0.22	2.58	5.28	9.73	13.63	17.94	0.06	1.68	3.79	7.39	10.62	14.23
117B	1.0958	1.45	5.85	9.9	16	21.07	26.48	0.91	4.38	7.72	12.85	17.18	21.83
111B	0.3421	1.45	5.85	9.9	16	21.07	26.48	0.91	4.38	7.72	12.85	17.18	21.83
101B	1.346	1.45	5.85	9.9	16	21.07	26.48	0.91	4.38	7.72	12.85	17.18	21.83
87B	1.0798	1.45	5.85	9.9	16	21.07	26.48	0.91	4.38	7.72	12.85	17.18	21.83
76B	0.5871	1.45	5.85	9.9	16	21.07	26.48	0.91	4.38	7.72	12.85	17.18	21.83

72B	0.0458	7.19	10.63	13.43	17.69	21.32	25.26	0	0	0.35	1.65	3.17	5.09
158B	8.6151	0	0	0.43	1.93	3.65	5.81	0	0	0.12	1.06	2.3	3.94
156B	8.0341	0	0	0.43	1.93	3.65	5.81	0	0	0.12	1.06	2.3	3.94
153B	9.1105	0	0	0.43	1.93	3.65	5.81	0	0	0.12	1.06	2.3	3.94
155B	8.7948	0	0	0.43	1.93	3.65	5.81	0	0	0.12	1.06	2.3	3.94
152B	7.0215	0	0	0.43	1.93	3.65	5.81	0	0	0.12	1.06	2.3	3.94
145B	7.1077	0	0	0.43	1.93	3.65	5.81	0	0	0.12	1.06	2.3	3.94
151B	17.3146	0	0	0.43	1.93	3.65	5.81	0	0	0.12	1.06	2.3	3.94
150B	14.0098	0	0	0.43	1.93	3.65	5.81	0	0	0.12	1.06	2.3	3.94
144B	5.1585	0	0	0.43	1.93	3.65	5.81	0	0	0.12	1.06	2.3	3.94
141B	8.497	0	0	0.43	1.93	3.65	5.81	0	0	0.12	1.06	2.3	3.94
140B	6.6374	0	0	0.43	1.93	3.65	5.81	0	0	0.12	1.06	2.3	3.94
136B	4.6672	0	0	0.43	1.93	3.65	5.81	0	0	0.12	1.06	2.3	3.94
109B	5.5099	0	0	0.43	1.93	3.65	5.81	0	0	0.12	1.06	2.3	3.94
104B	0.237	0	0	0.43	1.93	3.65	5.81	0	0	0.12	1.06	2.3	3.94
94B	0.2222	1.45	5.85	9.9	16	21.07	26.48	0.91	4.38	7.72	12.85	17.18	21.83
85B	0.8635	0.43	0.64	1.19	2.84	4.66	6.91	0	0	0.12	1.06	2.3	3.94
108B	2.2204	0	0	0.43	1.93	3.65	5.81	0	0	0.12	1.06	2.3	3.94
97B	0.5778	0	0	0.43	1.93	3.65	5.81	0	0	0.12	1.06	2.3	3.94
84B	0.577	0	0	0.43	1.93	3.65	5.81	0	0	0.12	1.06	2.3	3.94
77B	0.3375	0	0	0.43	1.93	3.65	5.81	0	0	0.12	1.06	2.3	3.94
170B	40.1262	0	0	0.43	1.91	3.62	5.76	0	0	0.12	1.04	2.27	3.88
165B	30.4792	0	0	0.43	1.93	3.65	5.8	0	0	0.12	1.06	2.29	3.92
163B	21.3692	0	0	0.43	1.93	3.64	5.8	0	0	0.12	1.06	2.29	3.92
169B	25.5197	0	0	0.42	1.9	3.6	5.74	0	0	0.12	1.04	2.25	3.86
166B	25.8628	0	0	0.43	1.92	3.64	5.79	0	0	0.12	1.05	2.29	3.92
162B	21.1643	0	0	0.43	1.93	3.65	5.8	0	0	0.12	1.06	2.29	3.92
157B	49.3678	0	0	0.42	1.9	3.6	5.74	0	0	0.12	1.04	2.25	3.86
183B	30.1552	0	0	0.42	1.91	3.61	5.75	0	0	0.12	1.04	2.26	3.87
182B	34.4272	0	0	0.42	1.88	3.56	5.67	0	0	0.11	1.02	2.21	3.8
176B	39.2619	0	0.01	0.48	2	3.7	5.84	0	0	0.15	1.1	2.32	3.93
172B	24.3078	0.38	3.13	6.11	10.88	15.03	19.57	0.15	2.13	4.47	8.37	11.83	15.65
180B	26.6437	0	0	0.42	1.89	3.59	5.72	0	0	0.12	1.03	2.24	3.85
177B	23.3298	0	0.07	0.76	2.59	4.56	6.96	0	0	0.31	1.54	3	4.85
167B	35.184	0	0.05	0.65	2.28	4.04	6.21	0	0	0.25	1.31	2.58	4.22
181B	27.4686	0	0	0.43	1.92	3.63	5.78	0	0	0.12	1.05	2.28	3.91
179B	18.9538	0	0	0.43	1.92	3.64	5.79	0	0	0.12	1.05	2.29	3.92
178B	37.8221	0	0	0.43	1.93	3.64	5.8	0	0	0.12	1.06	2.29	3.92
175B	39.617	0	0	0.43	1.91	3.62	5.76	0	0	0.12	1.04	2.27	3.88

174B	31.8271	0	0	0.43	1.92	3.63	5.78	0	0	0.12	1.05	2.28	3.9
171B	25.6624	0	0	0.42	1.88	3.56	5.68	0	0	0.11	1.02	2.22	3.81
168B	55.7798	0	0	0.42	1.89	3.58	5.71	0	0	0.12	1.03	2.24	3.84
173B	33.8457	0	0.57	1.94	4.65	7.27	10.32	0	0.22	1.12	3.14	5.19	7.62
164B	77.8097	0	0.17	1.07	3.17	5.34	7.95	0	0.02	0.51	1.98	3.62	5.66
160B	63.7179	0	0.03	0.63	2.33	4.2	6.5	0	0	0.23	1.35	2.71	4.47
161B	49.0023	0.06	1.8	4.08	7.97	11.47	15.37	0	1.08	2.79	5.88	8.73	11.96
159B	33.0438	0	0	0.43	1.91	3.62	5.76	0	0	0.12	1.04	2.27	3.89
154B	62.6803	0	0.01	0.49	2.05	3.81	6	0	0	0.15	1.14	2.41	4.08
147B	49.0482	0	0	0.43	1.91	3.62	5.76	0	0	0.12	1.04	2.27	3.88
149B	28.199	0	0	0.43	1.92	3.64	5.79	0	0	0.12	1.05	2.29	3.91
142B	43.1966	0	0	0.43	1.93	3.64	5.8	0	0	0.12	1.06	2.29	3.92
131B	36.0601	0	0.43	1.67	4.26	6.8	9.77	0	0.14	0.93	2.84	4.82	7.19
99B	59.8997	0	0.03	0.63	2.35	4.24	6.56	0	0	0.23	1.37	2.75	4.54
91B	0.2743	0	0	0.43	1.93	3.65	5.81	0	0	0.12	1.06	2.3	3.94
123B	3.8218	0	0	0.43	1.93	3.65	5.81	0	0	0.12	1.06	2.3	3.94
110B	1.921	0	0	0.43	1.93	3.65	5.81	0	0	0.12	1.06	2.3	3.94
98B	0.5563	0	0	0.43	1.93	3.65	5.81	0	0	0.12	1.06	2.3	3.94
83B	0.3139	0	0	0.43	1.93	3.65	5.81	0	0	0.12	1.06	2.3	3.94
89B	1.757	2.68	7.49	11.77	18.09	23.32	28.86	0.91	4.38	7.72	12.85	17.18	21.83
86B	1.3683	0.03	0.04	0.48	1.99	3.72	5.88	0	0	0.12	1.06	2.3	3.94
73B	1.6112	0	0	0.43	1.93	3.65	5.81	0	0	0.12	1.06	2.3	3.94
69B	2.1616	8	14.59	19.83	27.18	33.05	39.17	0.91	4.38	7.72	12.85	17.18	21.83
63B	1.2002	11.01	18.6	24.38	32.31	38.55	44.98	0.91	4.38	7.72	12.85	17.18	21.83
74B	1.4545	0	0	0.43	1.93	3.65	5.81	0	0	0.12	1.06	2.3	3.94
66B	0.9881	2.59	3.81	5.01	7.39	9.71	12.43	0	0	0.12	1.06	2.3	3.94
65B	1.3722	4.5	8.53	12.18	17.66	22.24	27.15	0.06	1.68	3.79	7.39	10.62	14.23
59B	0.1298	5.75	8.52	10.91	14.7	18.01	21.65	0	0	0.35	1.65	3.17	5.09
56B	0.5628	7.18	13.5	18.59	25.78	31.56	37.58	0.91	4.38	7.72	12.85	17.18	21.83
57B	1.4587	11.01	18.6	24.38	32.31	38.55	44.98	0.91	4.38	7.72	12.85	17.18	21.83
51B	1.0943	6.77	12.95	17.97	25.08	30.81	36.79	0.91	4.38	7.72	12.85	17.18	21.83
102B	3.7358	0	0	0.43	1.93	3.65	5.81	0	0	0.12	1.06	2.3	3.94
93B	3.0409	0	0	0.43	1.93	3.65	5.81	0	0	0.12	1.06	2.3	3.94
129B	9.1497	0	0	0.43	1.93	3.65	5.81	0	0	0.12	1.06	2.3	3.94
17B	3.6187	0	0	0.43	1.93	3.65	5.81	0	0	0.12	1.06	2.3	3.94
16B	11.9334	0	0	0.43	1.93	3.65	5.81	0	0	0.12	1.06	2.3	3.94
15B	3.3999	0	0	0.43	1.93	3.65	5.81	0	0	0.12	1.06	2.3	3.94
9B	8.3752	0	0	0.43	1.93	3.65	5.81	0	0	0.12	1.06	2.3	3.94
10B	5.9787	0	0	0.43	1.93	3.65	5.81	0	0	0.12	1.06	2.3	3.94

11B	2.4255	0	0	0.43	1.93	3.65	5.81	0	0	0.12	1.06	2.3	3.94
14B	8.6058	0	0.03	0.61	2.31	4.19	6.5	0	0	0.22	1.34	2.72	4.5
127B	5.0935	0	0	0.43	1.93	3.65	5.81	0	0	0.12	1.06	2.3	3.94
116B	2.662	0	0	0.43	1.93	3.65	5.81	0	0	0.12	1.06	2.3	3.94
80B	3.684	0	0	0.43	1.93	3.65	5.81	0	0	0.12	1.06	2.3	3.94
71B	0.8197	0	0	0.43	1.93	3.65	5.81	0	0	0.12	1.06	2.3	3.94
61B	0.533	3.09	8.03	12.39	18.79	24.07	29.65	0.91	4.38	7.72	12.85	17.18	21.83
55B	0.8555	5.54	11.31	16.11	22.99	28.56	34.41	0.91	4.38	7.72	12.85	17.18	21.83
49B	0.2367	8.27	14.96	20.24	27.65	33.55	39.7	0.91	4.38	7.72	12.85	17.18	21.83
46B	0.9601	15.1	24.07	30.58	39.29	46.04	52.91	0.91	4.38	7.72	12.85	17.18	21.83
41B	1.1212	14.38	21.19	26.04	32.66	37.88	43.29	0	0	0.35	1.65	3.17	5.09
32B	1.252	13.74	22.25	28.52	36.97	43.54	50.27	0.91	4.38	7.72	12.85	17.18	21.83
25B	0.8876	11.28	18.97	24.79	32.77	39.05	45.51	0.91	4.38	7.72	12.85	17.18	21.83
40B	4.0839	0	0	0.43	1.93	3.65	5.81	0	0	0.12	1.06	2.3	3.94
48B	7.7355	0	0	0.43	1.93	3.65	5.81	0	0	0.12	1.06	2.3	3.94
13B	6.7319	0	0	0.43	1.93	3.65	5.81	0	0	0.12	1.06	2.3	3.94
7B	11.7629	0	0	0.43	1.93	3.65	5.81	0	0	0.12	1.06	2.3	3.94
5B	7.1587	0	0	0.43	1.93	3.65	5.81	0	0	0.12	1.06	2.3	3.94
4B	14.1483	0	0	0.43	1.93	3.65	5.81	0	0	0.12	1.06	2.3	3.94
2B	9.3768	0	0	0.43	1.93	3.65	5.81	0	0	0.12	1.06	2.3	3.94
1B	16.1698	0	0	0.43	1.93	3.65	5.81	0	0	0.12	1.06	2.3	3.94
3B	7.5703	0	0	0.43	1.93	3.65	5.81	0	0	0.12	1.06	2.3	3.94
6B	10.8653	0	0	0.43	1.93	3.65	5.81	0	0	0.12	1.06	2.3	3.94
8B	15.9222	0	0	0.43	1.93	3.65	5.81	0	0	0.12	1.06	2.3	3.94
12B	14.8199	0	0	0.43	1.93	3.65	5.81	0	0	0.12	1.06	2.3	3.94
47B	2.6791	0	0	0.43	1.93	3.65	5.81	0	0	0.12	1.06	2.3	3.94
39B	1.67	0	0	0.43	1.93	3.65	5.81	0	0	0.12	1.06	2.3	3.94
28B	3.0484	0	0	0.43	1.93	3.65	5.81	0	0	0.12	1.06	2.3	3.94
27B	0.4867	0	0	0.43	1.93	3.65	5.81	0	0	0.12	1.06	2.3	3.94
21B	1.6133	0.16	1.68	3.8	7.5	10.86	14.64	0	0.84	2.39	5.27	7.98	11.07
20B	0.6806	0	0	0.43	1.93	3.65	5.81	0	0	0.12	1.06	2.3	3.94
18B	2.5866	0	0	0.43	1.93	3.65	5.81	0	0	0.12	1.06	2.3	3.94

APPENDIX IV

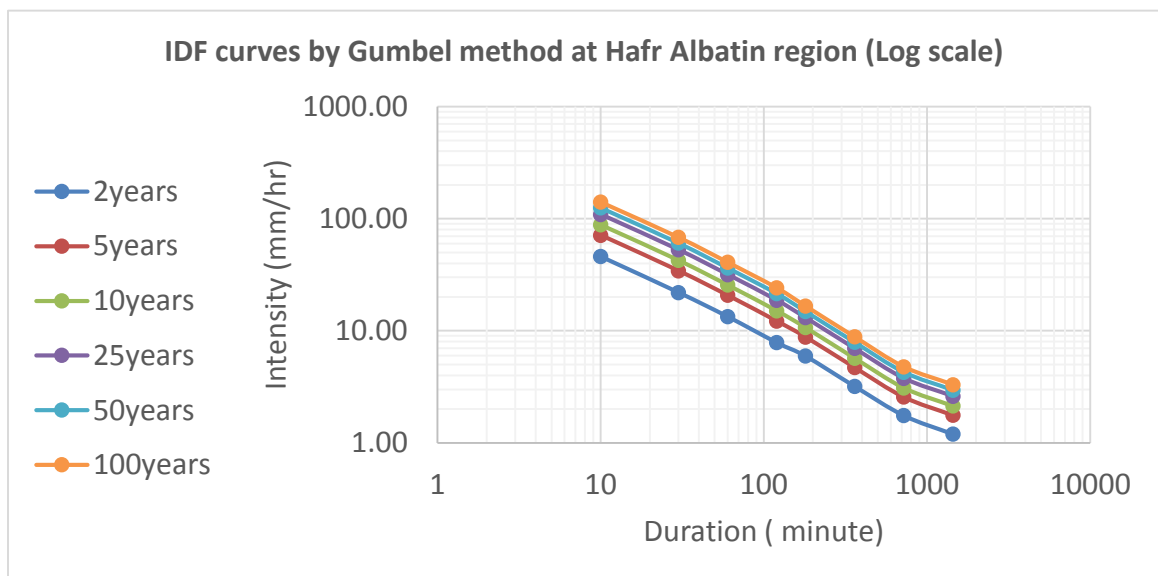
Peak discharge used in HEC-RAS

No.	Stream	Reach	RS	Peak flow					
				Q2	Q5	Q10	Q25	Q50	Q100
1	1	reach_1	13628.3	0.0001	0.01	0.71	2.78	5.15	8.25
2	10	reach_20	2353.18	9.07	18.48	27.4	62.96	108.23	163.94
3	11	reach_22	1981.89	12.52	23.99	34.38	63.51	108.9	164.73
4	12	reach_24	1030.46	17.61	38.94	59.88	93.18	123.57	174.22
5	13	reach_26	2253.26	18.6	40.65	62.21	96.47	127.66	174.65
6	14	reach_30	4740.13	19.61	42.72	65.55	102.33	136.63	190.81
7	2	reach_3	21887.6	0.0001	0.01	1.62	6.39	11.83	18.92
8	3	reach_5	10399.3	0.2	1.7	7.9	24.16	41.58	63.2
9	4	reach_7	24798.3	0.2	1.71	8.61	26.66	46.04	70.09
10	5	reach_9	6367.11	0.24	3.2	12.68	36.53	61.8	92.9
11	6	reach_11	7231.68	0.24	3.21	15.01	45.78	78.84	119.94
12	7	reach_13	12657.2	0.24	3.21	15.7	48.4	83.62	127.51
13	8	reach_15	4626.45	0.25	3.6	17.59	53.92	93.16	142.01
14	9	reach_17	2396.07	4.4	10.08	18.76	59.15	102.31	155.44
15	L1	reach_12	15154.8	0.0001	0.0001	0.43	1.71	3.17	5.06
16	L2	reach_19	13777.8	0.03	0.15	1.37	5.03	9.74	16.28
17	L3	reach_21	4319.04	0.46	0.75	1.04	1.54	2.03	2.62
18	L4	reach_23	6825.64	0.69	1.5	2.3	3.73	7.26	12.16
19	L5	reach_25	1131.16	0.82	1.46	2.01	2.81	3.45	4.13
20	L6	reach_32	754.31	0.0001	0.02	1.59	5.84	11.36	19.01
21	LL8	reach_33	5725.81	0.0001	0.02	1.59	5.82	11.32	18.96
22	LR7	reach_31	4532.65	0.09	0.13	0.2	0.49	0.9	1.44
23	R1	reach_4	26623.4	0.0001	0.0001	0.44	1.7	3.16	5.07
24	R2	reach_6	26588.4	0.0001	0.02	0.54	1.9	3.42	5.32
25	R3	reach_8	23058.6	0.2	1.83	4.3	9.91	15.77	22.83
26	R4	reach_10	21399.9	0.06	1.5	3.61	7.76	11.75	16.41
27	R5	reach_14	11209.6	0.0001	0.0001	0.27	1.04	1.93	3.11
28	R6	reach_16	4706.2	0.0001	0.35	1.19	3.07	5.03	7.39
29	R7	reach_18	5570.81	0.24	1.82	3.69	6.86	9.67	12.76
30	R8	reach_28	4641.6	3.26	11.95	21.45	37.1	51.27	67.21
31	RL10	reach_27	5412.53	1.41	6.92	12.98	22.94	31.96	42.1
32	RR9	reach_29	5311.28	1.56	4.03	6.76	11.36	15.58	20.38

APPENDIX V

Rainfall intensity for different duration and return period

Frequency (Years)	Duration(minutes)							
	10	30	60	120	180	360	720	1440
2	46.002	21.998	13.391	7.849	5.955	3.198	1.756	1.198
5	71.414	34.382	20.757	12.213	8.818	4.706	2.564	1.762
10	88.239	42.581	25.635	15.101	10.713	5.704	3.099	2.136
25	109.497	52.940	31.797	18.751	13.107	6.965	3.774	2.608
50	125.268	60.626	36.368	21.459	14.883	7.901	4.276	2.958
100	140.922	68.254	40.906	24.147	16.647	8.829	4.773	3.306



Vitae

Name : Ahmed Mohammed Al-Areeq

Nationality : Yemeni

Date of Birth : 1/Jan/1981

Email : a.m.alareeq@gmail.com

Address : KFUPM, Dhahran, Saudi Arabia, T.L:+966 55 788
7631.

Academic Background : **M.Sc.**, Civil Engineering, King Fahd University of
Petroleum and Minerals, Dhahran, Saudi Arabia.
B.Sc., Civil Engineering, Tamar University, Yemen.